University of South-Eastern Norway

www.usn.no

FMH606 Master's Thesis 2022

Electrical Power Engineering

Thermal overloading of MV metal enclosed switchgear

Cecilie D. Gløsmyr

Faculty of Technology, Natural sciences and Maritime Sciences
Campus Porsgrunn

University of South-Eastern Norway

www.usn.no

Course: FMH606 Master's Thesis, 2022

Title: Thermal overloading of MV metal enclosed switchgear

Number of pages: 146

Keywords: MV switchgear, temperature rise tests, thermal model

Student: Cecilie D. Gløsmyr

Supervisor: Elin Fjeld

External partner: **ABB AS**

Summary:

Going electric is an important step toward a more environmentally friendly world by reducing greenhouse gases. Some electrical devices might be able to withstand a short-term overloading, which for example can be used for fast charging of batteries or vehicles. A MV switchgear is one of the devices which have the possibility to handle a short-term overloading, without exceeding the IEC temperature limits.

The objective for this thesis is to develop and implement a thermal model which predicts the temperature rise of a specific MV switchgear, based on defined subsystems. This can be used to determine the possible overload time when different currents are applied.

Real temperature rise tests with different applied currents are executed to gather data for development of the thermal model's parameters and for verification. Parameter values like thermal time constants, heat transfer coefficients, resistance and surface areas are determined. The thermal model is implemented in Python 3.7 where the simulated thermal model is compared to the real temperature rise measurements.

The thermal model is able to simulate the temperature rise of the system with changing accuracy for different test cases. When only the initial current is applied until steady state, the average error is less than 10%. In the overload cases, some adjustments are needed to predict accurate temperatures. When the thermal time constant is adjusted, the thermal model is able to predict the temperature rise of the subsystems with a deviation less than 10% compared to the real data. Based on the thermal model, possible overload times for different applied currents is determined and presented.

Preface

This master's thesis is the final work of a master's degree in electrical Power Engineering at USN campus Porsgrunn. The thesis is developed and written in spring of 2022.

The software used for this project are Agilent BenchLink Data Logger3, Geogebra, MS Excel, MS PowerPoint, MS Project, MS Word and Python 3.7.

I am very grateful for all help and guidance from my supervisor Elin Fjeld, thank you. I would also like to say thank you to the external partners from ABB AS for the cooperation. A final thanks goes to all my friends and family for supporting me throughout my studies.

Porsgrunn, May 7th, 2022.

Cecilie Dortea Gløsmyr

Contents

Nomenclature

AC	Alternating current
Ag	Silver
Al	Aluminum
BEM	Boundary Element Methods
CFD	Computational Fluid Dynamics
Cold resistance	Resistance at initial temperature
Cu	Copper
C1, C2, C3	Switchgear cable modules
DC	Direct current
EPE	Electrical Power Engineering
FEA	Finite Element Analysis
FEM	Finite Element Method
FDM	Finite Difference Method
GIS	Gas Insulated Switchgear
HV	High Voltage
IEC	International Electrotechnical Commission
IEEE	Institute of Electrical and Electronics Engineers
LBS	Load break switch
LPTM	Lumped-Parameter Thermal Model
L1, L2, L3	Current phases
MS	Microsoft
MV	Medium voltage (1kV – 33kV)
Ni	Nickle

NOG	Non-oxidating gas
N_2	Nitrogen
OG	Oxidating gas
RMU	Ring main unit
SF6	Svovelheksafluorid gas
Steady state temperature	Temperature rise less than 1˚K/hour
SW	Switchgear
TNM	Thermal Network Method
USN	University of South-Eastern Norway
V4	Vacuum switchgear breaker
Warm resistance	Resistance at steady state temperature
XLPE	Cable type

Symbols

a	Radius of a-spot	[m]
A	Area	[m^2]
A_{base}	Surface area of base of switchgear enclosure	[m^2]
A_{cs}	Cross section area	[m^2]
A_e	Effective cooling surface area	[m^2]
A_{LBS}	Surface area of LBS	[m^2]
A_{surf}	Surface area	[m^2]
$A_{surf,sw}$	Surface area of switchgear	[m^2]
A_{wall}	Area of wall	[m^2]
b	Factor for effective cooling surface area	[-]
c	Specific heat	[J/kg K]
c	Temperature distribution factor	[-]
C	Heat capacity	[J/kg]
d	Temperature rise factor	[-]
f	Compensation factor for surroundings	[-]
f_{base}	Base factor	[-]
f_{corr}	Correction factor	[-]
f_{view}	View factor	[-]
g	Gravity	[m/s^2]
Gr	Grashof number	[-]
h	Heat transfer coefficient	[W/m^2K]
h_{conv}	Heat transfer coefficient by convection	[W/m^2K]

h_{LBS}	Heat transfer coefficient for LBS	[W/m^{2}K]
h_{tot}	Total heat transfer coefficient	[W/m^{2}K]
$h_{tot,\ bare}$	Total heat transfer coefficient for bare LBS (no covering)	[W/m^{2}K]
h_{wall}	Total heat transfer coefficient for surface wall	[W/m^{2}K]
H	Height	[m]
H_{busbar}	Height of busbar	[m]
$H_{LBS,m}$	Height of middle part of LBS	[m]
$H_{LBS,u\&l}$	Height of upper and lower part of LBS	[m]
H_{SW}	Switchgear height	[m]
I	Current	[A]
k	Enclosure constant	[-]
l	Length	[m]
l_{busbar}	Length of busbar	[m]
$l_{LBS,m}$	Length of LBS middle part	[m]
$l_{LBS,u\&l}$	Length of upper and lower part of LBS	[m]
l_{SW}	Length of switchgear	[m]
M	mass	[kg]
Nu	Nusselt number	[-]
P	Power (loss)	[W]
P_{cond}	Power transfer by conduction	[W]
P_{conv}	Power transfer by convection	[W]
$P_{dissipated}$	Dissipated power	[W]
P_{in}	Input power	[W]
P_{LBS}	Power input for LBS calculations	[W]

$P_{LBS,in}$	Power input to LBS	[W]
$P_{LBS,out}$	Power loss from LBS	[W]
Pr	Prandtl number	[m^2/s]
P_{rad}	Power transfer by radiation	[W]
P_{room}	Power to the room outside the enclosure	[W]
P_{stored}	Stored power	[W]
$P_{wall,in}$	Power input to wall	[W]
$P_{wall,out}$	Power output from wall	[W]
R	Resistance	[Ω]
R_{bulk}	Bulk resistance	[Ω]
R_{cold}	Cold/ initial resistance	[Ω]
R_{cont}	Contact resistance	[Ω]
R_{ref}	Resistance at reference temperature	[Ω]
R_{warm}	Warm resistance	[Ω]
R_1	Resistance from measurements	[Ω]
R_2	Theoretical resistance	[Ω]
ΔR	Resistance change by temperature	[μΩ/˚C]
T	Temperature	[˚K] or [$^\circ C$]
T_{air}	Air temperature	[˚K] or [$^\circ C$]
T_{amb}	Ambient temperature	[˚K] or [$^\circ C$]
T_{cold}	Cold/ initial temperature	[˚K] or [$^\circ C$]
T_{LBS}	Temperature at LBS	[˚K] or [$^\circ C$]
T_{max}	Highest/max temperature	[˚K] or [$^\circ C$]
T_{ref}	Reference temperature	[˚K] or [$^\circ C$]

T_{room}	Room temperature	[°K] or [°C]
$T_{s, rad}$	Absolute temperature of hot surface	[°K] or [°C]
T_{surf}	Surface temperature	[°K] or [°C]
T_{wall}	Wall temperature	[°K] or [°C]
T_{warm}	Warm temperature	[°K] or [°C]
T_0	Initial temperature	[°K] or [°C]
$T_{0, rad}$	Temperature on surrounding, colder surface	[°K] or [°C]
T_τ	Temperature at time constant	[°K] or [°C]
ΔT	Temperature change/ deviation	[°K] or [°C]
ΔT_{air}	Temperature change of air inside SW enclosure	[°K] or [°C]
$\Delta T_{air, mid}$	Temperature change of air inside SW enclosure at mid height	[°K] or [°C]
$\Delta T_{air, top}$	Temperature change of air inside SW enclosure at top height	[°K] or [°C]
ΔT_e	Temperature change between initial and steady state	[°K] or [°C]
$\Delta T_{enclosure\ air}$	Temperature change for enclosure air	[°K] or [°C]
ΔT_{LBS}	LBS temperature change	[°K] or [°C]
$\Delta T_{outsde\ wall}$	temperature change on outside wall	[°K] or [°C]
ΔT_{room}	Temperature change of room temperature	[°K] or [°C]
$\Delta\Delta T_{LBS}$	Over-temperature of LBS	[°K] or [°C]
V	Volume	[m^3]
w	Width	[m]
w_{busbar}	Width busbar	[m]
$w_{LBS,m}$	Width LBS middle part	[m]
$w_{LBS,u\&l}$	Width LBS upper and lower part	[m]
w_{SW}	Width of switchgear	[m]

x	Exponent	[-]
α	Temperature coefficient	$[\frac{1}{[^\circ C]}]$
β	Thermal expansion coefficient $1/T_0$	[1/K]
γ	Density	[kg/m^3]
Δ	Change	[-]
ε	Emissivity	[-]
η	Kinematic viscosity	[m^2/s]
λ	Thermal conductivity	[W/mK]
μ	Dynamic viscosity	[kg/ms]
ρ	Specific resistance	[Ωm]
ρ_1, ρ_2	Metals resistivity, a-spot	[Ωm]
σ_s	Stefan Boltsmann's constant	[W/m^2K^4]
τ	Time constant	[-]

1 Introduction

Chapter 1 describes the background for this thesis work, previous work and published papers on temperature rise and distribution in switchgears. Further the objective and method for the thesis is presented, before an overview of the report structure.

1.1 Background

Electrical solutions and devices have become an important part of people's daily life. This have led to more and more research and development in the field of electro with focus on digitalization, optimalization and user friendliness. Going electric is also an important part of reducing emission of greenhouse gases and being more environmentally friendly. Different sectors are researching and developing new and better solutions where people's needs are meet in an environmentally friendly way.

New solutions can for example be explored within the field of electric vehicles, battery charging and storing. Fast charging of electrical devices is increasing in importance and the possibility of overloading an equipment for a short time period is a wanted step. Some electrical equipment may be able to handle a short-term overloading without exceeding the temperature limits on the device, which depends on the equipment's thermal time constant. This technology can also be used for fast charging of electrical vehicles, ferries and charging of high capacity batteries, which is useful in situations like road construction sites. It must be mentioned that this can result in intermittent, high power demand on the supply. [1]

A MV switchgear might have the possibility to be overloaded for a short time period by utilizing its thermal time constant. This can be an important step in avoiding the need of upgrading/renewing switchgears in substations. This is costly and leads to a negative impact on the environment by discarding working switchgears. Switchgears can be run at different operating currents and do not only operate at the nominal or rated current, instead they can have a changing loading curve. How long the system can be overloaded depends on the loading and the system devices. The temperature limits for the devices are a restrictive factor and can be used to determine how long the system can withstand an overload without any damage. Cables, transformers and other devices connected to a switchgear must also be included in the analyze of overload possibility. The transformer is not likely to be the most critical device when it comes to current overloading. Due to the transformers larger mass, the device can usually withstand a higher overload than the cables and the switchgear. The former master's thesis [2] explored the cables by creating a thermal model. In this thesis work, a MV switchgear system will be researched.

In this thesis, the focus will be on a MV switchgear test system to find the needed values for developing a simplified thermal model. The model will be used to predict and map how the switchgear can be run safely without getting a too high temperature, with and without overloading. The model parameters will be gathered by executing tests on a real system. The test results will also be used for verification of the thermal model.

1.2 Previous work

MV switchgear and temperature rise tests are well documented with published papers and manuals describing the system, the temperature rise test procedure, and results of temperature rise tests on different systems. A temperature rise test is executed on a system to ensure that the system or product doesn't get overheated during operation. For example how long a MV switchgear can be loaded with a given input current before reaching the individual equipment temperature limits according to IEC standards. [3] Published papers (like [4] and [5]) on temperature rise test on switchgears shows the results from different executed methods. Most of the methods are based on stationary models where the main purpose is to find the final temperature, instead of dynamic models where the entire progress is covered.

One of the most common procedures are development of a 3D model of the system to create a simulation of the temperature rise with different applied currents. Some examples of popular software and methods are CFD, TNM, SINTEF and COMSOL Multiphysics. These can be used to design systems and simulate a range of real-world scenarios based on methods like finite difference method (FDM) and finite element method (FEM). Examples are described in section 2.6.

Another common test is executing physical temperature rise tests on a specific switchgear. None of the published reports or papers (found for this thesis) experiments with overloading by a higher applied current than the nominal current for the system, but lower or changing currents are tested. [6] The paper [5] describes temperature rise tests executed on an overhead line switchgear without ventilation for the applied currents I = 4400A, 3150A, 2500A, 1600A, with ventilation for I = 3150A and 4400A and with one phase set to zero for I = 4400A. Another paper [7] describes 15 different temperature rise test cases. For development of the dynamic model and not only 3D model development or stationary model description, the paper [4] explore the mathematic development in more details.

Included in the program for Electrical Power Engineering at USN campus Porsgrunn, laboratory work on a metal enclosed MV switchgear is performed. Procedures from these labs (temperature rise tests and resistance measurements) are used for this thesis. Previous master's theses have also been performed with different relevance to this particular thesis. Looking at the previous work done in these theses have been invaluable. Especially the master's theses [2] and [8]. These theses have granted me great inspiration for my own work.

The thesis in [2] have many of the same objectives as this thesis. It develops a thermal model for two types of cables based on temperature rise tests and calculated parameters. Due to the cables being a more homogenous system with a common structure (inside and outside part of the cable) and setup, the model is more diverse and can be adjusted easier to fit other cable systems. The MV switchgear system is more complicated. How the subsystems and measurement points are defined have a large effect on the results. The calculation of parameter values are not as straight forward as for the cable system, due to the many equipment inside the switchgear enclosure and how the heat transfer does not flow homogenous inside the system. This makes it more difficult to determine for example ideal measurement location and how the resistance changes. Finding reasonable parameter values to use in the thermal model will be a larger part of this thesis work and the parameter values will not be as flexible for other switchgear system. Most likely the parameter values

calculated here, is only valid for this specific MV switchgear. However, the methods and approaches can be used for other systems.

1.3 Objective

The objective of this thesis is to develop a simplified thermal model describing the temperature rise of the tested MV metal enclosed switchgear. The MV switchgear is specially adjusted for use at USN campus Porsgrunn and the thermal model is developed in Python 3.7. Temperature rise rests with different applied currents is performed on a real lab model to determine the needed parameters for the development of the thermal model. This includes fixed parameters like surface area, and parameters which changes with increasing temperature like resistance, heat transfer coefficient and time constant.

A further goal is to verify the model and determine possible overload times for different overload profiles. The verification of the thermal model is shown by simulating the actual temperature rise of the different cases vs the simulated temperature rise based on the thermal model. A goal is also to be able to present the possible overload time for different applied overload currents based on the thermal model.

1.4 Method

First a literature study is performed where the main goal is to gather information, published reports and papers describing temperature rise tests on a similar test system. Further is to look into published results of experiments executed with changing current and overload currents. Then, different temperature rise tests and resistance tests are executed on the real test system at the high current lab. This is done in parallel with development of the simplified thermal model. This development includes data collection, creating the mathematical equations and parameters. The model which simulates the temperature rise, is than implemented in Python programs. The data from the temperature rise test is exported to Python for comparison with the simulated result of the thermal model. Based on the simulations, the average error between the actual temperature rise and the simulated temperature rise is calculated to analyze the thermal model's accuracy. Some adjustments is made to increase the accuracy. Finally, an overview of possible overload times is created based on the thermal model.

1.5 Report structure

The report structure for this report is listed below.

- Ch 1: Introduction
- Ch 2: Theory
- Ch 3: System description and equipment
- Ch 4: Resistance test
- Ch 5: Steady state temperature rise tests
- Ch 6: Thermal model of MV switchgear
- Ch 7: Short duration overload test
- Ch 8: Data simulation
- Ch 9: Discussion

- Ch 10: Conclusion and future work
- References
- Appendices

2 Theory

This chapter includes theory about MV switchgear, heat generation in MV switchgear, thermal energy balance and heat transfer mechanism. Further it describes the calculations of the temperature rise tests in MV switchgear and LBS, given temperature limits, and lastly an introduction to a selection of 3D model simulation software's for further work in this field.

2.1 MV switchgear design

The main purpose of the switchgear is to protect, control and isolate electrical equipment. It usually consists of circuit breakers, fuses and switches connected by metal structure inside a metal enclosure. A common place to find switchgears are in industrial factories and throughout electric utility distribution and transmission systems. The switchgear's work process can vary based on the type of device, but a basic switchgear will act by interrupting the power flow to protect the equipment inside the enclosure from damage when an electric fault happens. [9] [10]

Three main switchgear classes are low-voltage switchgear, medium-voltage switchgear and high-voltage switchgear based on the voltage rating of the system.

- Low-voltage switchgear controls up to 1kV power.
- Medium-voltage switchgears controls between 1kV and 75kV power
- High-voltage switchgear controls power of 75kV or higher

The isolating media used to protect the energized switchgear from electrical fault is also used to classify the switchgear. Some examples of isolating media are air, gas, oil, fluid and solid. Some medium-voltage switchgears on the market today are gas-insulated switchgear, Air insulated switchgear, metal-clad switchgear, Pad-mounted switchgear, Vault or subsurface switchgear and Arc resistance switchgear. The gas-insulated switchgear (GIS) is sealed and filled with SF6 gas or more environmentally friendly gases like some fluorinated gas mixtures. [11] [12] The air insulated switchgear is not hermetically sealed as the GIS, but uses ventilation for dissipating heat. [13] [14] Figure 2.1 shows an example of metal clad, air insulated switchgear. [15] Figure 2.2 shows a MV gas-insulated switchgear. [16]

Figure 2.1: Metal clad switchgear. [15]

Figure 2.2: MV gas-insulated switchgear. [16]

2.2 Heat generation in MV switchgear

Heat generation in electrical equipment is mainly from the ohmic losses (often called copper losses) in the current path. The ohmic losses can be explained by the phenomena called Joule/ resistive heating. When the electrons of an electric current flows through an ironic lattice, the electrons collide with the lattice's ions. In each collision, some of the current's energy is absorbed by the lattice and converted into heat, which dissipates. Another possible source of heat generation is from iron losses. Iron loss appears due to the effect of eddy current losses and hysteresis losses when a magnetic field changes directional orientation in a ferromagnetic structure. The iron losses depend on the properties of the material (like magnetization) and the frequency of the current, and are more present in magnetic elements like iron. In this thesis, it is assumed only the ohmic losses are present. [17] [18] [19]

The main problem with heat generation, is the possibility that the device or equipment can't withstand the temperature. If the temperature increases over the equipment temperature limit, the equipment is in risk of malfunction, degradation of quality or failing entirely.

During normal operation of the MV switchgear, current is applied to the system. Due to ohmic losses in the equipment of the switchgear, like the conductors and contacts, a temperature rise is present. The main heat source is the power loss P caused by the mentioned ohmic resistance R when current I flows. The relationship is shown in Equation (2.1). [17]

$$P = RI^2 \tag{2.1}$$

Here I is the applied current and R is the total resistance of the current path. Based on Ohm's law it can be observed that the current value has an impact on the resulting power. Since the main heat source is the power loss P, the chosen applied current will be the largest factor defining the amount of generated heat. The resistance will also contribute. The total resistance R is the sum of the bulk resistance and the contact resistance. As shown in Equation (2.2) for a conductor. [17]

$$R = R_{bulk} + R_{cont} \tag{2.2}$$

The bulk resistance of the conductor R_{bulk} depends on the temperature, so it changes with increasing or decreasing temperature. The equation for R_{bulk} is shown in Equation (2.3). [20]

$$R_{bulk} = \rho * \frac{l}{A_{cs}}(1 + \alpha \Delta T) \tag{2.3}$$

Where ρ is specific resistance, A_{cs} is the cross-sectional area of the conductor, l is the length, α is the temperature coefficient and ΔT is the temperature difference. In a conductor, the effective area A_{cs} might be reduced by proximity and skin effect.

The value of the contact resistance R_{cont} depends on the surface between the contacts. The surface might not be uniform and instead have a rough surface, resulting in only direct contact in some spots (called a-spots). The contact resistance depends also on the connection force. A larger connection force result in a larger connection area and a higher temperature, which lead to a higher resistance. The value of the contact resistance is not calculated, but instead measured or estimated. [17]

2.2.1 Resistance increases due to temperature rise

The resistance depends on the conductor geometry and temperature. When electrons flow through a conductor (current flow is present), the electrons are hindered by moving/bouncing atoms and molecules within the conduct. With higher temperature, the atoms and molecules moves/bounces more within the object which makes it harder for the electrons to flow through without hitting any atom/ molecule. Resistance describes the difficulty for current to flow through the object. This means that with a higher temperature, it gets harder for the current to flow through the object, which is described by a higher resistance.

Heat is generated and the temperature increases when an electrical system is under operation, which increases the resistance of the system. The resistance of an electrical conductor is affected by this temperature difference as shown in Equation (2.4).

$$R_{warm} = R_{cold}(1 + \alpha(T_{warm} - T_{cold})) \quad (2.4)$$

Where R_{warm} is the resistance of the warm conductor, R_{cold} is the resistance of the cold conductor, α is the temperature coefficient, T_{warm} is the warm temperature and T_{cold} is the cold temperature. [17]

2.2.2 Skin effect

The skin effect changes the distribution of the current flow through a conductor. This happens because of changing magnetic fields (from eddy currents) when AC current flows through a conductor. When DC current flows, the current flows evenly distributed through the conductor. This is not the case for AC current. Most of the current flows near the conductor surface (or skin) and less in the center as shown in Figure 2.3.

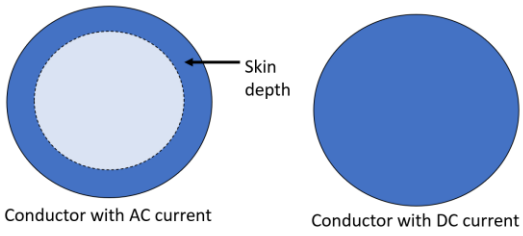

Figure 2.3: Current distribution through conductor with AC and DC current showing the skin effect.

The skin effect results in a smaller effective cross section area since mostly the outer part has current flowing through. Since the skin effect is caused by changing magnetic fields, the effect depends on the frequency of the current. For lower frequencies, the skin effect is higher. The properties (specific resistance and magnetic permeability) of the conductor materials will affect the size of the skin depth. [17]

From the former master's thesis [8] the contribution of the skin effect in LBS are considered when power is applied to the tested system (conductors in MV Switchgear). Based on the result from this thesis, the skin effect and also the proximity effect in MV switchgear system can be neglected [8] [21].

2.2.3 Proximity effect

When more than one conductor is present, the current flowing through the conductors can affect each other. First, for one conductor the skin effect can happen when AC current flows due to the changing magnetic field. Meaning the current flow mainly in the skin of the conductor. With for instance two conductors next to each other the current distribution in the conductors might again be influenced based on the layout. The magnetic field surrounding the conductors will induce eddy currents in the other conductor. This changes the distribution of the current flow. If the current in the two conductors flows in the same direction, most of the current will flow at the side of the conductors farthest away from each other. If the current in the two conductors flow in opposite directions, most of the current will flow at the side of the conductor which faces each other. Figure 2.4 shows the proximity effect when the AC current flows in the same and opposite direction.

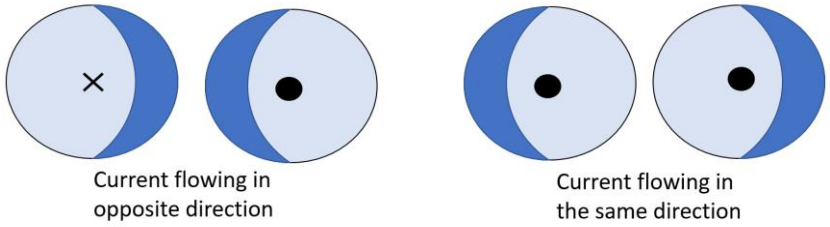

Figure 2.4: Proximity effect for current flowing in opposite and same direction.

Some challenges with the proximity effect are the reduced cross-section area leading to increased resistance and higher power loss. The effect also leads to increased frequency. The strength of the proximity effect depends on the distance between the parallel conductors, which become stronger the smaller the distance is. [17]

2.2.4 Contact type

An electrical contact is a device that creates an electrical connection between two members or surfaces. The contacts can be used to either ensure or interrupt a current flow, and the contact is open when the members are not connected. Anode is the member where the positive current enter, and cathode is the member where the current exits. Some of the challenges with contacts are changes in contact resistance, temperature, load, deformation and degradation.

Two of the main categories electrical contacts can be divided into are stationary and moving contacts. Stationary contacts have their members or connection surfaces permanently connected, while moving contacts have one or more moving member. Figure 2.5 shows an overview of the contact types. [20] [22]

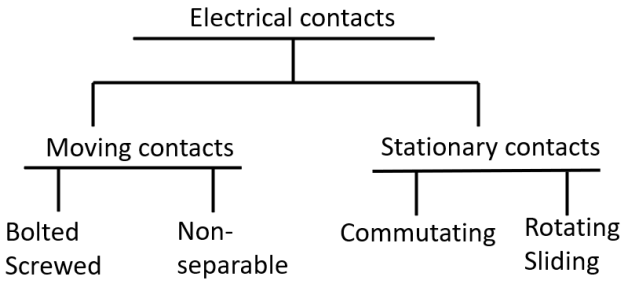

Figure 2.5: Overview of electrical contact categories.

Stationary contacts:

The stationary contacts can again be divided into bolted (or screwed) contacts and non-separable contacts (also called all-metal contacts). The bolted or screwed contacts have the conductors permanently connected by bolts, screws or clamps. This makes it possible to remove the bolt or screws when needed, without any damage to the contact. The bolted contacts, which uses clamps, have an interface (like a clamp plate, plastic) between the contact surfaces. This makes the clamped contacts functionality dependent on the contact pressure and resistance to plastic deformation. The non-separable contacts connect the members permanently together as well. These contacts are often within one contact member, have a high mechanical strength, direct contact and low transition resistance. [20] [22]

Moving contacts:

Moving contacts have one or more moving member and are divided into commutating contacts or sliding and rotating contacts. Commutating contacts are divided into separable and breaking. The separable contacts are different plug connectors, while breaking contacts are used for opening and closing an electric circuit. For sliding or rotating contacts, the connecting surfaces of the conductors slides over each other. This happens without the contact surfaces separating. Sliding and rotating contacts are often found in switches and circuit breakers. [20] [22]

2.2.5 a-spots and contact resistance

The surfaces where the contact parts of an electrical contact connect are not entirely even or flat. Instead, the connecting surfaces are more ruff with only small areas of actual metal to metal connection between the connecting surfaces. These areas are called a-spots as shown in Figure 2.6. The transferring current flows through the a-spots, which is the only conducting part. This decreases the active contact area, the passage for the current and the contact resistance. [20] [22]

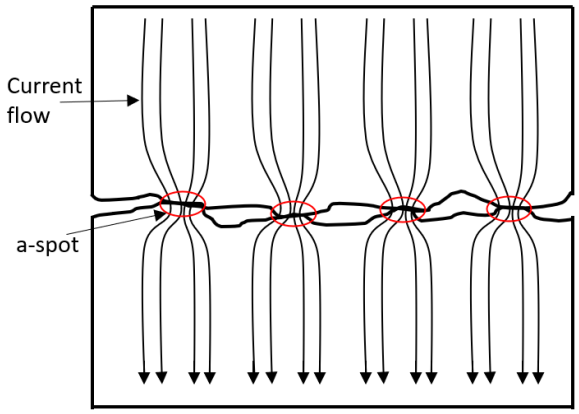

Figure 2.6: a-spot.

Construction resistance R_s is the electrical resistance of the contact, based on the restrictive current flow through the a-spots. For one a-spot the construction resistance is shown in Equation (2.5). [20]

$$R_s = \frac{\rho_1 - \rho_2}{4a} \tag{2.5}$$

Where ρ_1 and ρ_2 are the metals resistivity and a is the a-spots radius.

Film resistance is the resistance due to the metals surface not being clean. Instead, a thin layer of inorganic film (like oxide or sulphide) is located on the metals surface affecting the contacts resistance. This results in only part of the surface area connecting with its metallic surface, leading to a smaller effective surface area and increases the contact resistance.

The total contact resistance of a joint is the contact resistances added together with the resistance of the film, which usually only has a small contribution. Due to factors like changes in real contact area, pressure and resistive film, the contact resistance may vary or change. [20] [22]

When performing measurements on contact resistance, it will often be a deviation from the actual value due to not knowing where all the a-spots are located. The resistance at the a-spots is called constriction resistance. Even if all a-spots are known, it will still be a small distance between the measuring probes and the spots. The constriction resistance can be calculated or measured. If the measured construction resistance is higher than the calculated resistance, it often implies that the surface area is covered in film (which adds the additional resistance). Usually, the measurement of a contact is placed over the total surface area and includes more than only the a-spots. This effects the measured resistance and lower the accuracy. [22]

The contact resistance is also affected by temperature. The inflowing current heats up the contacts. The highest temperature is located at the contact surface, if the contact members consist of the same material. The temperature lowers, the longer away it gets from this area. The constriction resistance increases with a factor a little less than (1+αb) where α is the temperature coefficient of the resistivity and b is the temperature at the hottest point in the contact surface (above the bulk of the surface members). The factor would be exactly (1+αb) if the temperature was uniformly distributed. The resistance of the constriction has a factor

given as (1+2/3αb) where b is the max temperature. The same problems occur when determining these resistances as mentioned in the previous section. [22]

The voltage is of importance when determining the resistance and for security reason. It can be used to determine the melting point and boiling point of the contact to avoid any deformation, damage or risks. The melting point is the temperature at which the contact or metal in contact starts to "melt". Which in real life means deform due to the high temperature. This can happen when the applied power (or current) is increased. This can lead to a higher contact area and usually a small voltage drop. The deformation of the contact can also affect the contact's functionality. If the temperature gets higher than the melting point, the boiling point can be reached, usually at 0.8V for copper. A danger with reaching this high of a temperature can for example be explained by an open/ close contact. If the boiling point is reached as the contacts opens, an arc might be ignited (with an arc voltage between 10-15V) and the boiling can appear like an explosion. [22]

Another important factor which can have an effect is the torque. If connections or terminals are screwed together with wrong torque, it can lead to a run-away effect and electrical fires, contactor failures or phase loss which can for example cause motor damage. Electrical fire is a possible result of loose connections. The loose connection between the surfaces can lead to a run-away effect where the temperature keeps increasing and can end up resulting in an electric fire. In the case of an improper torque on for example only one of three phases, it can lead to the contactor burning up and resulting in a phase imbalance. This can lead too loss off one phase, resulting in only two phases working at a higher current than designed for. This can cause temperature damages or failure (reaching example melting point). Phase loss can also damage connection devices like the motor, if not proper protection is installed or the problem is not solved in time (immediately) [23].

2.3 Thermodynamics

The mathematics of the general thermal energy balance is presented first in this subchapter. The method for finding the final temperature in a temperature rise test of an MV switchgear based on the thermal energy balance is than presented. Then the heat transfer mechanism in the MV switchgear (conduction, convection and radiation) is described, the temperature limits of the MV switchgear and the method for finding the final temperature of the LBS in a temperature rise test. The last part describes different possible simulation software's that can be used for temperature simulations. [18] [24] [25]

2.3.1 Thermal energy balance

The thermal energy balance is part of the thermal analysis where one of the main goals are to determine how long a system can be loaded and still be within the equipment temperature limits. In the switchgear system the thermal energy balance describes the heat or energy dissipation during the runtime.

During the runtime when current is applied to the system, the power is either stored in the materials or lost as heat to the surroundings. In the power loss balance, the input power (P_{in}) to the system is equal a combination of the stored power (P_{stored}) in the materials/ equipment and the dissipated power ($P_{dissipated}$). The relationship is shown in Equation (2.6). [25]

$$P_{in} = P_{stored} + P_{dissipated} \tag{2.6}$$

The constant power input can be described as shown in Equation (2.7). [17]

$$P_{in} = RI^2 = \rho \frac{l}{A_{cs}} I^2 \tag{2.7}$$

Where R is resistance, I is current, ρ is resistivity, l is length and A_{cs} is the area of the cross-section. Equation (2.8) shows the power stored in the system. [25]

$$P_{stored} = c\gamma V \frac{d}{dt} \Delta T \tag{2.8}$$

Here c is the specific heat capacity and describes the materials ability to store heat, γ is density, V is volume and $\frac{d}{dt}\Delta T$ describes the change of temperature per time. The simplified dissipated heat or energy to the environment/ surroundings per second is shown in Equation (2.9). [25]

$$P_{dissipated} = hA_{surf}\Delta T \tag{2.9}$$

h is the heat transfer coefficient and A_{surf} is the area surface. Based on Equation (2.6), (2.7), (2.8) and (2.9). the power balance can be written as shown in Equation (2.10). [25]

$$\rho \frac{l}{A_{cs}} I^2 = c\gamma V \frac{d}{dt} \Delta T + hA_{surf}\Delta T \tag{2.10}$$

Thermal time constant:

The temperature rise can be calculated based on the energy (power) balance by solving the differential Equation (2.10), which result in Equation (2.11). [25]

$$\Delta T(t) = \Delta T_e(1 - e^{-t/\tau}) \tag{2.11}$$

Where ΔT_e is the temperature change between initial and final/ steady state temperature and τ is the thermal time constant. The time constant is the time it takes the system to reach 63.2% of the final, steady state temperature and are a feature of the lumped system analysis for thermal systems [26]. It can be used as an indication for how long the system can be overloaded (short term) without overheating it. For heavier (larger mass) systems, the time constant is longer/ higher. This means that the system can be overloaded for a longer time period, than for lower mass systems. A system with very low mass is not recommended to be overloaded. Equation (2.12) defines the time constant. [25]

$$\tau = \frac{cM}{hA_{surf}} = \frac{c\gamma V}{hA_{surf}} \tag{2.12}$$

Where M is mass, c is heat capacities, γ is density, h is the heat transfer coefficient and A_{surf} is the surface area. In the equation, cγV describes the thermal storage capacity and hA_{suft} describes the thermal dissipation capacity. The mass, density, volume and surface area are

usually fixed values. In for example a temperature rise, the parameters c and h are temperature dependent, which also makes τ temperature dependent.

If the time constant is positive, it indicates that the device is warmer than the ambient temperature. A higher heat capacity c leads to slower temperature changes, which leads to a longer (higher value) time constant. The heat capacity c is dependent on temperature change, where a higher temperature result in a lower c. The heat transfer coefficient h is dependent on the power input, the temperature deviation and the surface area. It changes with changing values for the input power and temperature deviation, assuming a fixed surface area. If the temperature increases, the heat transfer coefficient decreases. If the power input increases, the heat transfer coefficient increases. This connection is based on the heat transfer coefficient equation described in Equation (2.13). For the time constant, this result in the connection that increasing temperature gives a lower heat transfer coefficient which lower the time constant. [25]

Heat transfer coefficient:

The heat transfer coefficient h (by convection) of an enclosed switchgear without ventilation can be calculated by use of Equation (2.9) for temperature rise inside the enclosure. The rewriting will give Equation (2.13). [25]

$$h = \frac{P}{\Delta T * A_{surf}} \tag{2.13}$$

P is power dissipation in the enclosure, ΔT is the average temperature rise inside the enclosure and A is the surface area of the heat dissipation surface. This equation assumes a linear heat transfer process where radiation is neglected. Since the radiation is highly temperature dependent, it will most typically be a part of cooling the switchgear down. [27]

2.3.2 Thermal energy balance for finding final temperature in MV switchgear

The thermal energy balance can be used to determine the temperature rise in an MV switchgear. The change of temperature can be described by the dynamic state, the transition state and the stationary state. This procedure is used when determining the final temperatures of the system and not the temperature change every time step.

The dynamic state is the first state right after the current is applied and the system starts to heat up. In this initial state, the system has adiabatic conditions meaning all of the heat is stored in the system. The relationship is shown in Equation (2.14). [25]

$$P_{in} = P_{stored} \tag{2.14}$$

A complication is the possibility of an asymmetric short circuit current which can generate more heat than a symmetric short circuit current if the clearing time is short and the damping factor is small. In the simplified model, this possibility is excluded, and constant rms-value of fault current is assumed instead. In the transition from adiabatic conditions to stationary conditions, the power balance can be described as shown in Equation (2.15). [25]

$$P_{in} = P_{stored} + P_{dissipated} \tag{2.15}$$

The stationary phase starts when the temperatures are considered stable, and all the heat dissipates to the surroundings. The system is defined stable according to IEC in Equation (2.16) when:

$$\frac{d}{dt}\Delta T < 1K/hour \tag{2.16}$$

Equation (2.17) shows the relationship for the stationary phase where all the heat goes to the surroundings. [25]

$$P_{in} = P_{dissipated} \tag{2.17}$$

2.3.3 Heat transfer mechanisms in metal enclosed switchgear

During normal operations, a temperature increase on the current path inside the switchgear occurs due to ohmic losses (joule heating). The temperature difference between the hotter current path and the surroundings creates the heat transfer. The heat transfer mechanisms present are convection, radiation and conduction. [19] [24] [28]

Conduction:

Conduction is energy transfer caused by motion and interaction of molecules or atoms in an object. For the switchgear system, the conduction even out the temperature on the current path by transferring the heat from the hot spots to colder parts. For example, from contact to busbar. Conduction is also present in the heat transfer across the enclosure walls, unless the switchgear is hermetically sealed. The conductivity varies by temperature change if the material is gas or liquid. In solids, varied temperatures do not change the conductivity notable. Power transferred by 1 dimensional conduction is given in Equation (2.18). [24]

$$P_{cond} = \frac{\lambda}{l} A_{cs} \Delta T \tag{2.18}$$

Here λ is thermal conductivity, l is length, A_{cs} is cross-sectional area and ΔT is temperature difference. Figure 2.7 shows a model of conduction on a switch where the warmest point (hot spot) is the upper part of the contact. The heat will flow from this hotspot toward the busbar and lower part of the contact. This will distribute the heat from the hot spot within the physical devices which result in more heat along the current path. [24]

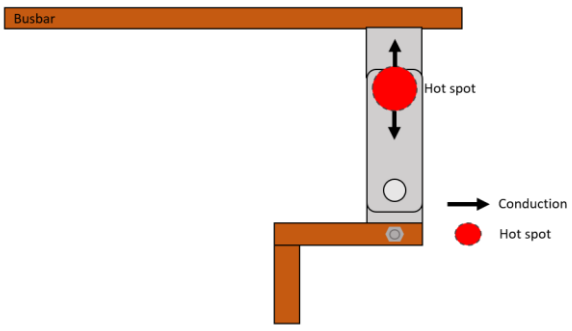

Figure 2.7: Model of conduction from a hot spot (contact) in a current path.

Convection:

Convection is energy transfer of heat from a warm area to a colder area inside an object or between them. In the case with a switchgear, convection is the heat transfer from the warmer current path to the gas inside the enclosure as shown in Figure 2.8. The heat is transferred to inner walls from convective movements of the gas caused by Buoyancy. Equation (2.19) shows the power transferred by convection P_{conv}. [24]

$$P_{conv} = hA_{surf}(T_{surf} - T_0) \tag{2.19}$$

Where A_{surf} is the surface area, T_{surf} is temperature at the surface and T_0 is the temperature of the surrounding medium. h is the heat transfer coefficient which depend on the type of fluid and the fluid velocity. In the switchgear the velocity is caused by natural/free convection and are usually between 5-10W/m^{2}K, but varies for different areas inside the switchgear. The convective heat transfer coefficient can be calculated as shown in Equation (2.20) [24].

$$h_{conv} = \frac{Nu * \lambda}{l} \tag{2.20}$$

Nu is Nusselt number which is given in Equation (2.21), λ is the thermal conductivity of the medium and l is the length. [24]

$$Nu = 0.53(Gr * Pr)^{0.25} \tag{2.21}$$

Gr is Grashof number and Pr is Prantl number. The formula for Granhofs number is shown in Equation (2.22) below. [24]

$$Gr = \frac{gl^3\beta(T_{warm} - T_{air})}{\eta^2} \tag{2.22}$$

Here g is gravity, l ins length, β is the thermal expansion coefficient, T_{warm} is the temperature of the hot surface area, T_{air} is the air temperature and η is the kinematic viscosity (of air) at 325K. Equation (2.23) gives Prantl number Pr. [24]

$$Pr = \frac{\mu c}{\lambda} \tag{2.23}$$

Where μ is dynamic viscosity, c is specific heat coefficient and λ is thermal conductivity.

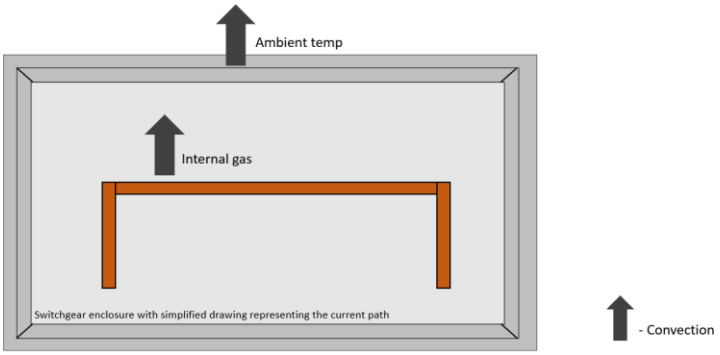

Figure 2.8: Representation of convection in the simplified switchgear enclosure model.

Radiation:

Radiation is energy transfer from absorption and emission of electromagnetic waves and do not need a medium for the transfer, meaning radiation can occur in vacuum. In the switchgear system, the energy is transferred by radiation to the inner walls from devices inside the enclosure with a higher temperature (overtemperature) as shown in Figure 2.9. Power transferred by radiation is given in Equation (2.24). [24]

$$P_{rad} = \varepsilon \sigma_s A_{surf} (T_{s,rad}^4 - T_{0,rad}^4) \tag{2.24}$$

Here ε is emissivity of the surface area, σ_s is the Stefan-Boltzman which is $5.67 * 10^{-8} W/m^2K^4$, A_{surf} is the surface area where the radiation emits from with temperature T_s and T_0 is the temperature at the larger, colder surface around where the radiation emits to. [23] The emissivity might change by time and depends on factors like oxidation. The emissivity is 1 for a black body, around 0.05-0.0025 for aluminum, 0.02 for polished copper and 0.065 for oxidized copper. The view factor is not included in Equation (2.24). The view factor is how the hot body views the surrounding and is usually between 0.7 and 0.9 in a MV switchgear. Adding the view factor to Equation (2.24) gives Equation (2.25). [24] [29] [30] [31]

$$P_{rad} = \varepsilon f_{view} \sigma_s A_{surf} (T_{s,rad}^4 - T_{0,rad}^4) \tag{2.25}$$

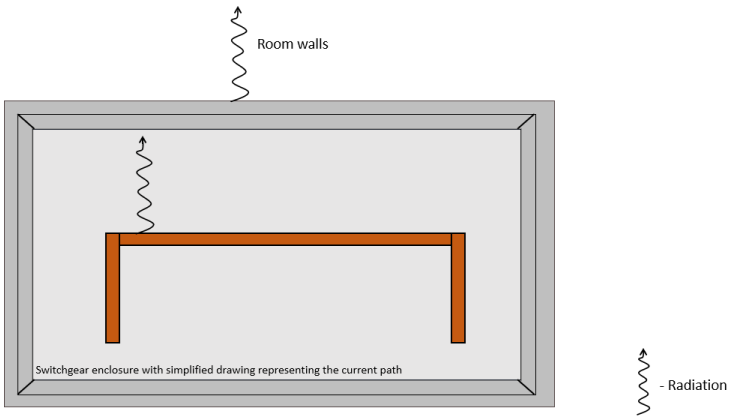

Figure 2.9: Representation of radiation in the simplified switchgear enclosure model.

Figure 2.10 shows a representation of the heat transfer inside and outside a sealed enclosed switchgear.

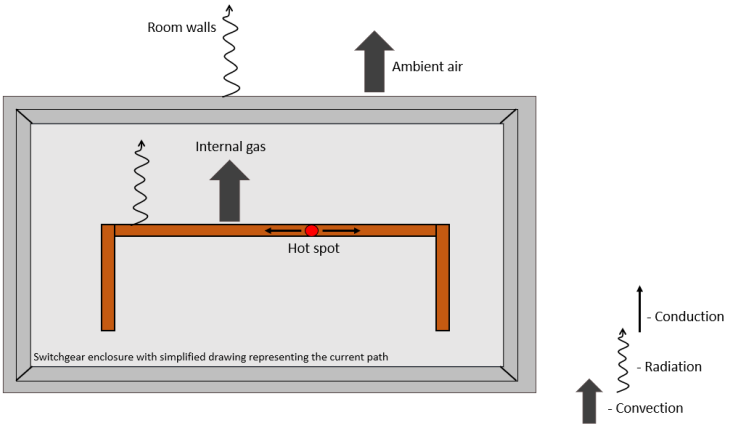

Figure 2.10: Representation of conduction, convection and radiation in the simplified switchgear model.

If parts of the current path are covered:

The transmission and distribution of convection, conduction and radiation will vary if parts of the current path are covered. The covering can be insulation around a switch, something covering parts of the busbar etc. This can prevent or reduce radiation and convection transfer from warmer spots, which can lead to a larger conduction from compensation. Figure 2.11 shows the model with and without covering around a switch. Covering can also change the measurement of the surface area of an equipment. [19]

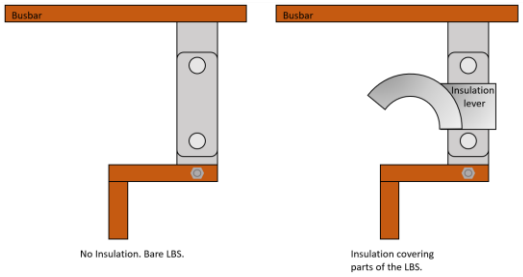

Figure 2.11: LBS model without and with insulation lever for visualization.

2.4 Temperature limits

To not damage the equipment from overheating, temperature limits are developed according to IEC standard. The temperature limits depend on the surrounding gas, the conduction material and the type of contact present.

Degradation is one of the possible damages from temperature. The degradation is faster with higher temperatures. Oxidation is one of the degradation mechanisms where the metal surface is exposed to oxygen and an electrolyte (example moisture from the air). The reaction can lead to corrosion on the metal surface, which is unwanted and can lead to malfunction. [32] The temperature limit will therefore depend on the surrounding gas and the devices material. The temperature limit for the contacts is also based on the type of contact. For example,

bolted contacts withstand often a higher pressure than spring loaded contacts (like open/close contacts). For the contacts, the temperature limits are also created based on a possible run-away effect. The contacts often end up being the warmest point in the current path. In the case of degradation, the contact resistance might increase, which makes the contacts warmer and again increases the resistance in a run-away effect.

The relevant temperature limits for HV and MV switchgear are shown in Figure 2.12 based on IEC standard. The first column with “Temperature” shows the maximum temperature for the contact or connection. The second column with “The temperature rise at ambient temperature of 40˚C” describes the maximum temperature rise or temperature deviation the contact or connection can have. The limits are developed based on an ambient room temperature not exceeding 40˚C. [3]

Nature of the part, of the material and of the dielectric (Refer to points 1, 2 and 3 in 7.5.6.2) (Refer to NOTE 1)	Maximum value	
	Temperature °C	Temperature rise at ambient air temperature not exceeding 40 °C (NOTE 2) K
1 Contacts (refer to point 4)		
Bare-copper or bare-copper alloy		
– in OG (refer to point 5)	75	35
– in NOG (refer to point 5)	115	75
– in oil	80	40
Silver-coated or nickel-coated (refer to point 6)		
– in OG (refer to point 5)	115	75
– in NOG (refer to point 5)	115	75
– in oil	90	50
Tin-coated (refer to point 6)		
– in OG (refer to point 5)	90	50
– in NOG (refer to point 5)	90	50
– in oil	90	50
2 Connection, bolted or the equivalent (refer to point 4)		
Bare-copper, bare-copper alloy or bare-aluminium alloy		
– in OG (refer to point 5)	100	60
– in NOG (refer to point 5)	115	75
– in oil	100	60
Silver-coated or nickel-coated (refer to point 6)		
– in OG (refer to point 5)	115	75
– in NOG (refer to point 5)	115	75
– in oil	100	60
Tin-coated		
– in OG (refer to point 5)	105	65
– in NOG (refer to point 5)	105	65
– in oil	100	60

Figure 2.12: IEC 62271-1 (2017): HV and MV switchgear temperature limits selection. [3]

OG stands for oxidating gas, NOG is non-oxidating gas. Further in this report the materials for copper, silver and nickel will be expressed by their elements name Cu, Ag and Ni.

2.5 Final temperature of the LBS in a temperature rise test

For the purpose of estimating how long the system can be overloaded without reaching the temperature limits of any of the equipment inside the switchgear, the most critical equipment from temperature rise is the main focus, instead of the entire switchgear. For the switchgear, the LBS has most often the highest/ fastest temperature rise (compared to its limit) and reaches its temperature limits first. Therefore, the temperature rise of the LBS can often be used for estimation of the highest temperatures. The temperature distribution of the LBS is not uniform and consists of the rotating contact, the open/close contact, and the connection points.

First the temperature rise of the air ΔT_{air} inside the switchgear can be estimated by using the method described in the following chapter. Then the over-temperature of the LBS contacts $\Delta\Delta T_{LBS}$ can be estimated and the temperature rise of the open/close contact ΔT_{LBS} can be calculated. Equation (2.26) shows the relationship. [33]

$$\Delta T_{LBS} = \Delta T_{air} + \Delta\Delta T_{LBS} \tag{2.26}$$

Temperature rise calculations - ΔT_{air}:

The procedure described in [33] can be used to determine the temperature rise of the air inside switchgear without forced ventilation. The method is based on calculating the temperature rise of the air in the top part and middle part of the switchgear. Equation (2.27) shows the temperature at mid heigh. [33] [34]

$$\Delta T_{air,mid} = k * d * P^{x} \tag{2.27}$$

Here k is the enclosure constant, d is the temperature rise factor, P is the power input and x is given as 0.804 for enclosure without ventilation openings. [34]. The enclosure constant depends on the effective cooling surface and the temperature rise factor depends on the number of horizontal partitions inside the enclosure. The temperature rise near the top is given in Equation (2.28). [33] [34]

$$\Delta T_{air,top} = c * \Delta T_{air,mid} \tag{2.28}$$

Where c is the temperature distribution factor depending on the heigh/ base factor f. The enclosure constant k is found by calculating the effective cooling surface area A_e and from the plot in Figure 2.13 finding the responding k value. Equation (2.29) shows the effective cooling surface area. [33] [34]

$$A_e = \sum A_{surf} * b \tag{2.29}$$

Here each of the surface areas A_{surf} of the enclosure is multiplied together with the b factor. The b factor corresponds to the different heat transfers for the different surfaces and whether the surface area is exposed or not. Table 2.1 shows some relevant b factor values. [34]

Table 2.1: b factors for calculating the effective cooling surface area of a switchgear. [34]

Surface:	**b**
Exposed top surface	1.4
Covered back wall	0.5
Covered side wall	0.5
Exposed front wall	0.9
Bottom	0

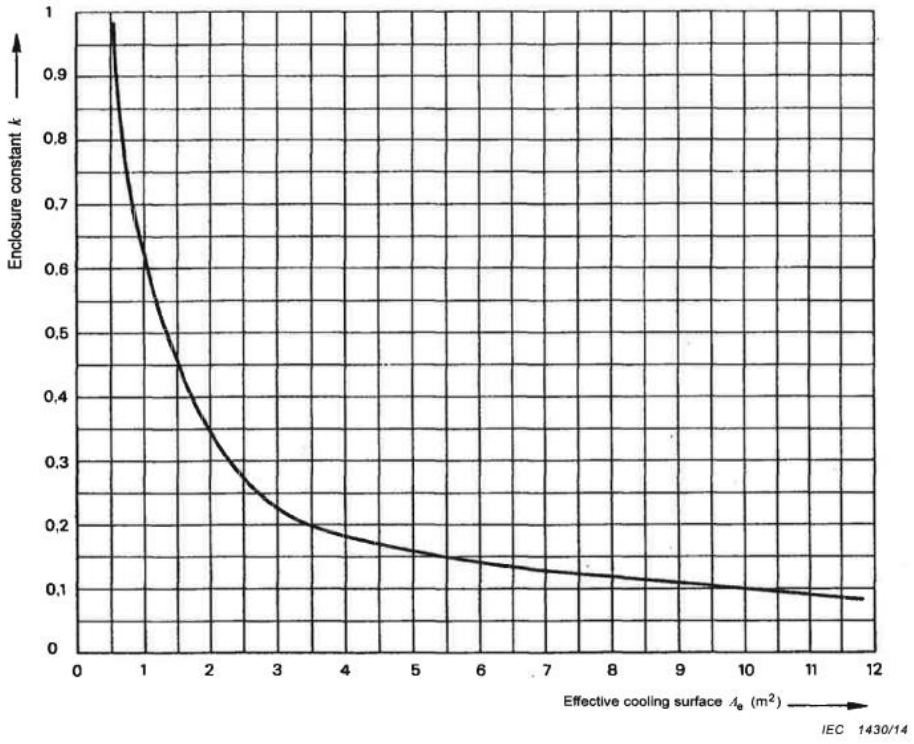

Figure 2.13: Enclosure constant k based on the effective cooling surface area A_e when $A_e > 1.25m^2$, IEC 1430/14. [34]

The temperature rise factor d for internal horizontal partitions is decided based on the number of horizontal partitions in the enclosure. In this switchgear, there is none horizontal partitions which gives d = 1. The temperature distribution factor c depends on the height/ base factor f_{base} as shown in Equation (2.30). [33] [34]

$$f_{base} = \frac{H^{1.35}}{A_{base}} \tag{2.30}$$

Here H is the height of the enclosure and A_{base} is the surface area of the base of the enclosure. c is found by using Figure 2.14.

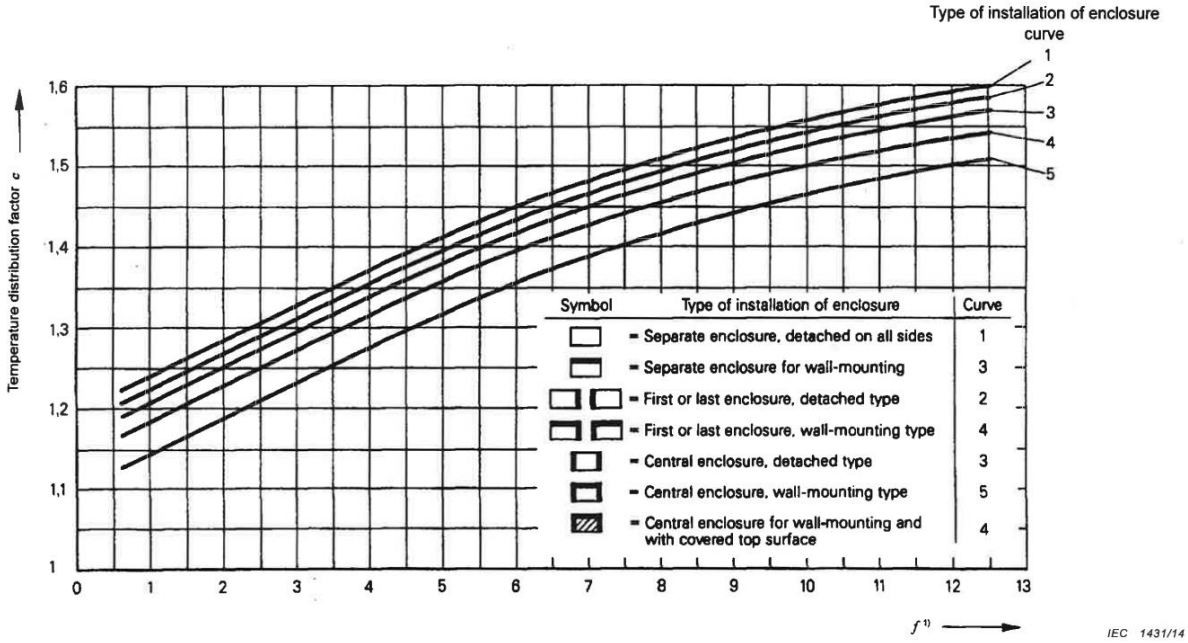

Figure 2.14: Temperature distribution factor c for enclosures without ventilation and effective cooling surface Ae > 1.25m^2, IEC 1431/14. [34]

Over-temperature of LBS by heat transfer coefficients - $\Delta\Delta T_{LBS}$:

Equation (2.31) can be used to determine the over-temperature of the LBS.

$$\Delta\Delta T_{LBS} = \frac{P_{LBS}}{h_{tot} * A_{LBS}} \tag{2.31}$$

The power input to the LBS P_{LBS} can be estimated by the same method as for the entire switchgear, but only including the contacts, connections and conductors related to the LBS. h_{tot} is the heat transfer coefficient, A_{LBS} is the heat emitting surface area of the LBS and are the area/dimension of the conductor and the geometry of the switch. [33] [34]

The heat transfer from the current path to the surrounding can be influenced by the degree and type of covering that may be on the LBS for proper function of the switch. This may lead to lower/ restricted heat transfer by radiation and convection, and an increased surface area with a possible higher emissivity as described in section 2.3.2. The heat transfer coefficient can be rewritten as shown in Equation (2.32). [33] [34]

$$h_{tot} = f_{corr} * h_{tot,bare} \tag{2.32}$$

Here f_{corr} is the correction factor and needs to be estimated from experimental studies. The f_{corr} used in this thesis is based on the study in [33] and set to 0.9-1.1. From the same study the heat transfer coefficient h_{tot} was estimated to be around 17 W/m^{2}K for bare conductors with emissivity between 0.2-0.3 and 23 W/m^{2}K when the emissivity was around 1. The coefficient depends on the heat sources orientation and the physical dimensions and will therefore vary based on design.

2.6 Simulation software

Several software programs are available on the market for temperature simulations where the user can create a 3D model of the system and explore how the system works in different scenarios and situations. A model like that can be used for steady state temperature simulations, calculations and predictions. Some examples are Comsol Multiphysics, SIMSCALE, Ansys Fluent and TMN.

Comsol Multiphysics is a simulation software for creating realistic Multiphysics and single-physic 3D models and have the functionality to simulate different real world scenarios and phenomena. Numerical methods like finite difference method (FDM), finite element method (FEM) and boundary element method (BEM) can be used in the simulations. Comsol Multiphysics can be combined directly with third-party software like CAD, MATLAB and SOLIDWORKS. [35] The paper [36] is one example where the software is used. For this paper the main goal was to use the software to estimate the current and temperature rise needed to create displacement in the micro beam. Figure 2.15 shows an example from the paper where 0.3V is applied and the total displacement and temperature distribution in aluminum is presented.

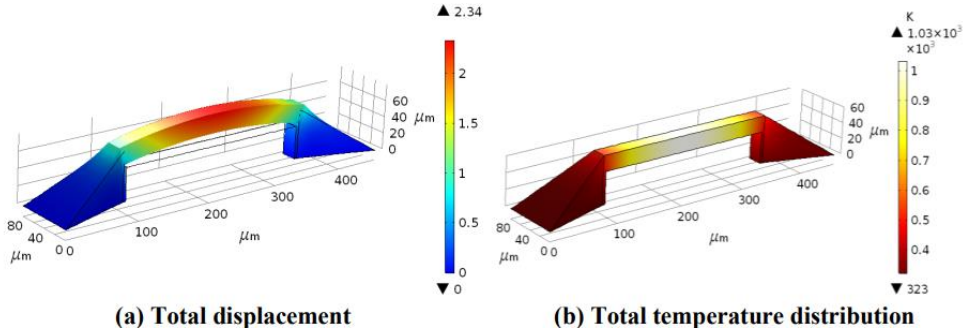

Figure 2.15: 3D model simulation of displacement and temperature in Comsol Multiphysics from. [36]

SIMSCALE is a heat transfer simulation software for testing and validating 3D designs based on the heat transfer mechanisms convection, conduction and radiation. It's an online product mainly used for optimalization designs by use of CFD (computational Fluid Dynamics) and FEA (Finite Element Analysis). [37]

Ansys Fluent is a software tools for designing and explore engineering systems by 3D designs. The Software focuses on optimalization of product designs, workflows and exploration in detail of real-world performances. [38] In the paper [21], the software is used for CFD-simulations to identify the temperature areas with low heat transfer in the switchgear. The switchgear simulation domain, the simulated temperature field and the simulated velocity field developed and presented in this paper by use of Ansys Fluent software is shown in Figure 2.16.

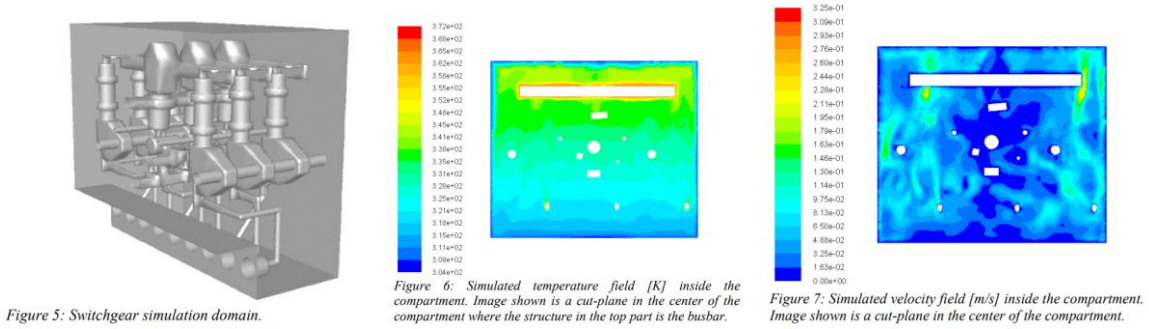

Figure 5: Switchgear simulation domain.

Figure 6: Simulated temperature field [K] inside the compartment. Image shown is a cut-plane in the center of the compartment where the structure in the top part is the busbar.

Figure 7: Simulated velocity field [m/s] inside the compartment. Image shown is a cut-plane in the center of the compartment.

Figure 2.16: Simulated temperature and velocity field from in Ansys Fluent software. [38]

Thermal network model (TNM) is used for calculating the temperature change in systems and devices. It is based on developing a mathematic formula or equation to describe the change of temperature in the system or device. One example is from the paper [39] where TNM is used to describe the system by network elements and calculates the temperature rise inside the switchgear. The simulations are than compared to measurements on the real system. Figure 2.17 shows the structure of the thermal network in this paper when TNM was used (left) and the thermal network of the (3 phase current) busbar with two sub conductors (right).

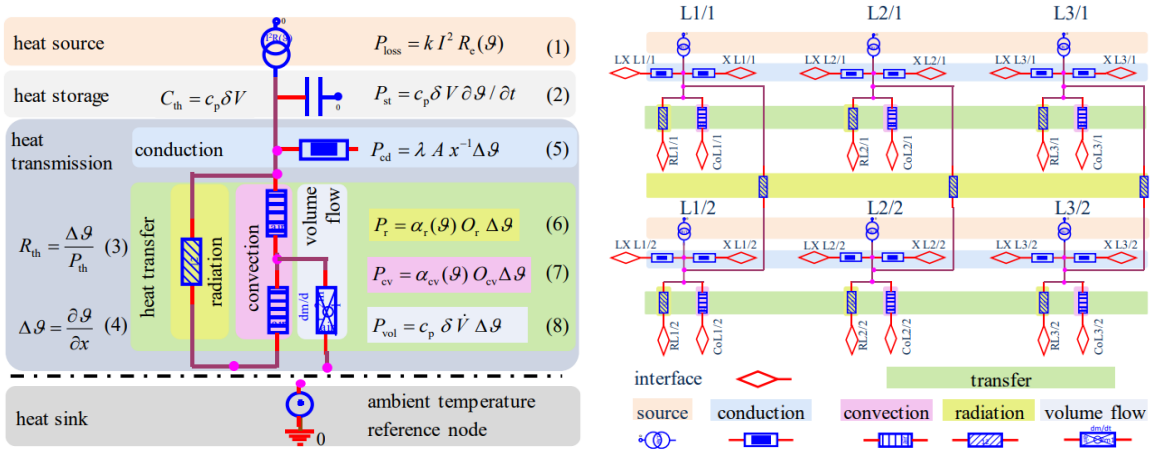

Figure 2.17: Thermal network model of busbar from [39].

None of these software products are used for this thesis. The reasons are that the goal of this thesis is to develop a simplified thermal model for the MV switchgear, not a detailed, advanced model. If that was the case, using one or more of these software products would have been an advantage. For this master's thesis, the need for learning how to use the software and create a 3D model was decided not necessary. Instead, the thermal model and calculations is implemented in Python 3.7. A version of TNM is probably the closest to what is used for this thesis. A possibility for future work on this MV switchgear can be to develop a more detailed thermal model with use of one of the previous mentioned software.

3 System description and equipment

This chapter describes the test system of the MV metal enclosed switchgear, the dimension of the enclosure and LBS, description of the temperature sensors (thermocouples), the equipment list and definition of subsystems.

3.1 MV metal enclosed switchgear

The test device is a MV metal enclosed switchgear RMU (ring main unit) from ABB. The device is a standard ABB MV metal enclosed switchgear with some adjustments for laboratory work at USN campus Porsgrunn. It has a removable back board and is filled with air instead of SF_6 gas, which it is designed for. The nominal current is 630A and voltage is 12/24kV. The switchgear has an upper and lower department as shown in Figure 3.1 and Figure 3.2. The upper department consists of the actual switchgear enclosure with the incoming cables, the current path, LBS etc. The lower department for this switchgear is empty, with no devices or equipment present. The actual functional switchgear consists therefore only in the upper part. Figure 3.1 shows the backside when the cover is on, which hides the current path. Figure 3.2 shows a model the switchgear from the back side created in MS PowerPoint.

Figure 3.1:Backside of switchgear with cover on.

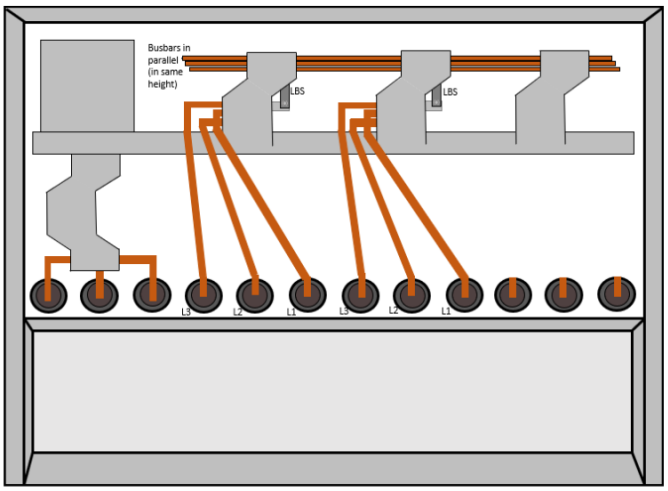

Figure 3.2: Model of the backside of switchgear without cover.

The switchgear is a 4-way unit and has three cable modules C1, C2, C3 and one vacuum switch breaker V4. C1 and V4 will not be used in this thesis work. The main current path is from C2 to C3. Each module consists of 3 phases L1, L2 and L3. AC or DC current is applied to the switchgear by connecting AC or DC cables between the current source and to the phases on the switchgear. For AC current, the cables are connected to each of the phases on module C2 as shown in Figure 3.3. When DC current are applied, two DC cables are connected between the DC source and on two of the phases on C2. Figure 3.3 and Figure 3.4

shows an image and created model of the switchgear from the front side, with view of the control panel and cable inputs/connections.

Figure 3.3: Frontside of switchgear.

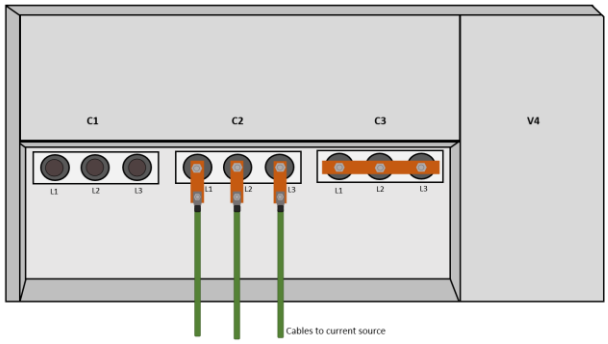

Figure 3.4: Model of the frontside of the switchgear.

The switchgear is designed with double sidewalls which increases the walls thickness. The material is aluminum. This can affect the heat transfer out of the enclosure. The frontside has the control panel where the operators have access to the device, which makes it important to increase safety by preventing a hot surface. This can be done by increasing the panels thickness or adding an insulating or protecting material. The functionality of the control panel itself also adds on the plates thickness.

Inside the switchgear (upper department) the current path is present with the three phases (L1, L2 and L3). For this thesis work, it is assumed all phases are similar and phase L1 is used for representation and measurements. The values for phase L2 and L3 will be set equal to the measured and calculated values on L1. All three paths consist of equal number of equal devices, which is presented in Figure 3.5. The only difference between the three phases is the length of the current path between the cable connection and to the first bolted connection. This leads to the only time the assumption is not used, is when calculating the total surface area of the current path (L1 + L2 + L3), where the surface area of each phase is measured individually and added together.

Each of the phases consists of 5 bolted connections, 2 load break switches (LBS) which each have one rotating contact (Ag/Ag) and an open/close contact (Ag/Ag) and cable connection at the start and end of the phase. The LBS is of knife blade type. The bolted connections are bolted busbar connection (Ag/Cu), bolted lower LBS connection (Cu/Ag) and bolted bushing connection (Cu/Cu). A simple model of one of the current paths is shown in Figure 3.5. The marking of the LBS shows what is included when doing measurements on the LBS and where the sensors are located.

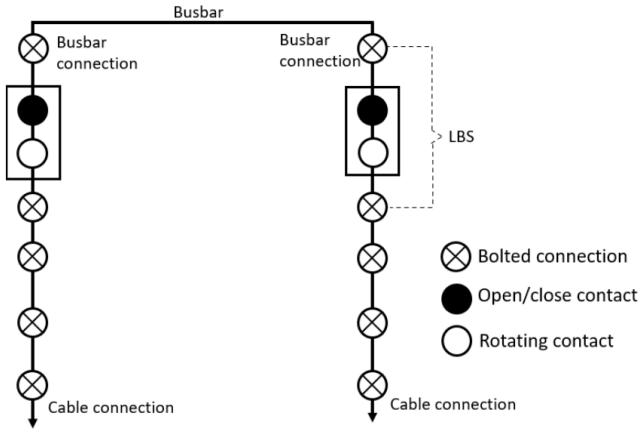

Figure 3.5: Model representation of one phase of the current path.

For the test device, only ohmic heating of the current path is assumed present. Contribution from skin effect, proximity effect and induced losses is assumed insignificant as described in section 2.2.2 and 2.2.3. Other possible heat sources (for example from the sun or panel oven) is not relevant and therefore neglected. The temperature rise tests are executed in January and February of 2022 and outside temperature was stable and cold. This resulted in a stable indoor temperature fluctuating between 18-21˚C. The device was not exposed to direct sunlight. This result in the power loss from ohmic resistance of the current path being the main heat source.

3.1.1 Switchgear dimensions

Figure 3.6 shows a model of the empty switchgear enclosure.

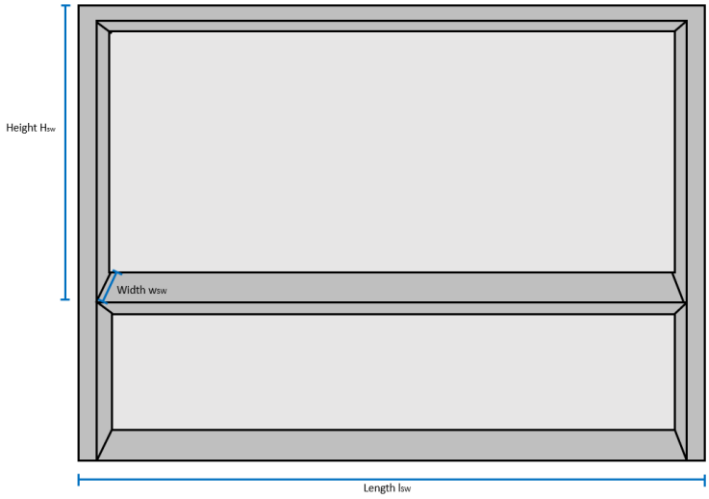

Figure 3.6: Switchgear dimensions.

The upper part of the enclosure is the location of the actual switchgear with the current path. The lower department is empty and not included in the definition of this switchgear. Table 3.1 shows the switchgear dimensions based on Figure 3.6 and measurements done on the real

device. The surface area of the switchgear is included, and the calculation is available in Appendix B.

Table 3.1: Switchgear dimensions.

Dimension	**Measurement [m]**
Width w_{SW}	0.52
Length l_{SW}	1.28
Height H_{sw}	0.845

The thickness of the different walls (top, bottom, sides, front and back) are not equal. The front is 23cm thick due to the control panel compared to the 3 mm thick back. The back and top are covered by one removable plate. The sides are constructed with doble side walls which increases the thickness of the wall. The dimensions of the walls are shown in Table 3.2.

Table 3.2: Wall thickness of switchgear enclosure.

Dimension	**Thickness [mm]**
Top/ back plate	3
Side wall	5
Bottom plate	4
Front plate	240

The surface area of the sides, top/ bottom, front/back wall and total area of the switchgear are calculated and presented in Table 3.3. The measured surface areas are the actual surface areas. The effective surface area is the calculated effective surface area based in IEC equations. [34] The calculations are available in Appendix C and part of the method described in section 2.5.

Table 3.3: Switchgear surface area.

Dimension	**Measured surface area [m^2]**	**Effective surface area [m^2]**
Side wall	0.44	0.22
Top/ bottom plate	0.67	0.93
Front/ back wall	1.08	0.97
Total surface area	4.37	3.8

3.1.2 Load break switch dimensions

A LBS is used for disconnecting or connecting the current in an electrical circuit. [40] For this thesis, the definition of how much of the current path is included as the LBS is based on the definition from the master's thesis [41] which uses a similar, but not the same LBS. In this thesis the knife blade LBS includes every part of the switch from the upper to lower switch Cu-Ag bolted connection as shown in Figure 3.7.

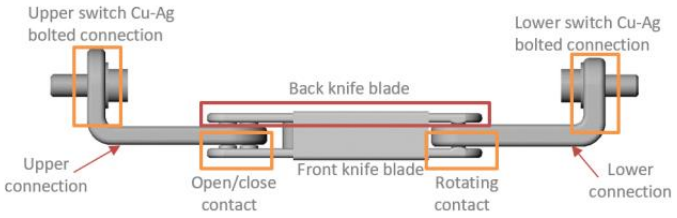

Figure 3.7: Definition of LBS from the master's thesis. [41]

A simplified 1-dimensional model of one of the LBS in the MV switchgear is shown in Figure 3.8. The LBS includes the open/close contact (Ag/Ag), the rotating contact (Ag/Ag) and the upper and lower bolted connections (Cu/Ag). The model is developed in MS PowerPoint. In the lab experiments this definition defines where the measurements of the LBS is executed and where the thermocouples for temperature measurements are placed. The LBS is divided into three parts when determining the dimensions. The middle part with the open/close contact and the rotating contact, and the upper and lower part including the connections. The upper and lower parts are similar. The lever for operating the LBS is not included.

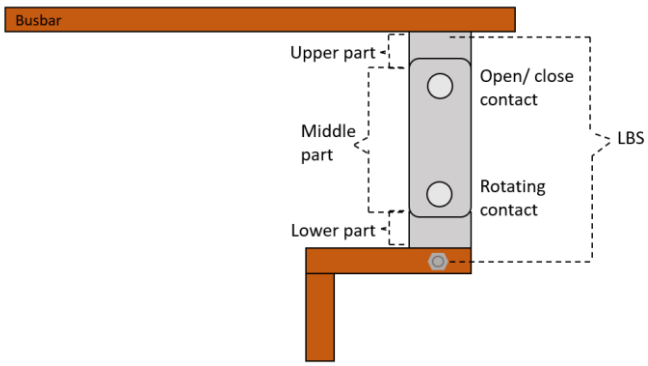

Figure 3.8: Simplified model of one LBS showing the definition for dimension.

The dimensions of the LBS for the upper and lower part and middle part are shown in Table 3.4. The calculated total surface area for one LBS is included in the last column. The calculations are available in Appendix B. The overlapping parts of the LBS is not added into the surface area twice.

Table 3.4: LBS dimensions.

Dimension	**Measurement [m]**
Width middle part $w_{LBS,m}$	0.005
Length middle part $l_{LBS,m}$	0.04
Height middle part $H_{LBS,m}$	0.13
Width upper and lower part $w_{LBS,u\&l}$	0.024
Length upper and lower part $l_{LBS,u\&l}$	0.027
Height upper and lower part $H_{LBS,u\&l}$	0.018
Surface area $A_{LBS,surf}$	$0.0152 m^2$

3.2 Sensor

Thermocouples for temperature measurements are the main sensors used for this thesis and are placed inside and outside the MV switchgear. The thermocouples are of type K, class 1 with a temperature range of -75˚C to 250˚C and an accuracy of ± 1.5˚C [42]. Figure 3.9 shows images of both ends of a thermocouple.

a) b)

Figure 3.9: Thermocouple. a) Twisted sensor conductor. b) Thermocouple plug.

The inner green cable is the positive side, where the conductor material is Ni-Cr. The white inner cable is the negative side, where the conductor material is Ni-Al. The measuring point of the thermocouple is where the positive and negative conductor material is twisted together. The measuring point is placed on a specific location on the system for temperature measurement and hold in place by Al-tape. The sensor measures the temperature at the first connection point for the two twisted vires of the thermocouple. To get valid measurements it is important to make sure the point where the twisted vires first meet is in contact with the surface where the temperature should be measured. If they are not in contact, its most likely the temperature of the air being measured instead of the surface. The plug end of the

thermocouple is connected to the logging device via a connection box shown in Figure 3.10. Inside the plugs, each of the positive and negative conductor materials are screwed underneath the corresponding screw. [42]

The connection boxes are connected to a data logger which sends the measurement data to a local computer, which logs the measurement data via the software Agilent BenchLink Data Logger 3. The data logger is shown in Figure 3.11. When a test is finished, the entire data set can be converted to excel format and retrieved from the software for further processing or use. The sensor overview for the laboratory tests is available in Appendix D.

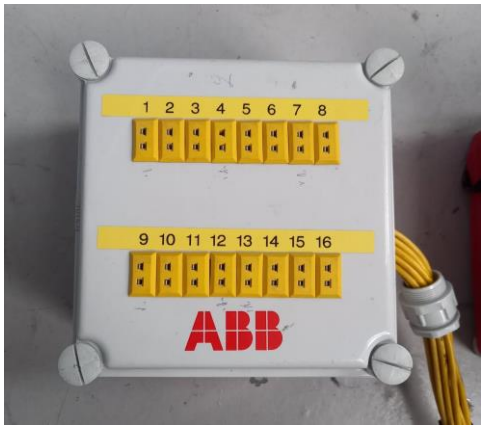

Figure 3.10: Connection box.

Figure 3.11: Data logger.

3.3 Equipment list

Table 3.5 shows the equipment list used for the laboratory tests. All equipment was available in the high current lab at USN campus Porsgrunn.

Table 3.5: Equipment list.

Type	Manufacturer	Model
MV Switchgear	ABB	3 phase 630A (RMU)
Current injector	Hilkar	Ak23
DC Power Supply	Delta Elektronika	SM1500-series
Data-logger	KEYSIGHT technologies	34972A LXI Data Acquistion/ Switch unit
Multimeter	Grossen Matrawatt	METRAHIT 30M

Connection box for thermocouples	ABB	
Thermocouples		Type K, class 1

3.4 Subsystem definition

For this thesis, the switchgear system is divided into two subsystems to describe the heat transfer. This is done to specify the heat transfer of the system in two steps for the development of the thermal model, which will be used further in the thesis. It is chosen to describe the system by two subsystems, but it would be possible to have more subsystem if wanted. Since the goal is to work with the warmest point to analyze and determine the system based on these limits, it is not necessary to have more than two subsystems for the development of this simplified thermal model.

The first subsystem is based on finding the most critical point/ device on the current path based on the temperature limits. Based on previous published paper (like [5] and [21]) and preformed tests, this device is the LBS on phase L1. Therefore, the first subsystem describes the heat transfer from the LBS to the surrounding air inside the enclosure.

The second subsystem is based on the heat transfer from the inside of the enclosure and out. Defining where this heat transfer is located is more difficult and the significance of chosen location is tested in section 5.3.2. The main challenge is to identify where on the outside of the enclosure is most ideal to represent the transfer. For the thesis, one of the outside side walls was chosen.

4 Resistance test

This chapter describes the purpose and procedure of the resistance test on the MV switchgear. The results of the executed test, and the resistance changed by temperature increase is calculated and presented.

4.1 Purpose

One of the important parameter inputs for the thermal model is the power input. Based on Ohm's law, the calculated power depends on the applied current and the resistance. The values of the resistances in the MV switchgear depends on the temperature. To be able to calculate the resistance change by temperature for different applied currents, a resistance test is executed. Measurements of the cold resistance and warm resistance at steady state for the different applied currents are done. This is performed by measuring the voltage drop and calculating the resistances by Ohm's law. The voltage drop is measured over phase L1 and over one of the LBS on phase 1. It is assumed the resistance is similar for all LBS and that the total resistance of phase L2 and L3 is equal to the total resistance of L1. The warm resistances will also be calculated at different temperatures by a given theoretically equation (2.4). The result of the two methods will be compared and analyzed to find a good representation for resistance change by increasing temperature at the LBS and L1 for this specific MV switchgear system.

4.2 Procedure

To calculate the cold and warm resistance, the voltage drop over phase L1 and over LBS on phase L1, module C2 is measured with use of a multimeter. 100A DC is the applied current. The thermocouples called senor 1 and sensor 2 is used for the LBS measurements. Sensor 1 is located at the upper bolted connection of the LBS and sensor 2 is located on the lower bolted connection of the LBS. Sensor 3 and 4 is of each end of phase L1 to measure over the phase. The setup of one phase is shown in Figure 4.1.

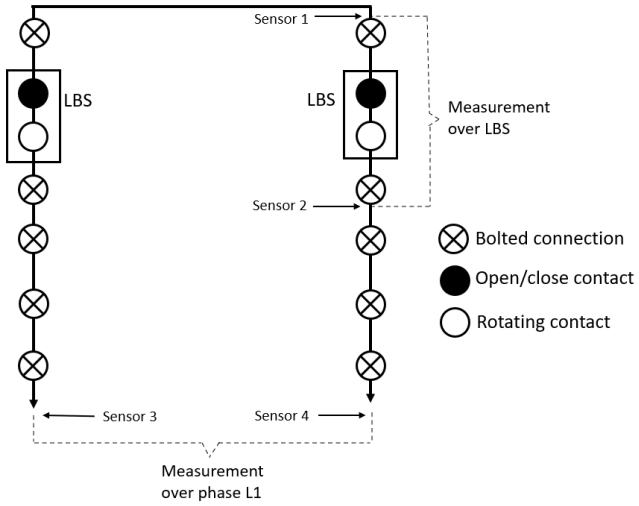

Figure 4.1: Model of one phase, current path with location of measurements.

It was decided to only measure the voltage drop over one LBS and phase L1. The test is based on using the decreasing temperature to determine when the measurements are executed. To make sure the measurements are done at the right temperature, the test and reconnection must be quick. Including several measurement points is time consuming, especially if the DC cables should be reconnected. The probability that the temperature would decrease below the wanted degree for the measurement is high. This would have made the tested values useless and at best inaccurate. Instead, only the voltage drop over L1 and one LBS will be measured. The calculated resistance for L1 will be used for phase L2 and L3.

The current path is injected with a stable DC current and the voltage drop is measured over the wanted location on the current path by use of the 4-wire method. The 4-wire method can be used in measuring resistances and excludes the problem of including the resistance of the ohmmeters own test leads. Instead, the voltage drop can be measured over the resistance by a voltmeter as shown by the setup in Figure 4.2. [17]

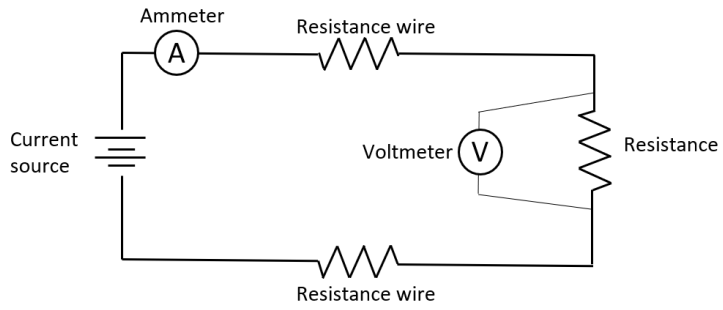

Figure 4.2: 4-wire method.

Voltage drop measurements:

The cold resistance is determined by applying 100A DC to the system and measure the voltage drop over the LBS and phase L1 when the system is cold (room temp).

For the warm resistance, the method for calculating the resistance is based on the already known steady state temperature on the LBS given in Table 4.1. (The temperature rise test in chapter 6 was performed before the resistance tests.) The switchgear is heated up until nearly max temperature is reached, then the current is turned off and the system cooled down. The resistance is wanted at steady state for each applied current. By monitoring the temperature at the LBS, the voltage drop over L1 and LBS can be measured when the temperature at LBS is equal the values given in Table 4.1. This gives the voltage drop at steady state for each applied current. Heating the switchgear and executing measurements as the system cools down saves time and decreases the number of needed cable reconnections.

Table 4.1: Steady state temperature for LBS.

	I = 400A	**I = 500A**	**I = 630A**	**I = 700A**	**I = 800A**	**I = 850A**
Steady state temperature at LBS [˚C]	48	63	87	103	110	110

4.3 Test result

Table 4.2 shows the measurement of the voltage drop and calculated resistances. The resistances R1 is calculated from Ohms law [43] and the resistances R2 is calculated from the theoretical Equation (2.4) describing the temperature rise in a conductor and is repeated below.

$$R_{warm} = R_{cold}[1 + \alpha(T_{warm} - T_{cold})]$$

Here R_{warm} is the resistance at temp T_{warm}, R_{cold} is the resistance at reference temperature T_{cold} and α is the temperature coefficient of the resistance for the conductor material. Conductor cupper hard is the present conductor material and is assumed to be $\alpha = 3.92*10^{-3}$ from table values. [17] The applied current in the resistance test is always 100A DC. The measurements are shown in Table 4.2 with the calculated resistances. R1 is calculated by Ohms law and R2 is calculated from Equation (2.4).

Table 4.2: Calculated resistance at different steady states.

	Temp LBS [˚C]	**Applied current I [A]**	**Voltage drop [mV]**	**Resistance R1 [μΩ]**	**Resistance R2 from eq. (2.4) [μΩ]**
LBS - L1	20	100 DC	2.8	28.1	28.1
Total L1	-	100 DC	22.9	229.2	229.8
LBS - L1	49	100 DC	28.7	28.7	31.4
Total L1	-	100 DC	23.1	231	254.8
LBS – L1	63	100 DC	2.9	29.2	32.9
Total L1	-	100 DC	23.3	245	267.9
LBS – L1	87	100 DC	3.1	30.6	35.6
Total L1	-	100 DC	26.5	265	288.9
LBS – L1	103	100 DC	3.2	32.3	37.3
Total L1	-	100 DC	28.0	280	303.1
LBS - L1	109.4	100 DC	3.3	33.0	38.1
Total L1	-	100 DC	28.6	286	308.2
LBS - L1	109.9	100 DC	3.4	33.7	38.1
Total L1	-	100 DC	28.7	287	308.6

Based on the calculated values in Table 4.2, a trendline for the resistance increase based on increasing temperature is developed in MS Excel. The trendlines are achieved by using the trendline function in Excel and visualizing the equation. Based on the data, a linear trendline fitted best and are therefore chosen to represent the resistance increase. Figure 4.3 and Figure 4.4 show the plotted resistance trendline for the LBS and L1 phase. R_1 (blue) is the calculated resistance based on Ohms law and R_2 (green) is the calculated resistance from Equation (2.4).

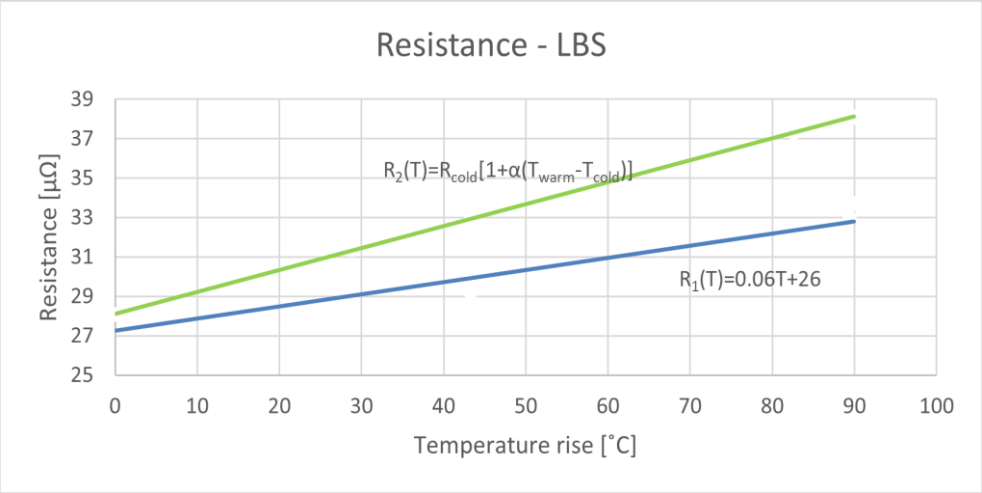

Figure 4.3: Resistance at different temperatures with trendlines for LBS.
R_1 is based on Ohms law and R_2 on Equation (2.4).

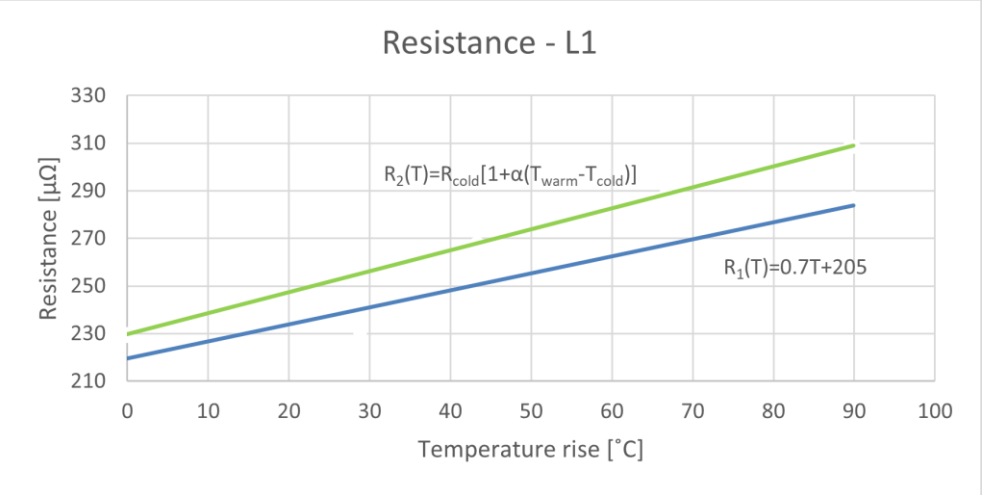

Figure 4.4: Resistance at different temperatures with trendlines for phase L1.
R_1 is based on Ohms law and R_2 on Equation (2.4).

Possible sources of error for the voltage drop measurements:

Some challenges and possible sources for error occurred during the resistance lab when the voltage drop over the LBS and L1 was measured. Since the resistance test was executed on a different day than the temperature rise tests, factors like room temperature can have been slightly different. Resulting in an inaccuracy for when (at which temperature) the voltage drop measurements should have been performed. The test depended on using the decreasing temperature to determine when the measurements was to be taken. It takes some time to observe the temperature, perform the measurements and noting the result. This can result in the voltage drop being measured at a lower or higher temperature than intended. Especially at the higher temperatures when the temperature drop was faster. An attempt to avoid this was to start the measurement process a few degrees higher than the temperature at the different steady states. For measurement over the LBS, thermocouples were mounted and used since it's not possible to measure inside the enclosure without opening it up. Resulting in the same amount of bulk included in every measurement. This was not the situation over phase L1, where the measuring probes was placed directly on the metal for every measurement. This can lead to a small variation of included bulk. Other more general possible sources of error like reading of the multimeter wrong is possible, but unlikely.

Comparison and discussion of resistance results:

The trendline for R_1(blue) on the LBS has a few deviations from the calculated R_1 resistance points (Table 4.2). This can be due to one of possible sources of error for the measuring of the voltage drop during this experiment, which is described above or that the temperature rise is not exactly linear. The trendline for R_2 (green) fits the calculated R_2 resistance points (Table 4.2) without any deviation. For phase L1, the result is similar. The calculated resistance points R_2 fits the trendline well, indicating a linear resistance increase by temperature change. The resistance points R_1 for L1 have some deviation from its trendline, but the deviation is smaller compared to R_1 for the LBS.

The resistance at LBS and L1 have both a higher temperature increase when using the theoretically equation for resistance of a conductor (R_2), than using the measured voltage drop to calculate the resistance. Since R_2 is based on Equation (2.4), the result would naturally follow the same trend with a similar increase. This makes it more likely to have the calculated resistance points more accurate to the trendline, compared to the measured values at R_1. In the calculations, the same R_{cold} value is used for both resistance calculation methods and the value for α is based on a 20˚C room temperature, which is similar to the actual room temperature. The measurements on the real system have in contrast a higher probability of inaccuracy based on the already mentioned possible sources of error. A possible reason for R_1 to be lower than R_2 is the inclusion of more bulk from several contacts, which result in a larger contact area and lower measured resistances compared to the theoretically calculated resistance from Equation (2.4). The amount of included bulk can be a reason the theoretically calculated resistances do not match the measured ones.

4.4 Adjustment of resistance equation for the thermal model

For the resistance change based on increasing temperature in the thermal model, a possible solution is to base the change on Equation (2.4) and fit it to match the real resistance from the voltage drop measurements (R_1 points). This can be done by adjusting the factor α in Equation (2.4) to fit the incline of the real measurements (R_1) and if necessary, add a factor to lift or lower the plot. This is done for both the LBS and L1 in two steps in online Geogebra.

Figure 4.5 shows the resistance R_1 based on measurements on the real system $h_{LBS,real}$ (green) vs the unadjusted resistance R_2 from the calculated theoretical Equation (2.4) $h_{LBS,theo}$ (blue) for the LBS.

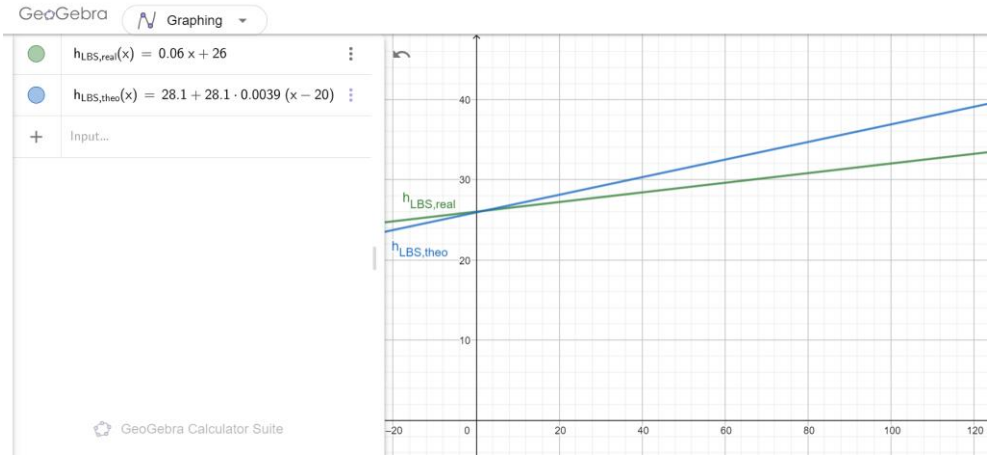

Figure 4.5: Resistance based on temperature change at LBS where the real resistance R_1 ($h_{LBS,real}$) vs the calculated resistance R_2 ($h_{LBS,theo}$) is plotted.

Figure 4.6 shows the real resistance R_1 $h_{LBS,real}$ (green), the unadjusted resistance R_2 from the theoretical equation $h_{LBS,theo}$ (blue) and the adjusted resistance $h_{LBS,adj}$ (red) for the LBS. For the adjusted resistance, α was first adjusted to have the same incline as $h_{LBS,real}$, which gives α equal 0.0021. Then, a factor of -0.9 was added to lower $h_{LBS,adj}$ to fit $h_{LBS,real}$.

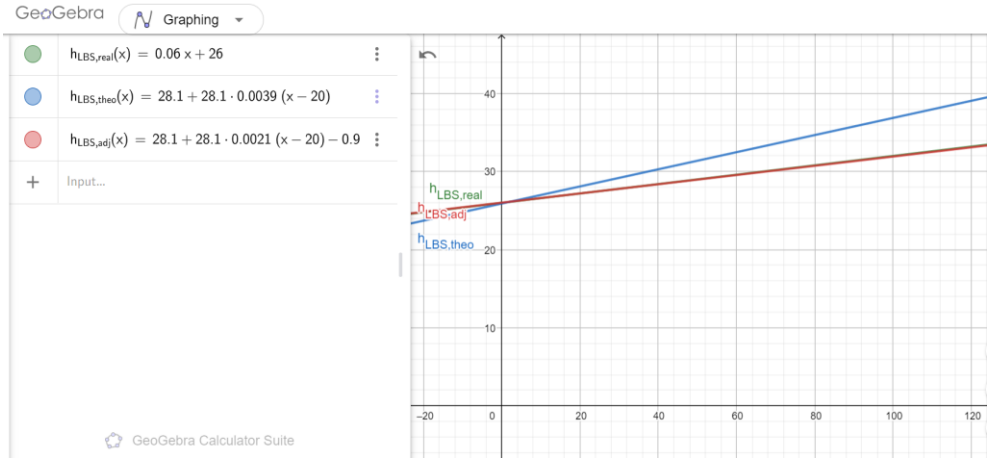

Figure 4.6: Resistance based on temperature change at LBS for the real resistance R_1 ($h_{LBS,real}$), the calculated resistance R_2 ($h_{LBS,theo}$) and the adjusted resistance ($h_{LBS,adj}$).

The same procedure is executed for the L1 resistance. Figure 4.7 shows the resistance from the real system R_1 (green) and the theoretical resistance R_2 (blue) based on Equation (2.4) for L1.

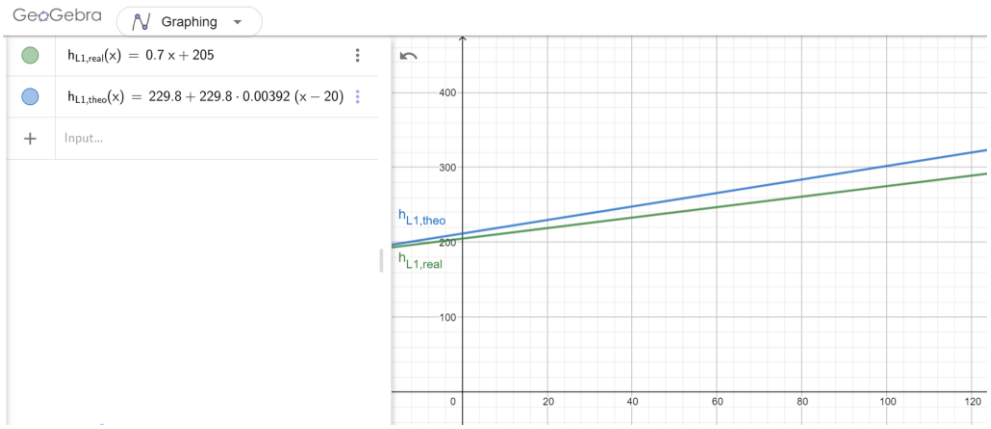

Figure 4.7: Resistance based on temperature change at phase L1. Plotted is the real resistance R1 ($h_{L1,real}$) vs the calculated resistance R2 ($h_{L1,theo}$).

By the same procedure as earlier, $h_{L1,adj}$ is adjusted from the theoretical equation to fit the real resistance. First α is adjusted to 0.00305, which gives the same incline as $h_{L1,real}$. $h_{L1,adj}$ lies 11˚C higher than the real resistance $h_{L1,real}$, so a factor of -11 is added at the end of $h_{L1,adj}$ to lower the line. This result in the lines plotted in Figure 4.8 where $h_{L1,real}$ and $h_{L1,adj}$ is equal.

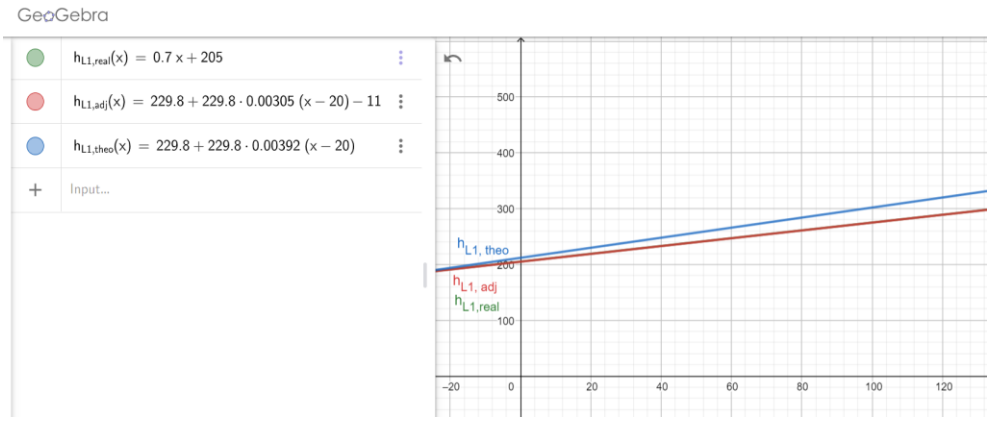

Figure 4.8: Resistance based on temperature change at L1 for the real resistance R1 ($h_{L1,real}$), the calculated resistance R2 ($h_{L1,theo}$) and the adjusted resistance ($h_{L1,adj}$).

For both the LBS and L1 the factor α is lowered. This is most likely due to the contacts within the switchgear and can be a result of the contact having another alloy than assumed. The $h_{LBS,adj}$ and $h_{L1,adj}$ equations will be used in the thermal model to calculate and update the resistance with the increasing temperature.

4.4.1 Parameter summary

The adjusted equation for L1 and LBS will be used for resistance calculations in the thermal model. The shift factor will be added at the end of the original equation. The parameter values are listed below in Table 4.3.

Table 4.3: Parameter values for resistance equation.

	LBS	**Phase L1**
T_{cold} [˚C]	20	20
R_{cold} [μΩ]	28.1	229
α	0.0021	0.00305
Shift factor	-0.9	-11

4.5 Determining contact resistance from total resistance

The percent of contact resistance of the total resistance for the LBS and L1 can be determined. From a previous executed resistance test (about one year ago as a lab exercise in the class Physics of Electrical Power Engineering [44]) [45] the cold resistance was calculated based on measuring the voltage drop on L1. In the test, the phase was divided into several parts and the resistance was calculated for each of the parts. Based on these values, the amount of bulk resistance and contact resistance for the LBS and L1 can be determined. Figure 4.9 shows the location of voltage drop measurements over phase L1 from the previous lab exercise.

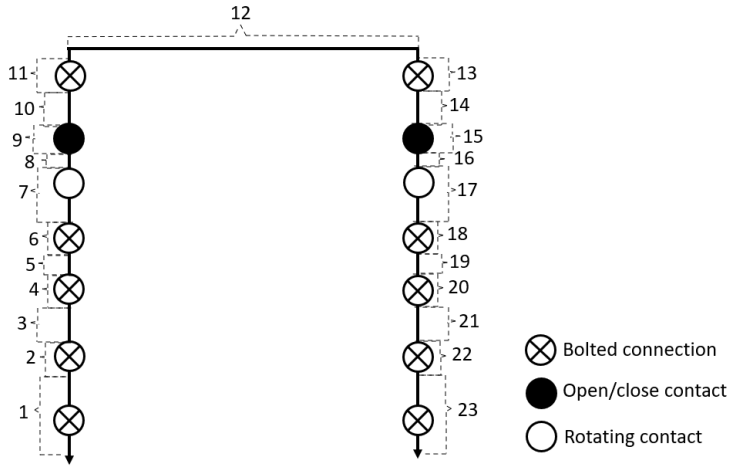

Figure 4.9: Measurement points on current path L1.

Table 4.4 shows the calculated result from the previous lab exercise. The current is 100A DC in all cases.

Table 4.4: Calculated resistance over current path L1. [45]

Meas. nr	Voltage drop [mV]	Calc. resistance [μΩ]	Meas. nr	Voltage drop [mV]	Calc. resistance [μΩ]
1	2.8	28	13	0.28	2.8
2	0.1	1	14	0.51	5.1
3	3.5	35	15	1.0	10
4	0.4	4	16	0.4	4
5	0.39	3.9	17	0.61	6.1
6	0.33	3.3	18	0.5	5
7	0.7	7	19	0.39	3.9
8	0.42	4.2	20	0.3	3
9	0.9	9	21	3.6	36
10	0.48	4.8	22	0.14	1.4
11	0.24	2.4	23	2.9	29
12	2.1	21	Total	22.99	229.9

The total cold resistance over the phase is 229.9μΩ. The LBS for the following resistance test is the measurement points 13, 14, 15, 16, 17 and 18 added together. Which for the cold resistance gives 33μΩ. [45] These values can be used to validate the new resistance measurements and to calculate how large amount of the LBS and L1 phase is contact resistance.

The cold resistances from R1 are calculated to be 28.1μΩ for the LBS and 229.8μΩ for L1. Compared to the cold resistance of the LBS and phase L1 from Table 4.4, the resistance value of the LBS is slightly lower with 28.1μΩ compared to 30.2μΩ. This is most likely due to the accuracy of included bulk in the measurements. The resistance measured over L1 is almost equal with 229.9μΩ from Table 4.4 compared to 229.8μΩ from the new measurements. This deviation can be neglected and are most likely occurring from the number of included decimals. The comparison increases the validity of the measurements of the cold resistance, which is used as a base for calculating the changing resistance.

The amount of the total resistance which is contact resistance can be calculated based on Table 4.4 and Figure 4.9. From Figure 4.9, measurement point 2, 4, 9, 11, 13, 15, 18, 20 and 22 are only contact resistances. The measurement point nr. 1, 7, 17 and 23 is partly contact resistance and bulk resistance. As a simplification, its assumed 50% of these resistances are bulk and 50% are contact resistance. Table 4.5 shows an overview of how much of the LBS resistance and L1 resistance is bulk.

Table 4.5: Contact resistance of the total resistance for the LBS and L1.

	R_{total} [μΩ]	R_{cont} [μΩ]	R_{cont} [%]
LBS	30.2	18.1	60
L1	229.8	76	34

For the LBS, 60% is calculated to be contact resistance of the total resistance. Some inaccuracy is present due to the simplification of how much is contact and bulk resistance in point 17. For the entire phase L1, 34% of the total resistance is calculated to be contact resistance. The same cause of inaccuracy is present here from point 1, 7, 17 and 23.

5 Steady state temperature rise tests

This chapter describes the temperature rise tests executed at the high current lab at USN campus Porsgrunn for determination of model parameters. The executed tests are temperature rise tests until steady state for a selection of applied currents.

5.1 Purpose

The purpose of the initial temperature rise tests is to create a base for the thermal model to be developed, and to be able to compare and verify the thermal model to the actual temperature rise in the switchgear. The first temperature rise tests to be executed are with applied current at 400A, 500A and 630A (nominal) until steady state. Ch 3. describes the system setup. The values and results of the temperature rise tests are used to calculate the heat transfer coefficients and the time constants. The thermal model can then be developed in Python 3.7.

5.2 Procedure

The temperature rise tests are executed at the high current lab at USN campus Porsgrunn. Thermocouple elements are placed on specified location to measure different temperatures of the current path, surface areas and air temperatures. The sensor overview is available in Appendix D. The thermocouples are plugged into the connection box so data can be transferred to the data acquisition unit. The Data acquisition unit is connected to a computer which logs the data by the computer software “Agilent BenchLink Data Logger 3”. This software measures the temperature every given time unit, and stores and plot the data. For the tests in this thesis, the temperature is measured every minute. AC cables are connected between the phases on the current source/ injector and module C2 on the switchgear. Module C3 is short circuited. The connection between the AC current source and the switchgear is shown in Figure 5.1. The thermocouples are connected to connection box on the front side of the switchgear and the data is sent to the computer in the background.

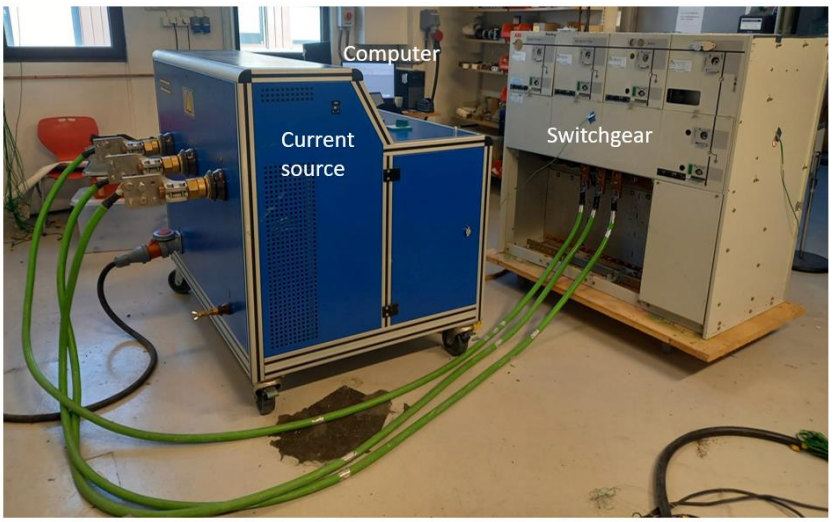

Figure 5.1: System setup.

When the preparation is finished, the logging system is turned on to verify that the thermocouples measure reasonable values (around 20˚C on the cold system – room temperature). After the logging has started, the current source is turned on and adjusted to wanted input current. Steady state can be declared when the temperature increases less than 1K per hour. [3] [34]

5.3 Result and discussion of temperature rise tests

This subchapter shows the result of the steady state tests and the calculation of the parameter values for the development of the thermal model.

5.3.1 Steady state temperature rise tests

The result of the temperature rise tests is described in this subchapter. The tests are run until steady state for applied current at I = 400A, 500A and 630A. The chosen measurement points presented are the LBS on phase L1, the enclosure air in same height as the LBS, the wall temperature on the outside of the enclosure and the room temperature.

Figure 5.2 shows the result of the temperature rise test when the switchgear was injected with 400A until steady state.

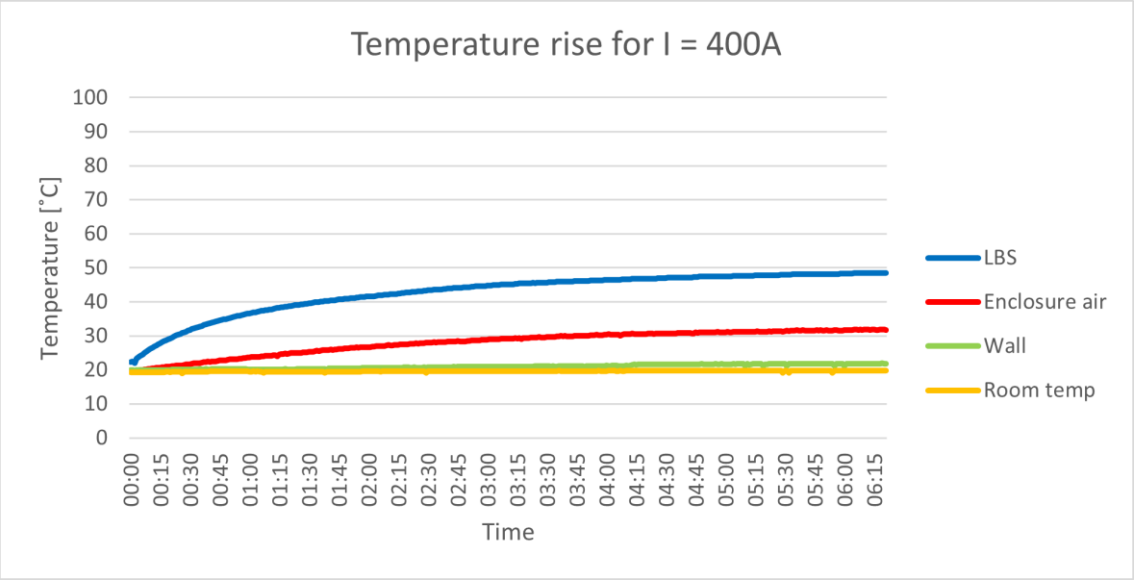

Figure 5.2: Temperature rise test until steady state with I = 400A.

The temperature at the LBS started at 22˚C and reached 48˚C at steady state, which was after about 6h and 10min. The enclosure air temperature increased from around 20˚C to 32 ˚C. The wall temperature and room temperature stayed relatively stable around 20˚C.

Figure 5.3 shows the result of the temperature rise test when applied current was I = 500A.

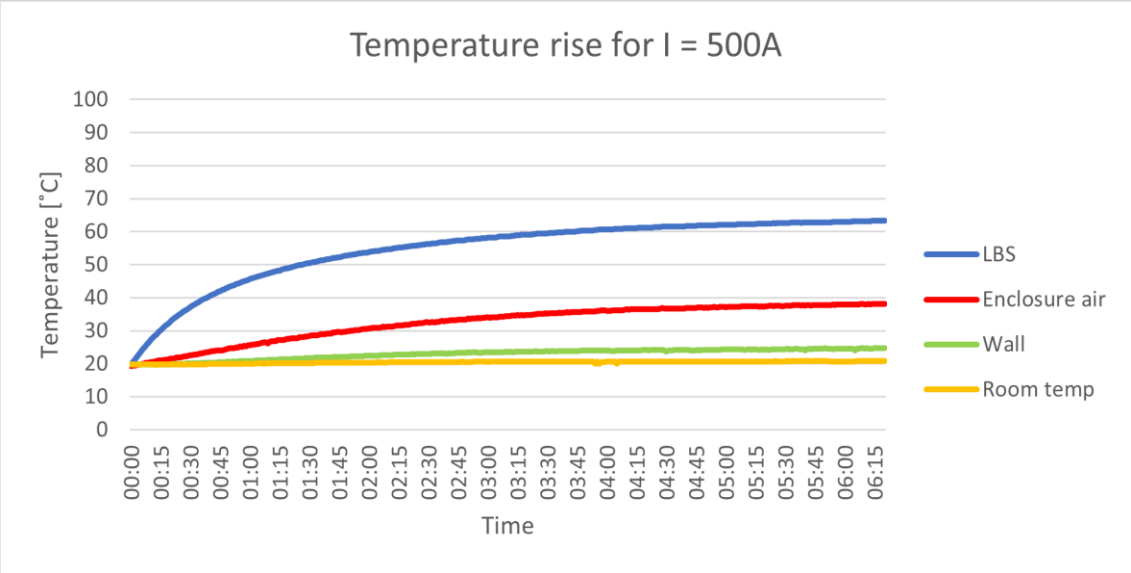

Figure 5.3: Temperature rise test until steady state with I = 500A.

When the applied current was I = 500A, steady state was reached after 6h and 10min. All of the measured temperatures started at approximately 20˚C and the room temperature stayed there. The LBS reached 63˚C, the enclosure air reached 38˚C and the outside wall temperature ended at 25˚C.

The temperature rise with I = 630A (nominal current) is shown in Figure 5.4.

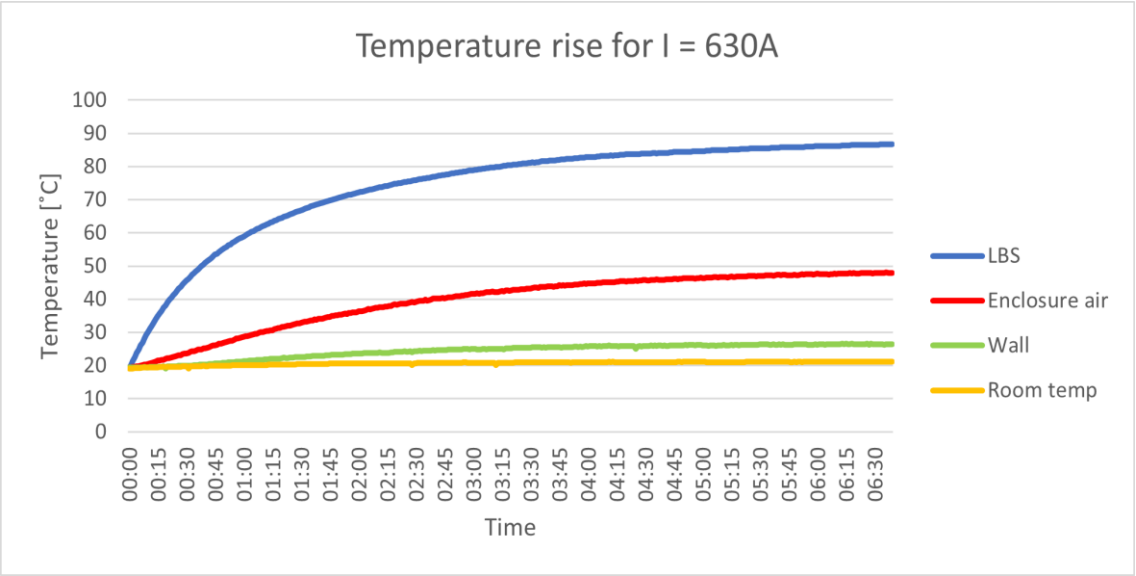

Figure 5.4: Temperature rise test until steady state with nominal I = 630A.

The temperature rise with applied nominal current I = 630A reached steady state after 6.5 hours. The measurements started at room temperature, 20˚C. The final temperature for the LBS was 67˚C, for the enclosure air it was 48˚C and at the outside wall the temperature reached 26˚C.

Table 5.1 shows an overview of the temperature rise ΔT_e for the three steady state cases with different applied currents, which can be used to calculate the temperature rise as shown in Equation (2.11). [25]

Table 5.1: Temperature rise ΔT_e of LBS, enclosure air and outside wall for different applied currents.

	$\Delta T_{e,LBS}$ [˚C]	$\Delta T_{e,enclosure\ air}$ [˚C]	$\Delta T_{e,outside\ wall}$ [˚C]
I = 400A	26.2	12.1	1.9
I = 500A	43.6	18.7	4.8
I = 630A	67.5	28.6	6.8

From the test results, it can be observed that the increase in applied current affect the temperature increase. For lower currents the temperature increase in the sensor points inside the switchgear enclosure (LBS, enclosure air) are lower than when higher current is applied to the system. The wall temperature (which is measured on the outside of the switchgear) is also affected by the applied current. This temperature change is not as large as the temperature change inside the enclosure. The generated heat due to power loss, heats up the inside of the enclosure (devices and air) and the wall. Based on the theory of heat dissipation (section 2.3.2), the system went through the adiabatic state in the beginning when all the power loss (heat) from the applied current path was used to heat up the current path. This phase led to a fast increase in temperature, especially at the LBS. When the transition phase started, the heat went from the current path to the surroundings, which here is the air inside the enclosure. This can be the reason for the slower temperature increase at the start of the test for the enclosure air and outside wall compared to the LBS. The measured temperature at the outside wall can also have a slower temperature increase due to the thickness of the double sidewalls as described in section 3.1 and cooling from the surrounding air. When the stationary phase hits, all the heat goes to the surroundings and the temperature increase slows down.

Based on the applied current for the three cases, it can be observed that the steady state temperature rise increases at the LBS (which is the assumed most critical point based on temperature limit) to around 30˚C at 400A, 40˚C at 500A and to nearly 70˚C at 630A. The IEC limit for silver coated contacts in OG is 115˚C and a max temperature rise at ambient air temperature (not exceeding 40˚C) of 75K. Since 1K increase is equal 1˚C increase, the max temperature rise of the LBS is 75K or 75˚C. The temperature rise at the LBS for all applied currents are within this limit. The temperature limits are available in [3].

Increasing the current in steps from 630A (overloading), will most likely increase the temperature significantly. It will therefore be important to observe the temperature rise to prevent overheating and equipment fail/ damaging. For lower currents than nominal, the system is not facing a risk of overheating. The switchgear does not use SF6 gas (as designed for), but air. This can have an effect on the result. According to [46], the temperature rise of SF_6 is higher than air, when the heat distribution in the switchgear is similar.

5.3.2 Importance of wall selection for wall subsystem

The outside wall chosen to represent the second subsystem is side 1, which was chosen before any tests were executed. With the data gathered from the temperature rise tests, it is possible to analyze and compare the different outside surface areas heat transfer coefficients to determine the optimal outside surface wall.

Optimal enclosure surface with assumed heat transfer coefficient:
The first analyze is with an assumed heat transfer coefficient. This test is based on comparing the measured steady state temperature at the different outside surface walls and calculate the temperature from an assumed heat transfer coefficient by Equation (2.13). A new temperature rise test is performed with applied nominal current I = 630A. The sensor setup is shown in Appendix D, where the temperature at each outside surface walls are measured. Table 5.2 shows the measured steady state temperatures.

Table 5.2: Steady state temperature on outside surface wall locations .

	Top	**Bottom**	**Side 1**	**Side 2**	**Front**	**Back**
Steady state temperature, outside wall [˚C]	40.8	26.9	26	31.2	25.2	35.1

The highest measured temperature was on the top of the enclosure. This is most likely due to the movement of the heat, which rises over colder air and results in the warmer air flowing toward the enclosure top. A contribution can be that the location of the current path inside the enclosure is close to the enclosure top. The top and back wall is the thinnest, resulting in a more effective heat transfer through these walls and a higher measured temperature compared to thicker walls. The front, bottom and side 1 of the enclosure measured the lowest final temperature between 25-27˚C, which indicates less heat transfer trough these surfaces or a more effective cooling compared to the rest. A possible reason side 2 gets warmer than side 1 is the lack of devices (inside the enclosure) close to side 1 compared to side 2. The front has a ticker surface wall due to the control panel which results in a lower measured temperature on the outside. This is also necessary to prevent users/ operators from touching a hot surface while working. The thickness of the different walls of the enclosure is listed in Table 3.2.

The heat transfer coefficient is set to 10 W/m^2K as an assumption, as done in [47]. The wall temperature for this heat transfer coefficient is calculated from Equation (2.13) and gives T_{wall} equal 29˚C. Based on this test, the most optimal enclosure wall to choose is the bottom or side 2, which is only approximately 2 degrees off. It is not known if the heat transfer coefficient of this specific switchgear actually is 10 W/m^2K. Therefore, the following section shows the calculated heat transfer coefficient based on the measured temperatures for each outside surface area.

Calculation of heat transfer coefficient for each outside surface area:
The heat transfer coefficient for the different outside surface areas can be calculated based on the measured temperatures. The calculation is performed in Python 3.7 and the code is available in Appendix E. The results are shown in Table 5.3.

Table 5.3: Heat transfer coefficient at different outside wall surfaces with applied current I = 630A.

	Top	**Bottom**	**Side 1**	**Side 2**	**Front**	**Back**
Heat transfer coefficient [W/m^{2}K]	4.3	12.7	15.3	7.9	16.6	5.9

Based on Table 5.3, a higher measured temperature results in a lower heat transfer coefficient. This is consistent with Equation (2.13). The bottom has the calculated heat transfer coefficient closest to 10W/m^{2}K. The deviation between the calculated heat transfer coefficients differs between 4.3W/m^{2}K and 16.6W/m^{2}K. Based on the results, the heat transfer of the different outside surface areas are not similar. It is therefore important to specify which surface wall is chosen to be used as a subsystem, since this will influence the results significantly. In a real situation it might be needed to monitor the temperature of all outside surface walls. In this test, only one measurement point at the center of each wall is used. A future analysis might include several measurement points on each wall to analyze differences.

5.3.3 Thermal time constants

The thermal time constant describes the response time after a step up or down of the input signal (here the applied current). Two time constants are used to describe the MV switchgear heat transfer system. The times constants are calculated for each of the three applied currents. In the following description, only the calculation with I = 630A is presented. The calculations when I = 400A and 500A is available in Appendix F. The first time constant is calculated based on the temperature at the LBS on current path L1. The highest measured temperature was 86.7˚C and the final room temperature was 21.1˚C. The second time constant is calculated by the temperature on the outside wall (side 1) which measured a max temperature at 26.3˚C. The highest room temperature was at 21.1˚C. The temperature at the time constants is found at 63.2% of the temperature rise and calculated with Equation (5.1). [48]

$$T_\tau = \left(\left(T_{max,sensor} - T_{max,air}\right) * 63.2\%\right) + T_{max,air} \tag{5.1}$$

For LBS:

$$T_{\tau,LBS} = \left((86.7℃ - 21.1℃) * 63.2\%\right) + 21.1℃ = 62.6℃ \approx 63℃$$

For surface wall:

$$T_{\tau,wall} = \left((26.3℃ - 21.1℃) * 63.2\%\right) + 21.1℃ = 24.4℃ \approx 24℃$$

The time constant can visually be found at these temperatures. The time constants for the LBS and the outside surface wall are shown respectively in Figure 5.5 and Figure 5.6. The results of the time constant calculations are shown in Table 5.4.

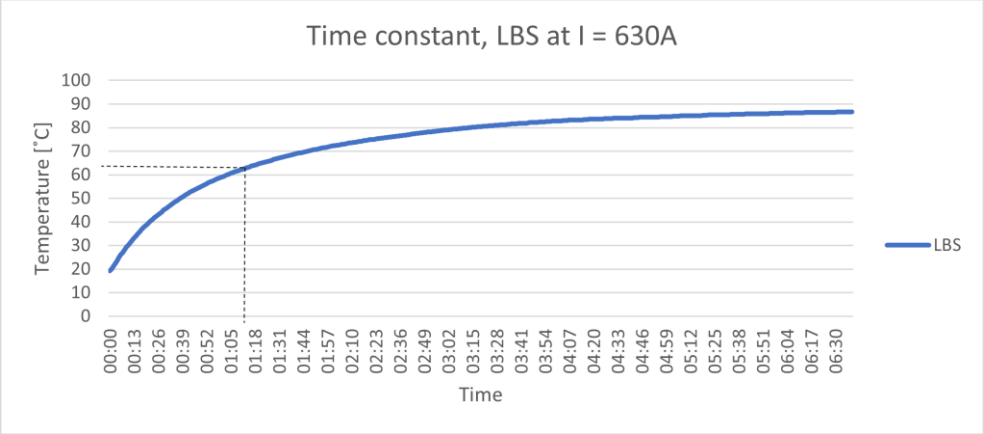

Figure 5.5: Time constant for LBS.

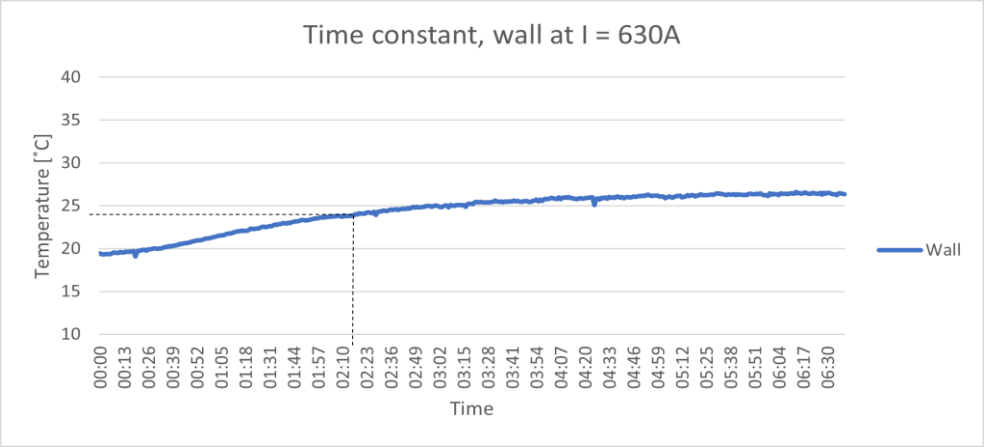

Figure 5.6: Time constant for outside wall.

The time constants with applied current I = 400A and I = 500A is calculated in Appendix F. Table 5.4 shows an overview of the time constants.

Table 5.4: Time constants for current path and outside wall.

	τ_{LBS} [min]	τ_{wall} [min]
I = 400A	90	150
I = 500A	80	140
I = 630A	70	135

Figure 5.7 shows the time constant vs temperature. The temperature is the measured steady state temperature for the LBS and outside wall for the three calculated cases in Table 5.4.

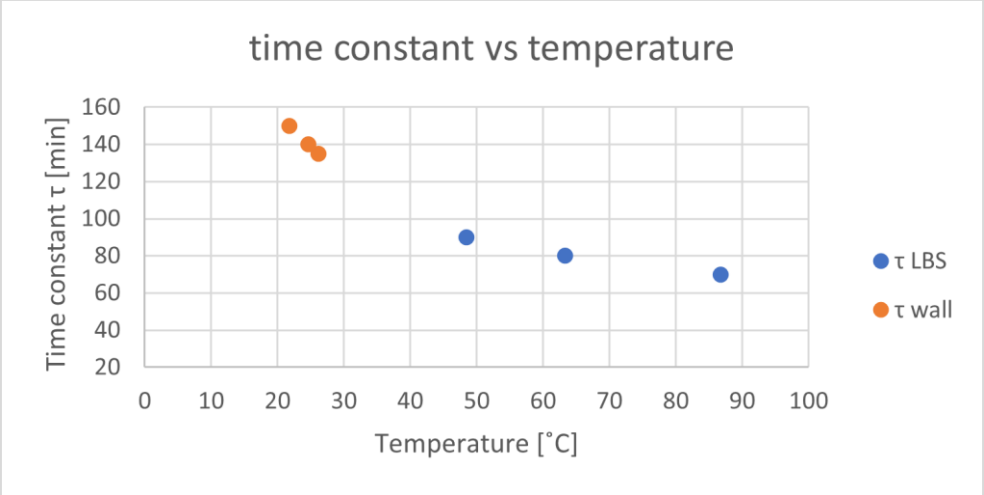

Figure 5.7: Time constant vs temperature for LBS and outside wall.

The time constant for both subsystems show a decreasing time constant with increasing current and temperature. This can be explained by Equation (2.12). The heat transfer coefficient increases with increasing temperature while cM and A is fixed. This results in a decreasing time constant. For the temperature rise, a larger time constant means it takes longer time for the temperature to increase to steady state/max temperature. This happens in these tests when the current is lower. It also results in a less steep slope, when the current is lower. In the opposite direction, it means that if a high current is applied (ex. 850A) the time constant will be smaller, and the temperature increase to steady state/max will be faster and steeper than any of the lower currents tested here.

Based on Table 5.4, the time constant for the outside wall decreases with a similar change as the time constant at the LBS. Including the temperature as a factor as shown in Figure 5.4, the outside wall time constant changes more aggressively than for the LBS. The LBS has a time constant change from 90min to 70min during a temperature change from 87˚C to 48˚C. The outside walls time constant changes from 150min to 135min when the temperature changes from 23˚C to 26˚C. This fits well with the observation of the LBS having a fast temperature rise from tests in section 5.3 and from previous papers like [21].

5.3.4 Heat transfer coefficients

The two heat transfer coefficient is calculated in Python 3.7. The code is available in Appendix E. The first heat transfer coefficient h_{LBS} is used to describe the inner systems where the heat flows from the warmest point on the current path (which is the LBS) to the surrounding air. The second heat transfer coefficient h_{wall} is used to describe the subsystem where heat flows from the air inside the enclosure and out. It is based on the measurements from the outside wall. The method used to calculate the heat transfer coefficients is shown in Equation (5.2).

$$h = \frac{R * I^2}{A_{surf} * (T_{max} - T_{air})} \tag{5.2}$$

Here R is the warm resistance, I is the input current, A_{surf} is the effective surface area, T_{max} is the highest temperature and T_{air} is the air temperature.

For h_{LBS} the temperature is measured at the LBS sensor on phase L1. The resistance is the calculated resistance for LBS from the adjusted equation in section 4.3 and A_{surf} is the effective surface area of the LBS. The power input for the second heat transfer coefficient h_{wall} is based on the incoming power to the system which heats up the current path. The used resistance is therefore the resistance of the current path (L1 times 3), which was calculated in section 4.3. A_{surf} is the effective surface area of the enclosure wall. The calculated heat transfer coefficients for the three different applied currents are presented in Table 5.5.

Table 5.5: Heat transfer coefficient for the three different applied currents.

	h_{LBS} [W/m^{2}K]	h_{wall} [W/m^{2}K]
I = 400A	10.6	12.6
I = 500A	11.3	13.4
I = 630A	13.2	15.4

The heat transfer vs steady state temperature for each of the applied current is plotted in Figure 5.8.

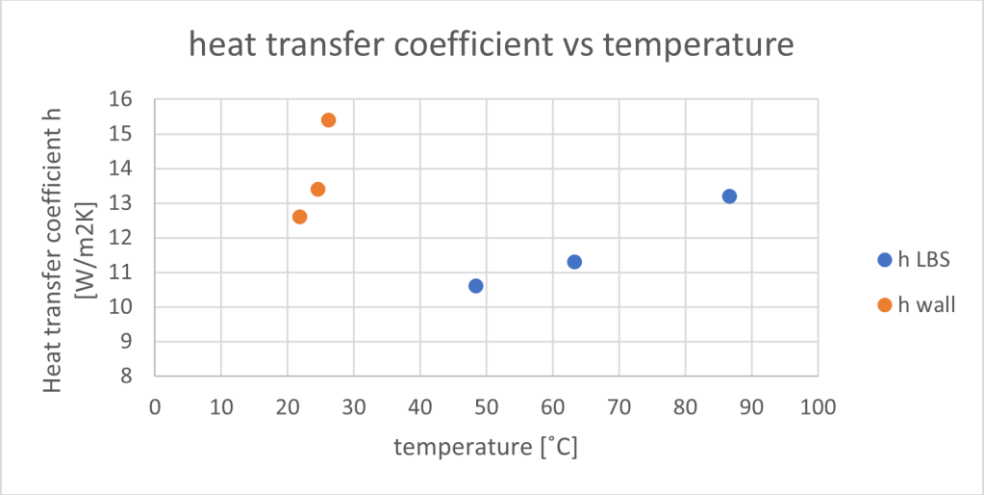

Figure 5.8: Heat transfer coefficient vs temperature for LBS and outside wall.

The heat transfer coefficients have an increasing value with increasing applied current, which can be explained by Equation (5.2). For this case, the surface area is assumed fixed. The temperature and the resistance increases with higher temperature, but the largest factor is the current squared which results in an increasing heat transfer coefficient in most cases. The heat transfer coefficient of the outside wall has a more rapid increase than the LBS, when the temperature and current increases. The outside wall heat transfer coefficient has a higher value than the LBS at lower steady state temperature when the same current is applied.

It is challenging to determine especially the second heat transfer coefficients due the ununiform switchgear system. The switchgear is not an empty box, but have devices and equipment inside, which can affect the heat transfer of the system in addition to the different thicknesses of the different walls as described in section 3.1. This makes it more challenging to define and gather correct parameter values, which leads to some assumptions and simplifications. The heat transfer is calculated based on one of the side walls (side 1). Another wall would have resulted in a different result. Calculating the effective surface area

can also lead to challenges based on the definition (what is included). The value of the heat transfer coefficient h_{wall} has therefore a higher possibility of being inaccurate for describing the heat transfer from the enclosure air through the walls and to the surrounding air outside the switchgear. To make sure the values are within acceptable limits and makes sense, reference values are used from already published papers calculating the heat transfer coefficients on similar systems. From the paper [33] the heat transfer coefficient on the LBS was calculated to be between 10-17W/m^{2}K, around 17W/m^{2}K for bare conductors with emission at 0.2-0.3 and 23W/m^{2}K for bare conductors with emission at 1 (black body). This is only used as an indication and the values are highly dependent on the specific system. The heat transfer coefficient of the wall is higher than expected based on the lower temperature deviation. A reason for this can be the calculated surface area or a higher emission constant than assumed, which is part of the definition of radiation as shown in Equation (2.25). Another possible reason is that the chosen outside wall is not the optimal wall for describing the second heat transfer.

6 Thermal model of MV switchgear

The thermal model of the MV switchgear is modelled by the general thermal energy balance for dynamic systems. The system is modelled as a lumped parameter system for simplification. [48] Which in this system makes the temperatures in the two subsystems uniformly distributed. The temperatures used for developing the thermal model is the temperature of the LBS, the air surrounding the LBS, enclosure wall and room temperature outside the enclosure. Equation (6.1) shows the general thermal energy balance. [50]

$$\frac{dT}{dt} = \frac{1}{C}(P_{in} - P_{out}) \tag{6.1}$$

Where dT/dt describes the temperature change, C is the heat capacity of the system, h is the heat transfer coefficient, A is the surface area and T is temperature. Equation (6.2) shows the heat capacity C.

$$C = cM = \tau hA \tag{6.2}$$

Where c is the specific heat capacity, M is the system mass and τ is the thermal time constant in min. For the system, the temperature change per time unit can be written as shown in equation (6.3) and (6.4) for the two subsystems, called LBS and wall. The subsystem LBS describes the heat transfer from the LBS to the surrounding air inside the enclosure, and the subsystem wall describes the heat transfer from the inside the enclosure and out of the enclosure through the wall. Temperature change for the LBS to surrounding air is shown in Equation (6.3) and for the surrounding air to outside enclosure Equation (6.4).

$$\frac{dT_{LBS}}{dt} = \frac{1}{C}(P_{LBS,in} - P_{LBS,out}) \tag{6.3}$$

$$\frac{dT_{wall}}{dt} = \frac{1}{C}(P_{wall,in} - P_{wall,out}) \tag{6.4}$$

The input power according to Ohm's law is shown in Equation (6.5). The output powers for the thermal model development in Equation (6.6) and (6.7) are based on Equation (2.13).

$$P_{in} = RI^2 \tag{6.5}$$

$$P_{LBS,out} = h_{LBS}A_{LBS}(T_{LBS} - T_{air}) \tag{6.6}$$

$$P_{wall,out} = h_{wall}A_{wall}(T_{wall} - T_{room}) \tag{6.7}$$

The resistance R changes value by increasing temperature according to Equation (2.4) with values given in Table 4.3. The dynamic model for the temperature rise inside the switchgear for each subsystem can be summed up as shown below in Equation (6.8) and (6.9).

$$\frac{dT_{LBS}}{dt} = \frac{1}{C}[(RI^2) - (h_{LBS}A_{LBS}(T_{LBS} - T_{air})] \tag{6.8}$$

$$\frac{dT_{wall}}{dt} = \frac{1}{C}[(RI^2) - (h_{wall}A_{wall}(T_{wall} - T_{room})] \tag{6.9}$$

7 Short duration overload test

This chapter shows the results of the temperature rise test with initial applied current at 400A, 500A or 630A before the system is overloaded with current at 700A, 800A or 850A. The test cases will be used later for comparison and verification of the thermal model. To be able to observe and analyze the overloading of the system it is decided to go over the IEC temperature limit of a temperature rise of 75K, but not exceeding the 115˚C limit. [3] Without exceeding the 75K temperature limit for the LBS, an overload after applying 630A would result in a temperature increase less than 10˚C. This is not enough at the LBS to determine the slope or gather any useful data. The temperature limit of the switch is decided based on the material of the switch, indicating the switch can handle a temperature of 115˚C. In on normal operation, the limits are not recommended to be exceed based on this assumption. This is done for research purposes of stressing the system.

7.1 Overloading with initially I = 400A

The result of the temperature rise test for applied current I = 400A until steady state and then overloaded with 700A is shown in Figure 7.1. Since the temperature never reached 115˚C when the applied current was 700A, a new steady state was reached. The LBS, enclosure air, outside wall and room temperature are plotted.

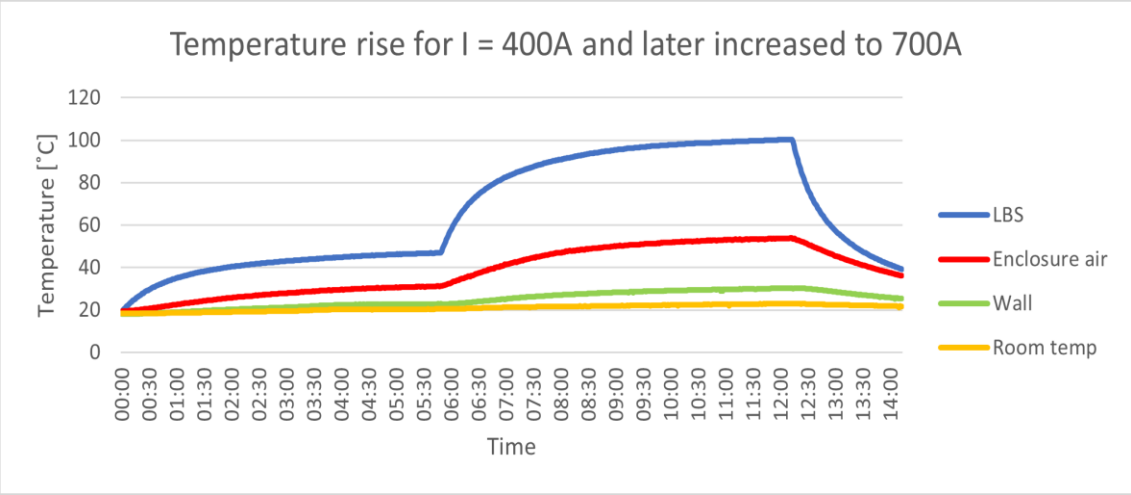

Figure 7.1: Temperature rise with I = 400A, which later is changed to 700A.

The system was applied with 400A until steady state, at approximately 5h and 50min. The current was then increased to 700A for the overloading. The LBS did not reach the 115˚C IEC limits, so the system stabilized at a higher steady state after about 12h and 15min of the total run time and approximately 6h and 45min after the current change. The current was then turned off and the system cooled down. At steady state with 700A, the LBS sensor measured the highest temperature at 100.4˚C. The final temperature rise of the LBS was 80˚C, 30˚C for the enclosure air and around 10˚C at the outside wall.

Figure 7.2 shows the temperature rise when 400A was applied until steady state, then overloaded with 800A. The current was turned off when LBS sensor reached 110˚C.

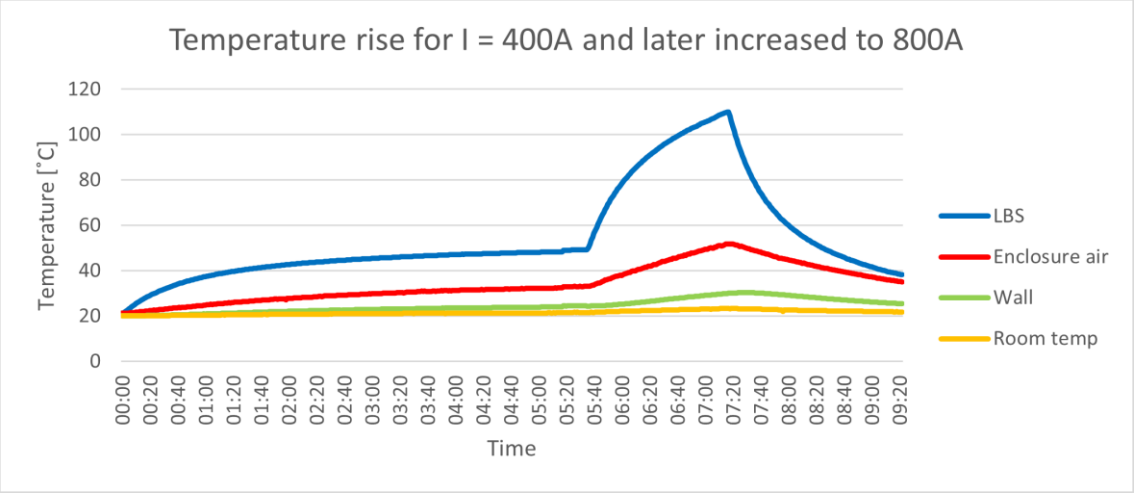

Figure 7.2: Temperature rise with initially I = 400A and later changed to 800A.

The system reached steady state after approximately 5.5 hours with I = 400A. The applied current was then changed to 800A. The temperature at the LBS reached almost it's 115˚C limit after approximately 2 hours under overloading. The current was then turned off, and the test was stopped. The enclosure air had a temperature increase of around 30˚C and the outside wall at around 10˚C.

The result of the temperature rise when the system was loaded with I = 400A until steady state and then overloaded with 850A (until the LBS temperature limit was almost reached) is shown in Figure 7.3.

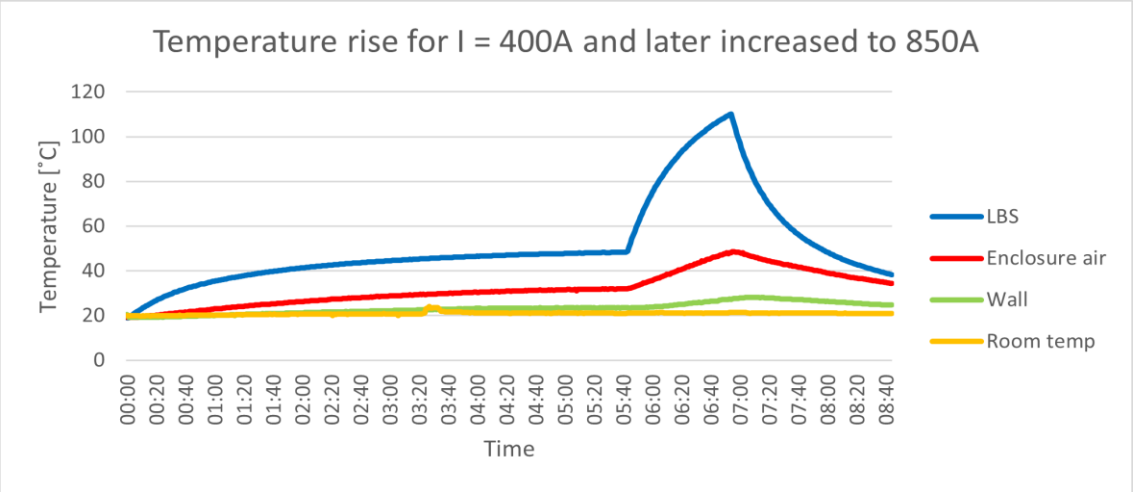

Figure 7.3: Temperature rise with I = 400A and overloaded later to 850A.

The temperature reached steady state after approximately 5h and 45min with 400A applied current. At this time, the current was adjusted to 850A. the LBS sensor was the first sensor to almost reach its temperature limit with 110˚C after about 1h and 15min after the overload started. The current source was then turn off and the temperature decreased. The temperature rise of the enclosure air was around 30˚C and slightly lower than 10˚C at the outside wall. The increase in room temperature at approximately 3.5h is unclear, but most likely an error or movement at the measurement point.

7.2 Overloading with initially I = 500A

The switchgear was loaded with I = 500A until steady state, before being overloaded with I = 700A. The result is shown in Figure 7.4.

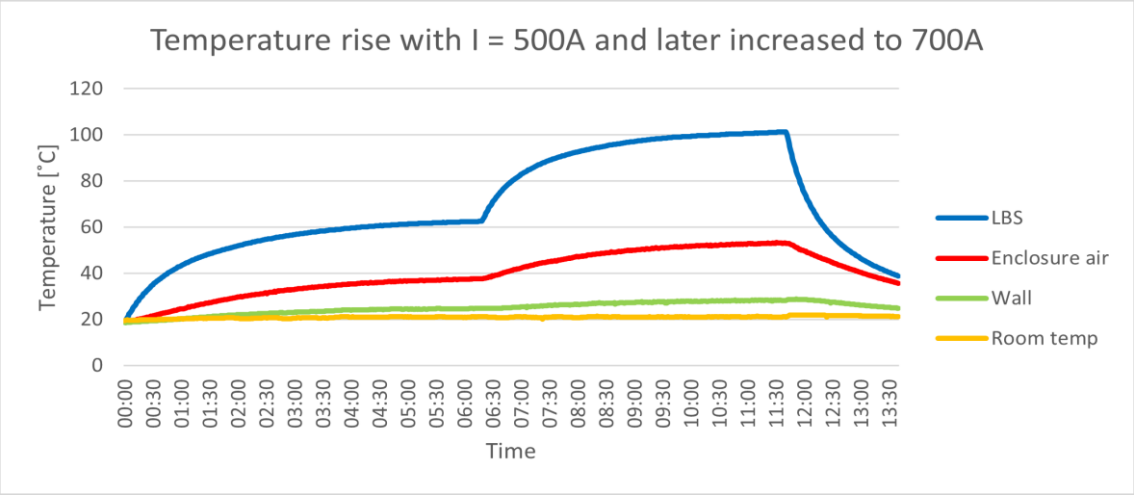

Figure 7.4: Temperature rise with I = 500A and later overloaded to 700A.

The system was first loaded with nominal current I = 500A until steady state was reached. This took approximately 6,5 hours. The applied current was then changed to 700A. The LBS sensor did not measure temperatures close to given 115˚C temperature limits, so a new steady state was reached. The highest measured temperature was by LBS sensor with 101˚C. After the new steady state was reached (at around 12 hours total runtime), the applied current was turned off and the system cooled down. The enclosure air had a temperature increase of around 35˚C and the wall at around 8˚C.

Figure 7.5 shows the change of temperature when the switchgear was overloaded with I = 800A after reaching steady state with applied current at I = 500A.

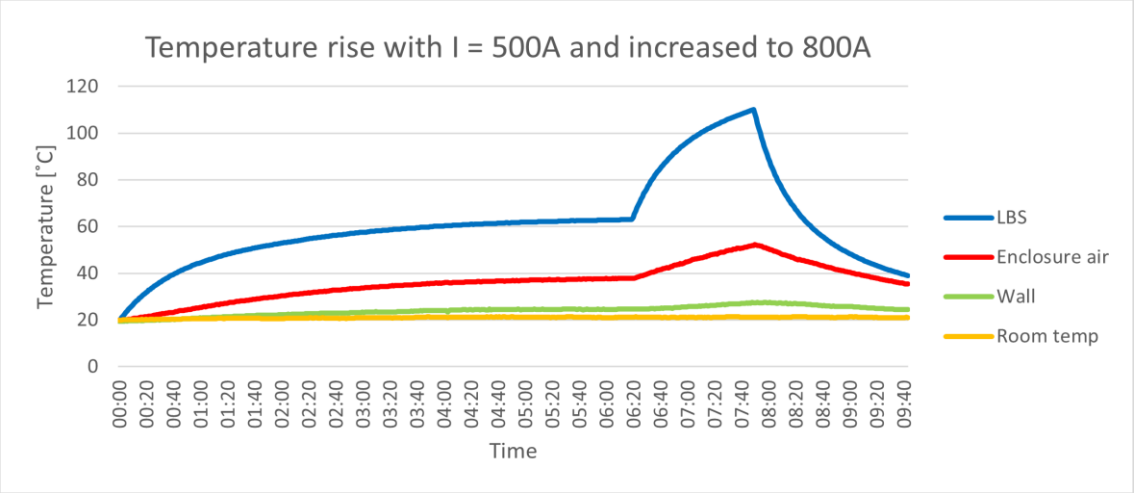

Figure 7.5: Temperature rise with initially I = 500A and later changed to 800A.

Steady state with 500A was reached after approximately 6h and 30min. Then the system was overloaded with 800A until the LBS sensor reached its temperature limit. This happened after approximately 7h and 50min after the applied current was changed. For the enclosure air, the temperature rise was around 30˚C and the around 5˚C at the wall.

Figure 7.6 shows the temperature rise test when the system was loaded with 500A until steady state and then overloaded with 850A for a shorter time period.

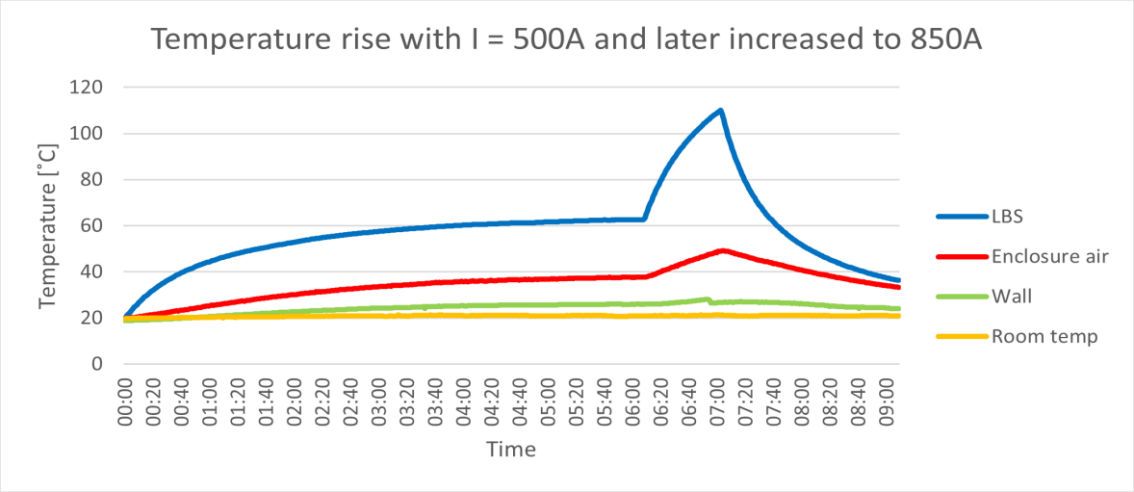

Figure 7.6: Temperature rise with I = 500A and later overloaded to 850A.

The temperature stabilized at steady state after approximately 6h and 10min with I = 630A. At this time the current was adjusted to 850A for the overloading. The LBS sensor was the first sensor to almost reach its temperature limit after about 1 hour of overloading. The current was then set to zero and the system cooled down. The temperature increase of the enclosure air was measured to be around 30˚C and around 5˚C at the outside wall.

7.3 Overloading with initially I = 630A

The system was loaded with 630A until steady state before being overloaded with 700A. Figure 7.7 shows the result of the temperature rise test.

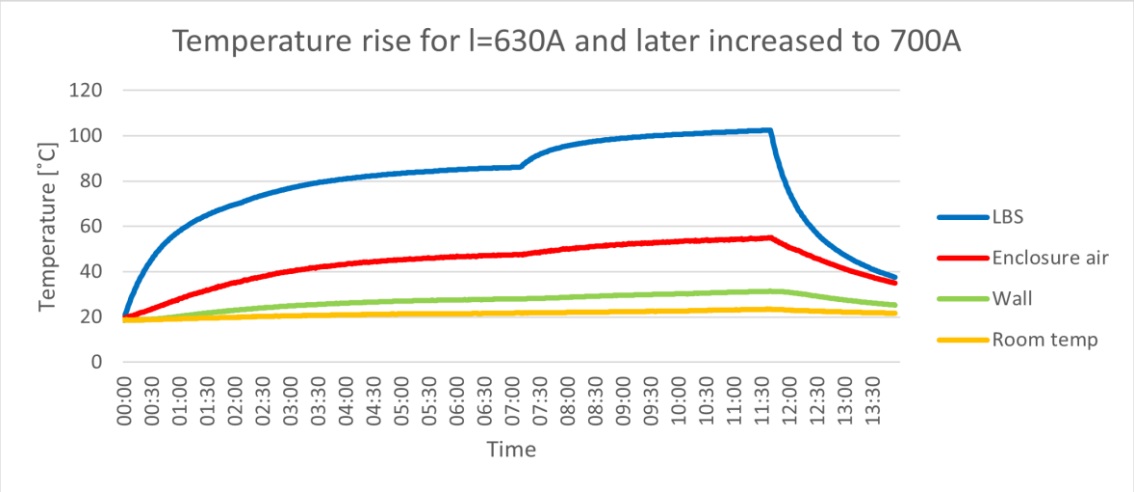

Figure 7.7: Temperature rise with nominal I = 630A and later overloaded to 700A.

The temperature reached steady state with applied current I = 630A after approximately 7 hours and 15min. At this time the system was overloaded by increasing the current to 700A. Before the overload, the temperature at the LBS was close to the IEC limit (75K temperature increase) at steady state. The temperature was measured to be at 86˚C, which is a temperature rise of 66K. Based on the IEC limit, the LBS can only have a temperature rise from steady state of less than 10˚C or 10K to be within this limit. It is not recommended to try to push this limit by overloading the system. For the purpose of the research in this thesis, the limit is exceeded to get usable values in development and verification of the thermal model. To be able to execute the overload tests, the ability of the material of the LBS is used. The LBS itself can handle temperature up to 115˚C according to IEC. Due to the temperature rise limit being exceeded, the risk of damaging the device, degradation etc. is higher. As done for the previous tests, the system was tested for overload until a temperature of 110˚C (close to 115 ˚C) was reached.

The LBS did not reach 110˚C during the overload and a new steady state was reach instead. The 75K temperature limit was reached approximately 1 hour after the current was changed. The temperature increase of the enclosure air was around 35˚C and 10˚C at the outside wall.

Figure 7.8 shows the system when it was loaded with 630A until steady state before being overloaded with 800A.

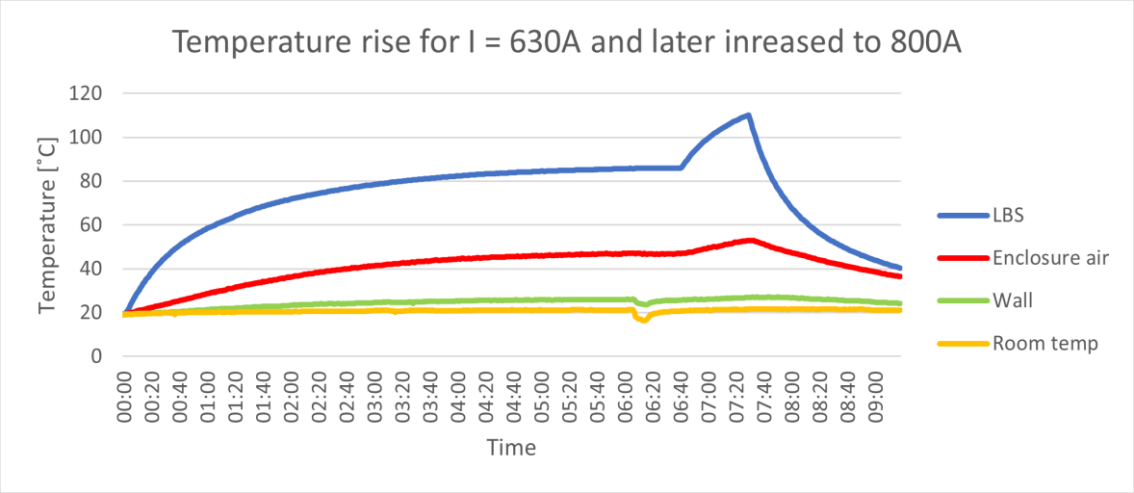

Figure 7.8: Temperature rise with I = 630A and later overloaded to 800A.

The system reached steady state after approximately 6h and 40min runtime. Then the system was overloaded with 800A for approximately 45min before the current was turned off. The highest measured temperature was 110˚C on LBS sensor after 7h and 30min runtime. The temperature increase at the enclosure air was around 30˚C and 7˚C at the outside wall. The dip in the measurement at the wall and room temperature after 6 hours and 15 min in the room temperature measurement was due to the gate in the lab being opened by other lab users. The gate was opened for about 15min and the outside air (in February) mixed with the inside air in the lab, decreasing the room temperature.

Figure 7.9 shows the temperature rise for the system when nominal current was applied until steady state. The system is then overloaded with 850A.

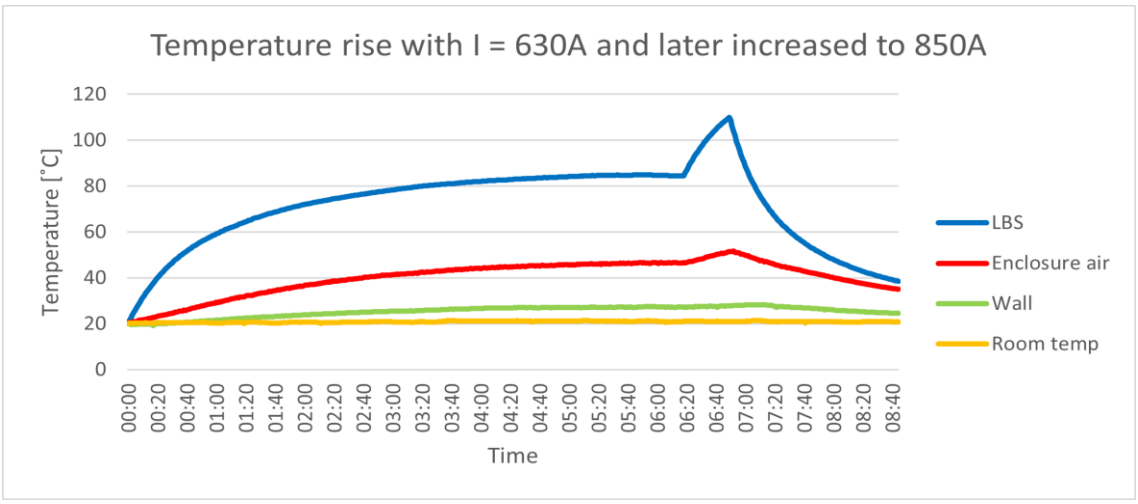

Figure 7.9: Temperature rise with initially I = 063A and later changed to 850A.

After the system reached steady state with I = 630A (after approximately 6h and 20min), the current is increased to 850A. LBS sensor reached 110˚C 30min later, after 6 hours and 50min

total runtime. The current was then turned off and the system cooled down. The temperature increase at the enclosure air was approximately 30˚C and 8˚C at the outside wall.

7.4 Discussion of the overload tests

The observation from comparing the different slopes of the overload currents (700A, 800A, 850A) shows that the temperature increase gets faster/ steeper with higher applied current. With the 700A current, the maximum temperature is around 100˚C or a temperature increase of 80K at the LBS. This is lower than the maximum temperature limit of 115˚C limit and 5K over the 75K temperature increase limit. For all 800A and 850A cases the applied current was turned off when the LBS reached 110˚C, which is close to the 115˚C limit and 15K over the temperature increase limit for the switch. Based on the initial temperature of the LBS at approximately 20˚C. The slope increase in the overload cases is more aggressive with higher currents, resulting in a shorter time before the temperature limits is reached as shown in Table 7.1.

Comparing the different initial current cases gives the observation that the chosen initial current highly affects the time the system can be overloaded. The LBS are in center of the analyze since it's the device which reaches its limits first and therefore the most vulnerable to damage. When 400A is the initial current, it takes longer time in the overload phases for the system to reach its limit. This is natural since the steady state temperature in the 400A cases is at approximately 50˚C compared to the 630A cases when the overload starts at nearly 90˚C. This means that if an overload is to be performed in the system, it is important to know the initial temperature, the temperature when the current is changed and the applied currents to be able to have an indication of possible overload time/ time before the limits are reached. From the test result, it can be observed that an overload current of 700A or higher results in a too high temperature at the LBS according to the IEC limits of the temperature rise for MV switchgears. It is therefore not recommended to apply a current larger than 630A if no temperature overload is intended.

Cooling is a very important factor in the possibility of overloading. In the system, cooling is mainly from the surrounding air (room temp at 20˚C), but can also be from the cables. If the cable connection to the switchgear has a colder temperature than the switchgear, it can be a part of the cooling. In situations, the cables can also be warmer than the switchgear and be a factor in warming the system. This shift can change during a test run. For this thesis, the focus is on the surrounding air as the main cooling factor to the system. A possible reason the outside wall temperature increase in most cases is 10˚C or lower can be the cooling effect from the surroundings. The room or ambient temperature is 20˚C. Even with the heat transfer through the walls in the second subsystem (which heats up the outside wall), the cooling effect has a large enough effect to prevent higher temperatures of this outside wall. A lower surrounding air temperature decreases the risk of overheating the system due to the higher cooling factor.

Due to the risk of damaging the system, it is not recommended to overload the system without having totally control over every factor influencing the system and its environment. Cooling can have an important influence on how much the system can handle. Some switchgears have more controlled ventilation and location which is in favor for safety. The risk of overloading the system several times can affect the switch and change its functionality

or increase the percentage of damaging and degradation. Which again can change or influence the temperature increase of the switch from one operation to the next.

If the system is overloaded, it is recommended to frequently check the devices inside the switchgear for damage. When it comes to overloading the switches in this thesis, the switches were checked for damage like discoloring after the tests. None was detected. The damaging or degradation risk is higher when the temperature limits are pushed, which is a concern. It is also possible to repeat resistance test over the LBS after each test run to look for changes and in that way detect degradation or damage. Table 7.2 shows an overview of the cooling time from max temperature until the temperature was down to the steady state value of the initial current.

Overload time for LBS:

Table 7.1 shows the time it takes all 9 test cases to go from the first steady state to the temperature limit for the LBS (75K increase) with an ambient temperature of 20˚C. [3]

Table 7.1: Overload time for each test case until a temperature increase of 75K is reached at LBS.

Overload I / **Initial I**	**700A**	**800A**	**850A**
400A	3h	1h	40min
500A	2h	40min	30min
630A	1h	15min	10min

Cooling time to steady state temperature for LBS:

The time it takes the temperature to cool down from max temperature to the start temperature of the overload period is shown in Table 7.2.

Table 7.2: Cooling time from max to steady state at the LBS.

Overload I / **Initial I**	**700A**	**800A**	**850A**
400A	1h	1h	45min
500A	30min	25min	20min
630A	10min	10min	10min

8 Data simulation

Chapter 8 shows the simulated results of the thermal model for the different temperature rise tests until steady state (I = 400A, I = 500A and I = 630A with and without overloading. The model and model parameters are based on information and data gathered from the physical test at the lab and calculated values. The presented results show the real temperature rise (lab data) vs. the simulated temperature rise from the thermal model. For verification of the thermal model, overload cases are tested and presented. The average deviation between the real data and the result of the thermal model is calculated to give an indication of the accuracy. The simulations shows the temperature rise at the LBS and the outside surface wall, which represents the two subsystems. The Python scripts are available in Appendix G.

8.1 Simulated vs. real temperature rise without overloading

The thermal model is developed to be able to simulate the temperature rise of the switchgear system. Defined by the subsystems LBS and surface wall. The continuously simulated result is developed based on the thermal model shown in Equation (6.8) and (6.9). The real data (dotted lines) are measurements from the real lab system and are retrieved from excel and plotted in the same Python program. The following figures shows the simulated and real temperature rise at the LBS and enclosure air. The changing input factor is the input current. Figure 8.1 shows the result when applied current is I = 400A, Figure 8.2 when I = 500A and Figure 8.3 when nominal current I = 630A is applied.

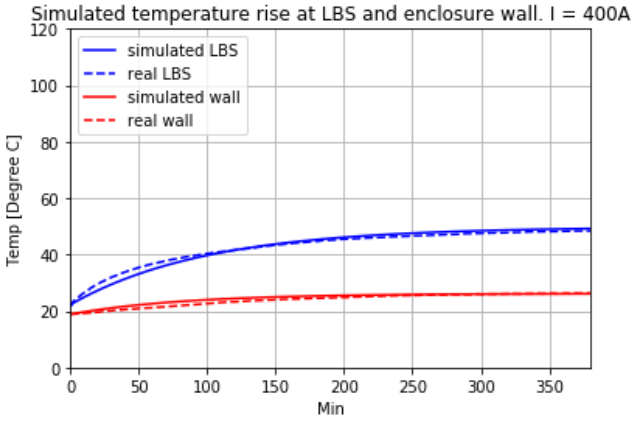

Figure 8.1: Simulated and real temperature rise with I = 400A.

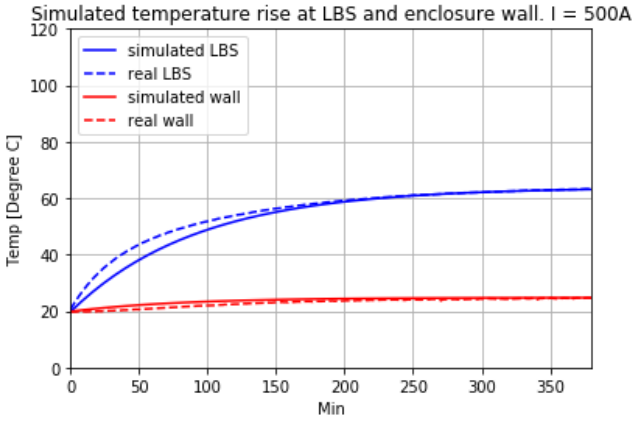

Figure 8.2: Simulated and real temperature rise with I = 500A.

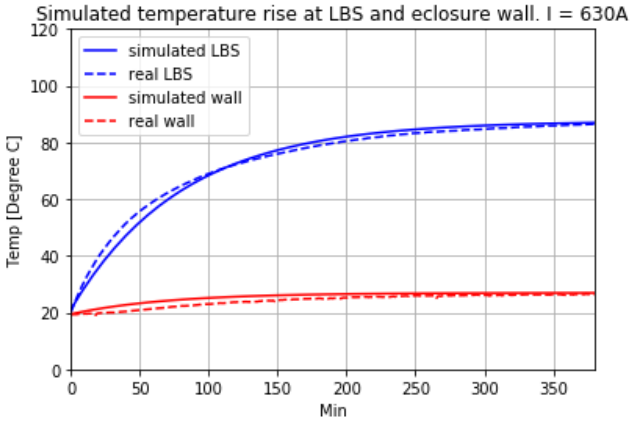

Figure 8.3: Simulated and real temperature rise with I = 630A.

The real vs simulated temperature rises at the LBS and outside wall gives similar plots. The simulated wall temperature is slightly larger than the real values at around 0-250min in all cases, but not notable. The initial and final temperature at the outside wall for the simulated and real data are equal. For the LBS there is a deviation between the real measurements and the simulated temperature from 0-200min in the 500A case. For the 400A and 630A the simulated data is slightly lower from approximately 0-100min and slightly higher after.

The inaccuracies can be due to the use of a simplified model, which do not include every aspect of the system and have some assumption and neglections included. This can affect the calculation of the parameter values and result in unideal values for the model. Since the simulated plots shows a slower temperature rise in the start of the simulation period, it can be assumed some of the input parameters are not optimal.

The calculated average error or deviation between the real and simulated model for each timestep (1min) is shown in Table 8.1. The average temperature deviation is calculated based on Equation (8.1).

$$\frac{error}{total\ (\Delta T)} * 100\% \tag{8.1}$$

Table 8.1: Average temperature deviation between the real and simulated models for the two subsystems.

	I = 400A	**I = 500A**	**I = 630A**
LBS ΔT [˚C]	26.2	43.6	67.5
LBS error [˚C]	1.4	3.3	1.4
LBS error [%]	5.3	7.6	2.1
Outside wall ΔT [˚C]	1.9	4.8	6.8
Outside wall error [˚C]	0.1	0.2	0.6
Outside wall error [%]	5.3	4.2	8.8

The average temperature deviation between the real data and simulated thermal model indicates how accurate the thermal model is compared to the real data. The deviation is presented in actual temperature error and in percentage. ΔT is the temperature deviation between steady state temperature and initial temperature for each case. The thermal model has an average error less than 10% in all cases, which are considered acceptable for the purpose of this study.

8.2 Simulated vs. real temperature rise with overloading

Simulation of the temperature rise with overloading at LBS and outside surface wall based on the thermal model and the real measurements on the switchgear is shown in this sub chapter. The temperature rise tests with overload is executed and simulated with the purpose of verifying the developed thermal model and the input parameters. The simulations are also used to analyze how accurate the thermal model predicts the temperature rise compared to the real measurement data. The change of applied current during the test run can be used to determine if the thermal model is good enough to predict how the temperature increase act for this specific switchgear system (based on the two subsystems) at higher applied currents than nominal current. Being able to predict the temperature rise accurately can be used in future test cases to disclude the need for executing a real temperature rise tests and to get an indication of how long it takes the subsystems to reach its temperature limits.

8.2.1 Parameter values from initial model

The 9 overload cases have initial current at 400A, 500A or 630A. At a given time, the current is changed to 700A, 800A or 850A. The given time is when steady state is reached. The only parameter values changed in the overload cases are the applied current. Parameter values like the time constant and heat transfer coefficient is not adjusted. This is to observe how the models preform with different currents without any changes.

Initial current at I = 400A:

Figure 8.4, Figure 8.4 and Figure 8.5 shows the simulated vs. real temperature rise with initial current at 400A. During the test period, the current is adjusted to respectively 700A, 800A and 850A.

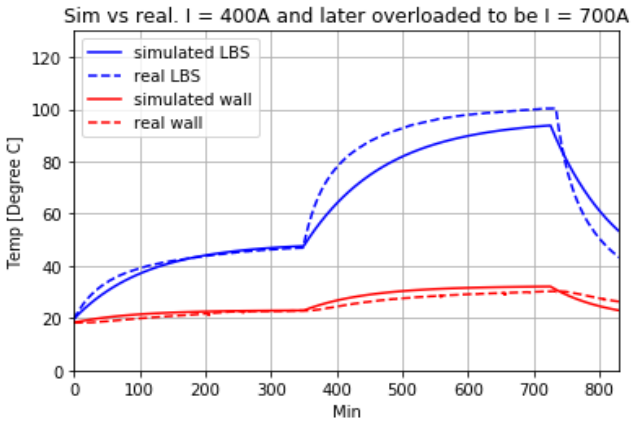

Figure 8.4: Sim vs real temperature rise at subsystems for I = 400A, which is changed to I = 700A during runtime.

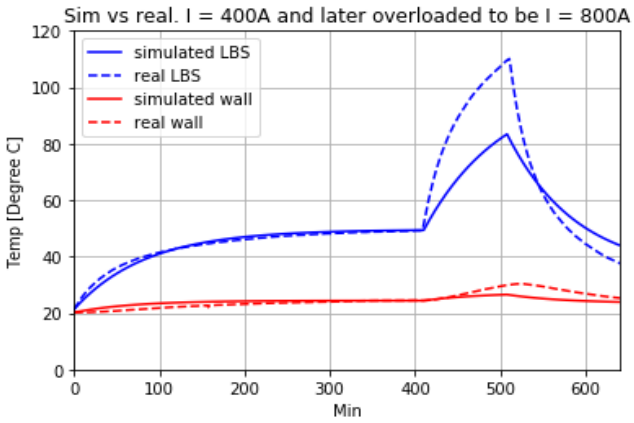

Figure 8.5: Sim vs real temperature rise at subsystems for I = 400A, which is changed to I = 800A during runtime.

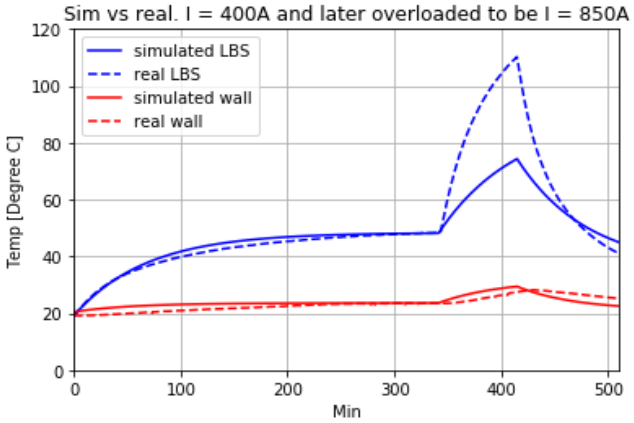

Figure 8.6: Sim vs real temperature rise at subsystems for I = 400A, which is changed to I = 850A during runtime.

For all overload cases, the thermal model seems to fit the real data best with only a small deviation when the applied current is 400A. When the current is changed to either 700A, 800A or 850A, the deviation between the real data and simulated model is larger. The simulated model of the LBS predicts a lower temperature than the real data in all cases. For the wall temperature, the simulated model predicts a higher temperature in the 700A and 850A cases. The prediction of the wall temperature in the 800A case is lower than the real data. In the 700A and 850A cases, the simulated temperature of the wall is higher than the real measurements.

Initial current at I = 500A:

The simulated vs. real temperature rise with initial current at 500A and overloaded later is shown in Figure 8.7, Figure 8.7 and Figure 8.9. Respectively, the current is overloaded with 700A, 800A and 850A in each figure.

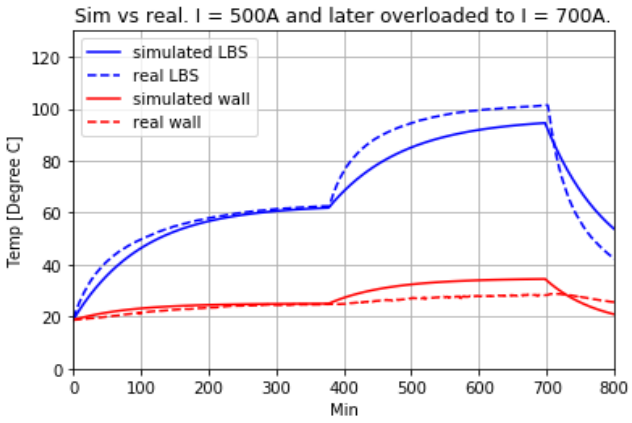

Figure 8.7: Sim vs real temperature rise at subsystems for I = 500A, which is changed to I = 700A during runtime.

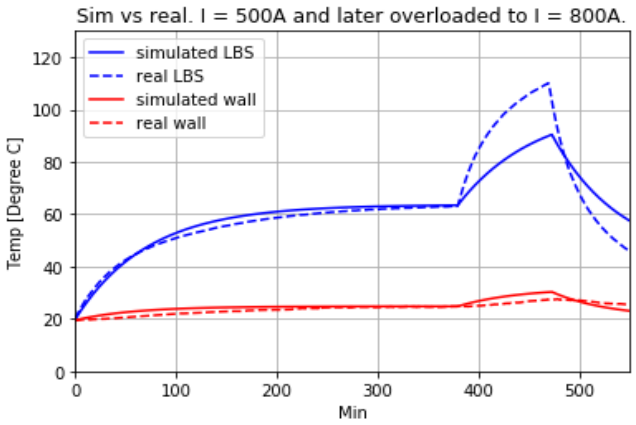

Figure 8.8: Sim vs real temperature rise at subsystems for I = 500A, which is changed to I = 800A during runtime.

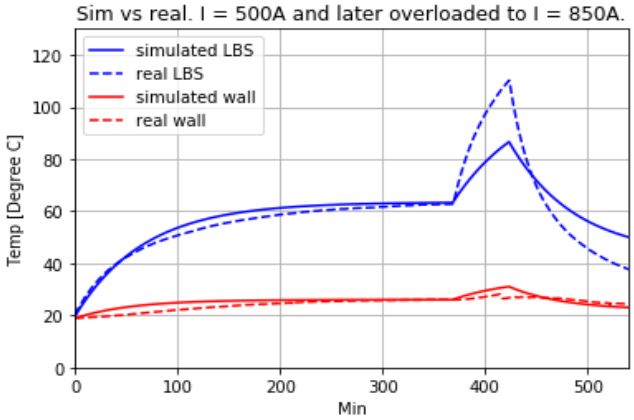

Figure 8.9: Sim vs real temperature rise at subsystems for I = 500A, which is changed to I = 850A during runtime.

When the initial current (500A) is applied, the deviation between the real and simulated data is small compared to the overload phases. The simulated model predicts a lower temperature at the LBS in the overload period in all cases, while the prediction of the outside wall temperature in the overload phases is higher than the real data. Compared to the cases when the initial current was 400A, the deviation between the simulated and real data in the overload phase for the LBS is similar or smaller when the initial current was 500A. At the wall, the deviation in the overload period is larger in the 500A-700A case compared to the 400A-700A. The deviation between the real and simulated temperature rise is more similar in the 400A-800A compared to 500A-800A case, and in the 400A-850A case compared to 500A-850A.

Initial current at I = 630A:

Figure 8.10, Figure 8.11 and Figure 8.12 shows the simulated vs. real temperature rise with initial current at 630A (nominal). The current is during the runtime adjusted to respectively 700A, 800A and 850A.

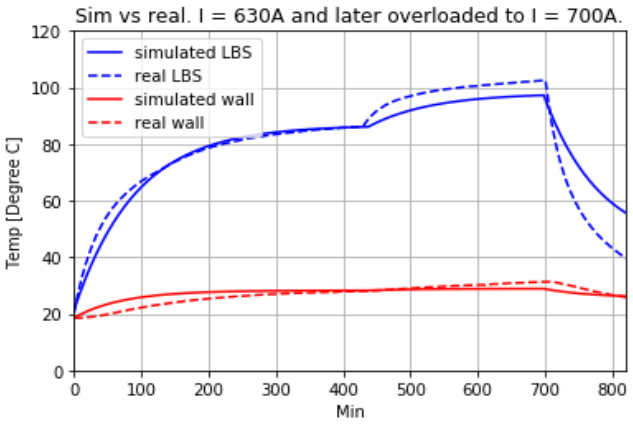

Figure 8.10: Sim vs real temperature rise at subsystems for nominal I = 630A, which is changed to I = 700A during runtime.

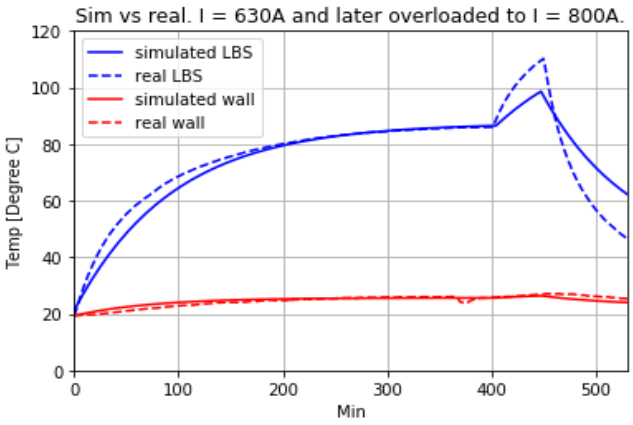

Figure 8.11: Sim vs real temperature rise at subsystems for nominal I = 630A, which is changed to I = 800A during runtime.

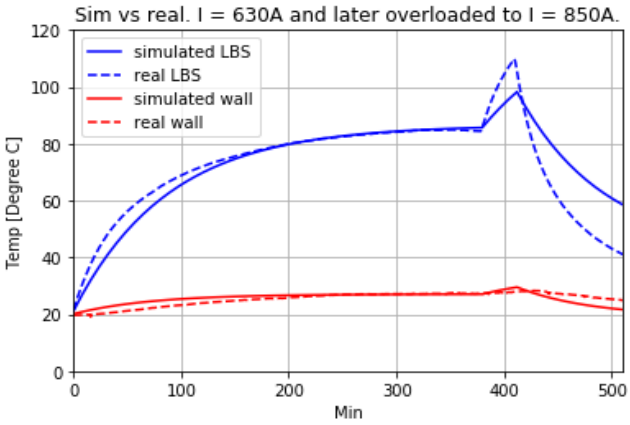

Figure 8.12: Sim vs real temperature rise at subsystems for nominal I = 630A, which is changed to I = 850A during runtime.

The deviation between the real and simulated temperature rise is smaller when the initial current is applied than in the overload phases. This is similar to the previous tests with 400A and 500A as initial current. For the LBS, the real data is higher than what the simulated model predicts in all cases. The real data is also higher at the wall in the 700A case, while the real data is lower in the 850A. In the 800A case, the real and simulated data in the overload phase is similar. Compared to the tests with 400A and 500A, the overload phase for the 630A cases at the LBS have a lover deviation between the real and simulated temperature rise. For the wall, the simulated and real temperature rise in the overload periods are more similar in the 630A cases.

Average deviation/ error:
The average deviation between the simulated and real models are calculated for the overload cases. The calculations are available in Appendix H. The final result is presented in Table 8.2 for the LBS and in Table 8.3 for the wall. The approach is equal the description in section 8.1.

Table 8.2: Average error between the real and simulated plots for the LBS.

Overload I / Initial I	700A	800A	850A
400A	5.3%	3.9%	4.4%
500A	4.4%	1%	0.3%
630A	0.8%	1.1%	7.8%

Table 8.3: Average error between the real and simulated plots for the wall.

Overload I / Initial I	700A	800A	850A
400A	11%	5.7%	6.7%
500A	19.8%	7.9%	8.7%
630A	1.6%	6%	21.5%

The average error describes the average temperature deviation or error between the real and simulated data. It includes the entire test run period from the current is turned on, adjusted and turned off. As seen from Table 8.2 the error changes for the LBS between 0.3% and 7.8%, indicating an average error lower than 10% between the real data and the simulated data. For the outside wall temperature, the average temperature error is between 1.6% and 21.5%. The high deviation between the real and simulated data in the 630A-850A case and 500A-700A case is due to the larger deviation between the real and simulated data in the overload and cooling period.

The average error does not view the actual max and min error. Based on the results presented in the previous figures, the error or deviation fluctuates largely in most cases. In the plots, there is usually a period of time where the deviation is higher, and a period of time where deviation is close to zero. The average temperature deviation can instead only be used as an indication of the thermal model's accuracy. The simulated thermal model is more accurate

based on the calculated average deviation to the real data for the LBS than the outside wall. In most cases the error or deviation between the simulated and real model is smaller when the initial current (400A, 500A or 630A) is used and a larger deviation in the overload or cooling periods (700A, 800A or 850A).

The simulations of the LBS have a less steep temperature rise than what the real data shows. The thermal model underestimates the possible overload times, which indicates that the time constant of the overload period in the thermal model is not correct or fitted for the situations. This is most likely due to the time constant used in the overload cases is the same as for the initial current. Based on the underestimations, the thermal time constant should be shorter for higher applied currents. The next step (sub chapter) will be to manually adjust the time constant in the overload periods/ for the overload currents of the 9 cases. This is done to try to improve the simulation by reducing the deviation between the real and simulated temperature rise in the overload periods.

8.2.2 Manual adjustment of time constants

Based on the observations in section 8.2.1, the next step is changing the time constant in the overload periods of the 9 cases to better fit the real data. Based on the test cases in section 8.2.1, the thermal model is not able to predict accurately the temperature increase when the current is changed. The lower predictions indicate a to high time constant. Instead of running temperature rise tests with 700A, 800A and 850A (which would have resulted in too high temperatures based on the temperature limit of the LBS), the ideal time constant for each 9 cases would be gathered by manually adjusting them in the software code, Appendix G. The procedure is to change (only) the time constant in the overload phase in the code until the temperature increase seems reasonable and are more similar to the real temperature rise. The found/ new time constants are collected and a pattern is developed to be able to indicate how the time constant changes based on the initial and overload currents.

Initial current at I = 400A:

Figure 8.13, Figure 8.14 and Figure 8.15 shows the simulated thermal model vs the real data when the initial current is 400A. For these cases, the time constant is manually adjusted in the overload period (when the current is 700A, 800A or 850A) to fit the real data. Overview of the time constants are shown in Table 8.4 and Table 8.5.

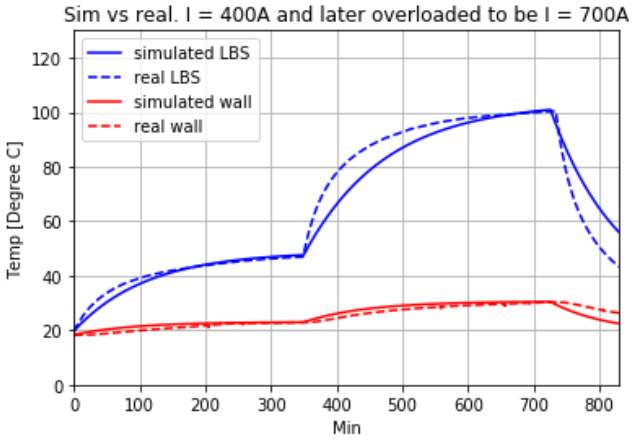

Figure 8.13: Sim vs real temperature rise with manually adjusted time constant when I = 700A. Initial current is 400A.

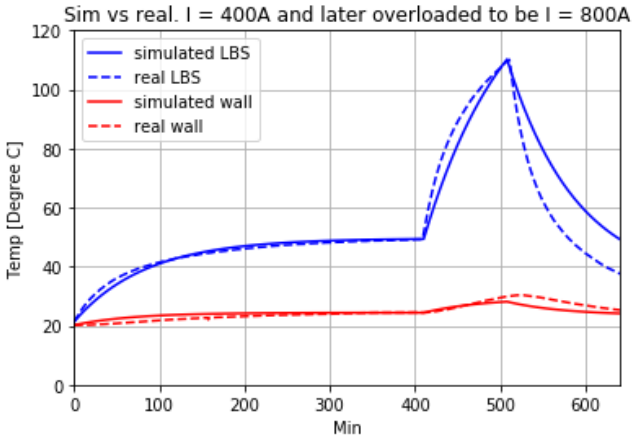

Figure 8.14:Sim vs real temperature rise with manually adjusted time constant when I = 800A. Initial current is 400A.

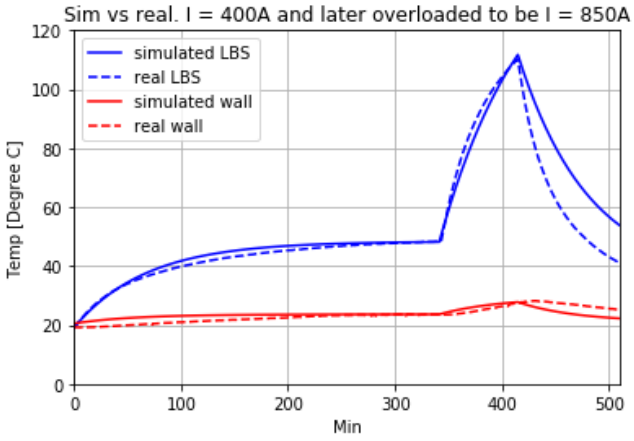

Figure 8.15: Sim vs real temperature rise with manually adjusted time constant when I = 850A. Initial current is 400A.

The new time constant in the overload period at the LBS is changed from 90min to 82min in the 400A-700A case, 58min in the 400A-800A and 45 min in the 400A-850A. For the outside wall, the new time constant is 170min in the 400A-700A case, 180min in the 400A-800A case and 190min in the 400A-850A case. The new simulated maximum temperatures of the three test cases at the LBS and wall is similar to the real data. Which indicates that the new time constant in the overload periods are more accurate for these cases. The optimal time constant for the LBS decreases for each case, while it increases at the outside wall. A decreasing time constant indicates that the slope of the temperature increase is steeper, and the temperature reaches maximum temperature quicker. For the LBS, the time constant decreases for increasing overload current (with same initial current and overload start temperature) with nearly 40min. This indicates that the overload current highly affects the time constant.

A possible reason the wall is not affected as the LBS is the similar temperature deviation between start and end temperature in all cases. In theory, the slopes are steeper for higher

overload currents which should have resulted in the time constant decreasing with increasing overload current. The opposite is present, which can indicate that only adjusting the time constant in the code is not ideal. It is also possible the program is not detailed enough to adjust accurate for so similar temperature increases.

With the new time constants, the temperature rise in the overload period does not match the real data exactly and some deviation is present, but the deviation is smaller compared to using the unadjusted time constants. No changes are done in the cooling period from step 1.

Initial current at I = 500A:

The simulated thermal model with manually adjusted time constant for the overload period vs the real data is shown in Figure 8.16, Figure 8.17 and Figure 8.18 when the initial current is 500A. Table 8.4 and Table 8.5 shows the time constant in the overload period.

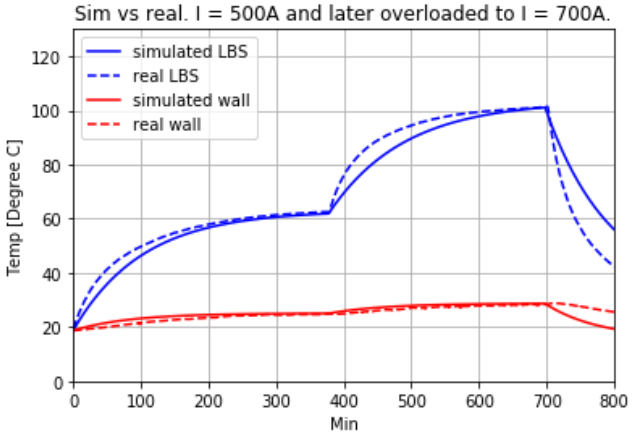

Figure 8.16: Sim vs real temperature rise with manually adjusted time constant when I = 700A. Initial current is 500A.

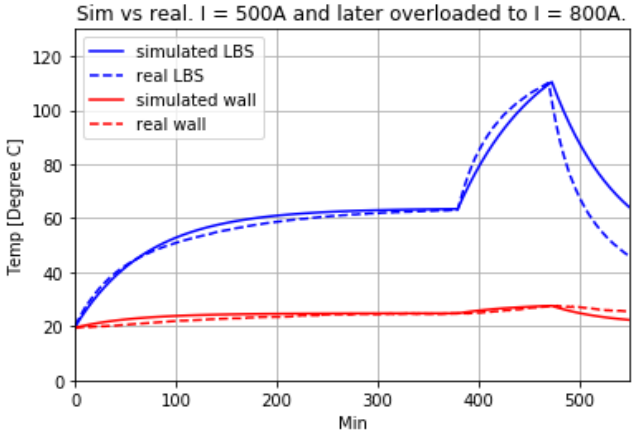

Figure 8.17: Sim vs real temperature rise with manually adjusted time constant when I = 800A. Initial current is 500A.

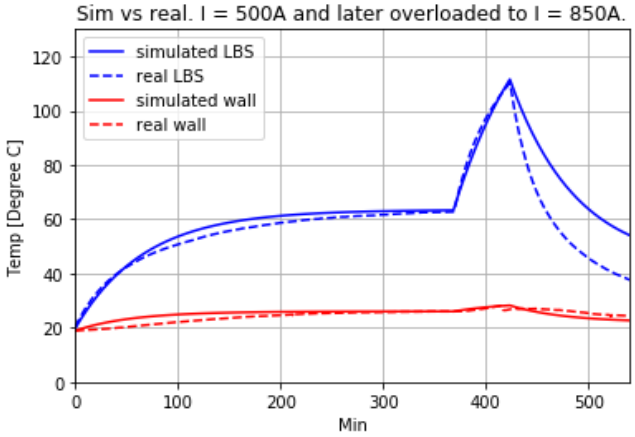

Figure 8.18: Sim vs real temperature rise with manually adjusted time constant when I = 850A. Initial current is 500A

Adjusting the time constant in the overload period improves the accuracy of the cases when the initial current is 500A as well. The time constant at the LBS when the current is 500A is

80min. In the 500A-700A the time constant is adjusted to 73min, 56min in the 500A-800A case and 48min in the 500A-850A case. The situation is similar to the previous three cases (initial current at 400A), which has a decreasing optimal time constant. The time constant at the outside wall is changed to 200min for the 500A-700A and 500A-800A cases and 220min at the 500A-850A case. The new time constants for the outside wall are not as expected with an increasing time constant with increasing overload current. Possible reasons are similar to the three previous cases when initial current was 400A. The new plots show a more similar simulation between the real data and the simulated thermal model in the overload period, and equal maximum temperature. The parameter values in the cooling period are not adjusted.

Initial current at I = 630A:

Figure 8.19, Figure 8.20 and Figure 8.21 shows the real data vs the simulated thermal model with manually adjusted time constant in the overload period. The initial current in all cases is the nominal current 630A.

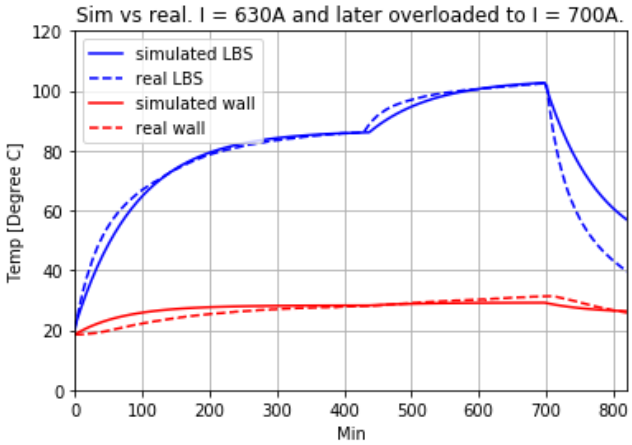

Figure 8.19: Sim vs real temperature rise with manually adjusted time constant when I = 700A. Initial current is 630A.

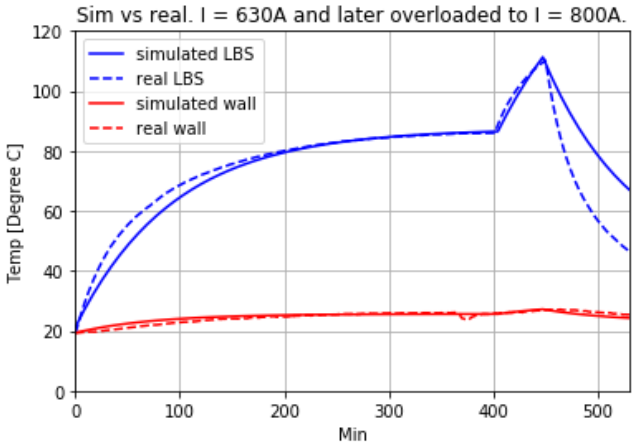

Figure 8.20: Sim vs real temperature rise with manually adjusted time constant when I = 800A. Initial current is 630A.

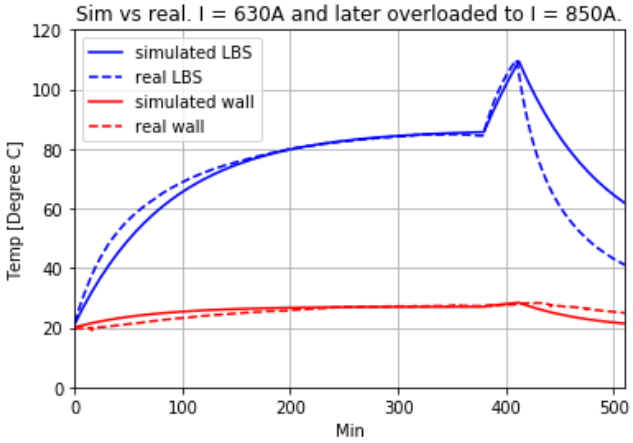

Figure 8.21:Sim vs real temperature rise with manually adjusted time constant when I = 850A. Initial current is 630A.

The time constant at the LBS is adjusted for the 630A-700A in the overload period to 64min, in the 630A-800A case to 54min and in the 630A-850A case to 50min. The time constant when the current is 500A is 70min. The thermal model predicts more accurate overload period with the adjusted time constants compared to using the 500A time constant. For the outside wall, the time constants are not adjusted in the three cases. The code was not able to get any improvements by changing the time constant when the overload current was on, probably due to the small temperature change. The parameter values in the cooling period are not changed from step 1.

Manually adjusted time constant in overload period:

Table 8.4 and Table 8.5 shows the time constant in the overload period of the 9 cases, which gives the most similar temperature rise as the real data. The time constant is adjusted manually. The time constant at the LBS and wall when the current is 400A, 500A or 630A is shown in Table 5.4.

Table 8.4: Manually adjusted time constant for the overload period for the LBS.

Overload I / **Initial I**	**700A**	**800A**	**850A**
400A	82min	58min	45min
500A	73min	56min	48min
630A	64min	54min	50min

Table 8.5: Manually adjusted time constant for the overload period for the wall.

Overload I / **Initial I**	**700A**	**800A**	**850A**
400A	170min	180min	190min
500A	200min	200min	220min
630A	135min	135min	135min

Figure 8.22 shows the thermal time constant vs applied current. The blue dots show the time constant at initial currents. The orange dots show the time constant at the overload currents, when initial current is 400A. The green dots show the time constant when 500A is the initial current and the red dots show the time constants when 630A is the initial current. The linear trendlines are included and the actual time constant values are displayed over the dots. Figure 8.23 shows the thermal time constant with same setup for the outside wall.

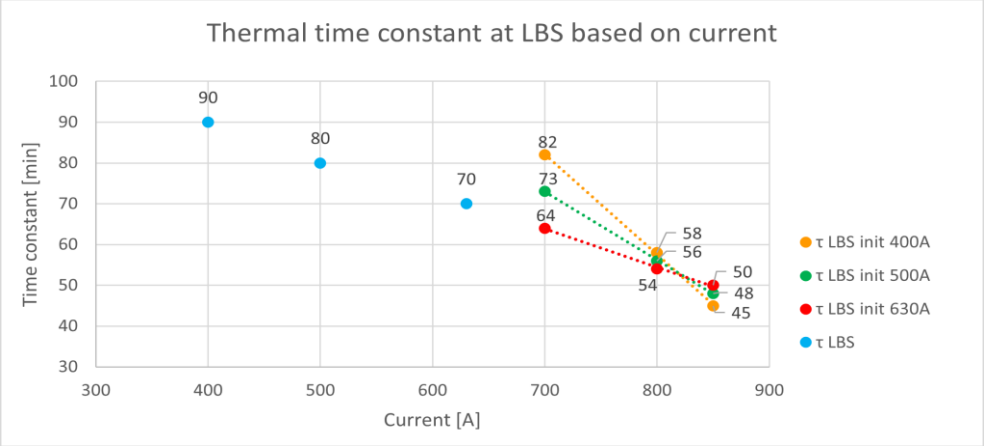

Figure 8.22: Time constant at LBS for different currents.

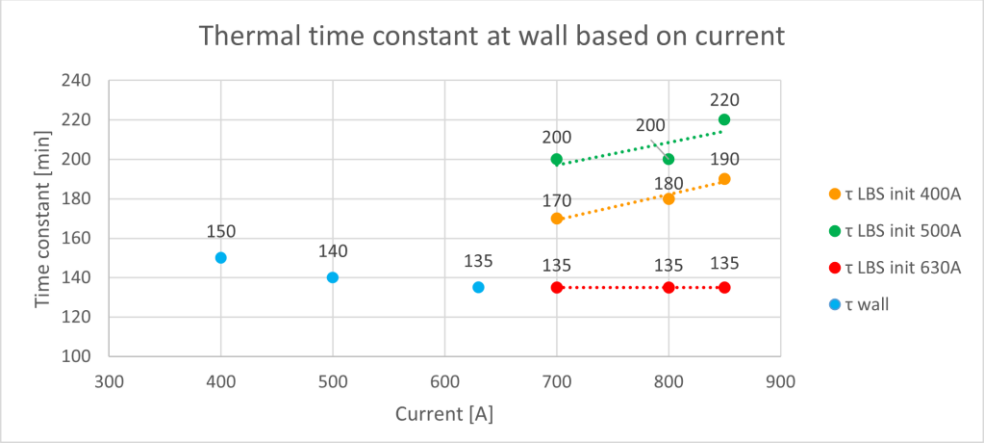

Figure 8.23: Time constant at outside wall for different currents.

The time constants for the LBS and wall do not seem to fit a similar pattern for the overload periods. For the LBS, the time constants decreases with increasing overload current. For each of the overload currents, the ideal time constant is different based on the initial current. For the 700A overload current, an initial current of 400A gives the highest time constant. The opposite is shown when the overload current is 850A. Here an initial current of 400A gives the lowest time constant. Figure 8.22 shows that the initial current affects the time constant of the overload current, but the patterns doesn't correspond to each other. The time constant at the overload current for the wall do not seem to follow a natural pattern, where the time constant increases for higher overload currents and is fixed when the initial current is 630A.

Since the time constants are manual adjusted in the simulated thermal model in each individual case, it is not unexpected that the model predict different ideal time constant values in the overload cases. This can be due to the different accuracy of the other model parameter for each case. It is logical that some error is present when trying to determine the time constant, especially since the actual steady state temperature and slope at the 800A and 850A case is unknown. A more ideal method is to perform a real temperature rise test for the overload current at the lab to gather the time constants. This is not possible with the

temperature restrictions for this thesis. Instead, some adjustments and assumptions on how the time constants changes with increasing current can be done.

Average deviation/ error:
Table 8.6 and Table 8.7 shows the average deviation between the real data and the simulated thermal model with adjusted time constant. The calculation is available in Appendix H.

Table 8.6: Average error between the real and simulated plots for LBS.

Overload I / Initial I	700A	800A	850A
400A	1.9%	1.8%	3%
500A	1.6%	3.1%	4.5%
630A	1.3%	1%	6%

Table 8.7: Average error between the real and simulated plots for wall.

Overload I / Initial I	700A	800A	850A
400A	1.4%	2.9%	2.7%
500A	2.1%	0.8%	4.3%
630A	2%	4%	8.9%

The average deviation/ error is smaller than before the time constant was adjusted in the overload periods. The average error for the LBS and wall is less than 10%, which is considered acceptable for this thesis work. This indicates the importance of the time constant. Some of this deviation is due to the cooling period, where the time constant is not changed.

8.2.3 Practical adjustment of time constants

As seen from section 8.2.2 the manually adjusted time constant in the simulation results has less error between the real data and the simulated thermal model, compared to not changing the time constant as seen in section 8.2.1 This indicates that changing the time constant is important for the simulated thermal model to give more accurate predictions. The time constants in section 8.2.2 do however does not follow a natural pattern for different initial currents. To be able to make further simulations for several currents, it is decided to simplify

the time constant pattern. This is mainly used to be able to create an overview where the possible initial current and overload current can be determined based on the wanted overload time.

The adjustment of time constant for the LBS is to linearize the changing time constant as close to the result from Figure 8.22 with the actual measured time constant from the 400A, 500A and 630A (blue dots) and the time constant when the initial current is 630A (read dots). This gives the new time constants as shown in Table 8.8, which is considered the best fit for the LBS.

Table 8.8: New time constants for LBS (best fit).

	400A	**500A**	**600A**	**700A**	**800A**	**900A**
τ_{LBS} [min]	90	80	70	60	50	40

For the time constants at the wall, the simulation is not able to give realistic results as shown in section 8.2.2. Since the temperature rise at the outside wall can be considered similar for several cases and have a temperature rise around 10˚C for most cases, it can be assumed the time constant do not change significantly in the simulation. In real life and based on the actual measurements from chapter 6, it can be observed that the slope of the temperature rise is different for different applied currents. Based on the simulation however, it seems like the changes is too small for the simulation to make good predictions of the time constant. To simplify the problem, it is decided to set the time constant of the outside wall fixed at 140min for all applied currents.

8.3 Possible overload times

The possible overload times for different applied currents are presented in

Figure 8.24. Both of the IEC limits [3] are taken into account. The first limit to be reached is the 75K temperature increase at the LBS, which becomes the base for this chart. The figure values on the x-axis and y-axis are presented as factors where the x-axis shows the initial current divided on the rated current (630A). The y-axis is the overload current divided on the rated current (630A).

The data from this chart is based on the simulated thermal model with the simplification from section 8.2.3 where the thermal time constant is changed. By using the thermal model simulation, the possible overload current for different overload times can be determined. Several data points are gathered from the simulated thermal model where the initial current is set, the overload time chosen, and the possible overload current can then be read from the chart. The gathered data points are shown in Appendix I. Due to using the thermal model with the new simplifications for time constant, the result in

Figure 8.24 does not correspond exactly to the real overload time from the temperature rise tests on the lab model or the previous overload simulations from section 758.2 or 8.2.2. To get the equations for the different curves, the data points is implemented in Excel and a polynomial trendline is drawn between the points. The equations are used in a Python script

which prints out the result of Figure 8.24. The Excel sheet and Python code is available in Appendix I.

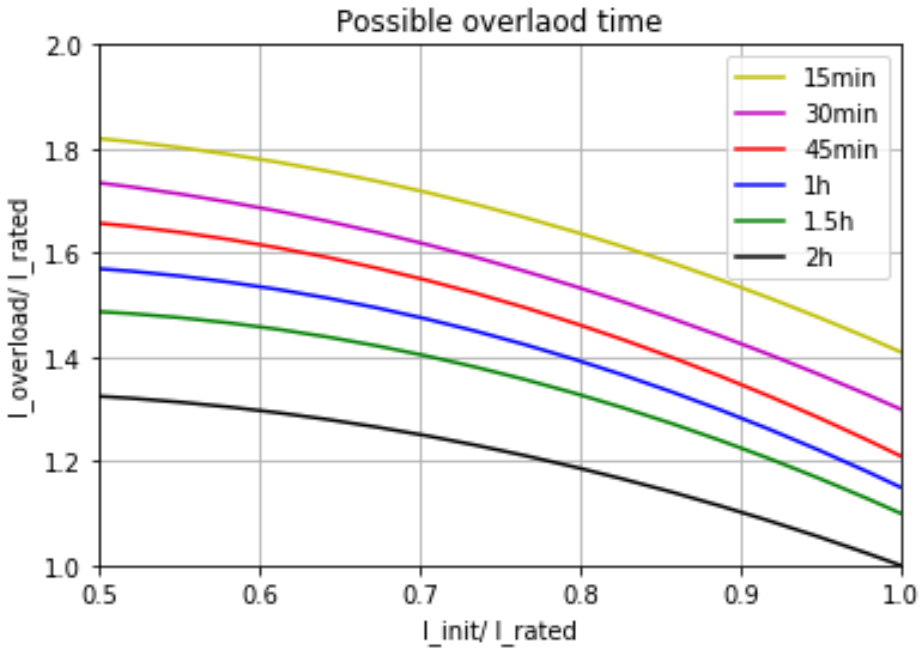

Figure 8.24: Possible overload times.

Some possible overload times from the laboratory test is presented in Table 7.1. An overload time of 2h is possible from the lab tests when the initial current is 500A and the overload current is 700A. From the chart, an overload time of 2h when the initial current is 500A gives a possible overload time of approximately 1.2 (750A). From the lab experiments, the system can be overloaded for 1h in the 400A-800A case and the 630A-700A case. An initial current of 400A and an overload of 1h gives about 1.5 (950A) based on Figure 8.24. If the initial current is 630A and a 1h overload is wanted, the possible overload time is about 1.15 (725A) based on the chart. A 30min overload is possible from the lab experiments when the initial current was 500A and the overload current was 850A. From Figure 8.24, an initial current of 500A and an overload time of 30min corresponds to approximately 1.5 (950A). An overload time of 15min is possible based on the lab experiments in the 630A-800A case. 15min overload time when the initial current is 630A gives 1.4 (880A) from the chart.

From the comparison, the chart in Figure 8.24 allows for a higher overload current than the result from the lab experiments. The chart allows for an overload current up to 150A higher than the measurements from than lab (in the 400A-800A case). For the other compared cases, the allowed overload current is estimated to be between 25A and 100A higher than what is observed from the lab measurements. This is due to the deviation between the thermal model simulations and the actual real temperature rise of the system from the lab experiments. For the development of the chart, the time constant was adjusted from the optimal time constants in each case to be able to develop the plots. This increases the deviation between the real and simulated temperature rise, which leads to the deviation occurring in the chart from the actual tests result on the real system. This makes the chart risky to use since it indicates a higher allowed overload current, then what the result from the laboratory tests does. The chart is self

is accurate to the thermal model with the simplified time constant pattern, and predicts the temperature rise accordingly.

9 Discussion

The discussion chapter includes the laboratory setup with placement of the sensors, the temperature rise tests and the resistance test. Further the thermal model and parameter values are discussed, before the results of the simulation of the real temperature rise vs the simulated thermal model.

9.1 Laboratory setup

Switchgear system:
The switchgear is an MV metal enclosed switchgear located at the high current lab at USN campus Porsgrunn. The top/back plate of the switchgear is removable. The switchgear has three cable modules, one vacuum switch breaker and is a 4-way unit. The switchgear is not a homogeneous or symmetric device, which makes it more difficult to analyze compared to a symmetric device like a cable. This result in some simplifications for the development of the thermal mode, which increases the possibility for inaccuracies in determining the heat transfer in the system. The switchgear is designed to be filled with SF_6 gas, but is filled with air instead. This can affect the temperature increase. Based on published papers [46], the temperature increase is lower when air is used instead of SF6 gas within a switchgear enclosure. This result in the pressure being equal ambient pressure. The changes on the switchgear can be assumed to change the temperature rise of the switchgear compared to the standard device.

The current path within the enclosure consists of three phases where each phase have one busbar, two LBS and ten bolted connections. Each LBS includes an open/close contact and a rotating contact. The highest temperature compared to the IEC temperature limits are usually on the LBS. [5] [21] The IEC limits are certificated for 40˚C room temperature. [3] In the lab at USN, the room temperature was around 20˚C, which leads to a larger cooling factor from the surroundings compared to a 40˚C room temperature. For system overloading with a higher applied current than nominal current, the lower room temperature can affect the temperature rise and result in the possibility to overload the system longer or to a higher temperature without damaging the devices. This is utilized in the thesis to allow for a higher temperature rise than IEC, but this might not be possible in other surroundings.

When overloading the switchgear system, not only the switchgear must be included in the analysis. The connected devices like cables and transformers must be able to withstand the present overload. This can decrease the possible overload time for the extended system view. The surroundings (not only room temperature but surrounding devices or equipment) should as well be included in the analysis. For the connected devices, it is possible to find the time constants (as done for the switchgear) to determine the temperature rise. The transformer usually have a larger time constant due to the larger mass. From [2], the time constant for XLPE cables was found to be 40min in flat formation and around 60min in trefoil formation which can be a limiting factor.

Thermocouples, sensors:
Temperature rise tests with and without overloading and a resistance test was executed. 20 thermocouple sensors was used for the temperature measurements. The sensors accuracy is ± 1.5˚C [42] For this thesis, the uncertainty is acceptable. The sensors were placed on the inside and outside of the switchgear to measure temperatures of the devices, surface areas and air. Due to the large surface areas of the device, the possibility of not measuring at ideal location is high. The temperature might not be homogenously distributed throughout the surface area, leading to small temperature variation of the surface. In this thesis work, only one measuring point it used for each surface area. The chosen location might not be the most representing measuring point. This can increase the inaccuracy of the ideal temperature measurements for a location.

If the sensor's measuring point is not placed directly on the surface, the sensor might measure the air temperature instead of the surface temperature. Since the thermocouples are taped to the enclosure walls and devices, it is possible some unwanted movements can change the sensor's locations and measure the air instead of the surface. This was not detected in this thesis work. Unwanted movements of the sensors can also happen within one test or between different tests. This can lead to some inaccuracy, but none large deviation at any of the sensor values was detected, exception one time when the laboratory door was opened (Figure 7.8).

9.2 Lab tests

Temperature rise test:

The applied current falls during the temperature rise test due to increasing resistance. This was monitored and adjusted during the experiments, but results in a more approximately analysis of the test results (only one decimal in the values). Since all three phases must be adjusted separately, the applied current was not always exactly equal between the three phases, which also leads to some inaccuracy.

Steady state was declared after manually calculating when the temperature deviation between one hour was less than 1˚C. How quickly it was observed that steady state had occurred can have been different between the tests. This can lead to some misinformation in the plots, but is not affecting any of the calculated parameters or results in other way. The different measurement points within one test might reach steady state at different times as well. This can result in the temperature at one sensor location already has reached steady state, while waiting for other sensors to measure steady state.

Only one test was executed each day, which results in a small deviation in initial temperature between the tests. The room (and initial) temperature differs between 18-21˚C. This can affect the thermal model's prediction of the temperature rise in each case by increasing the inaccuracy between the different cases. Based on the thermal model, this is not the main reason for the deviation of the simulated temperature rise vs the real lab measurements.

Resistance test:

The resistance test performed for determining the resistance as a function of temperature was executed based on utilizing the decreasing temperature and measuring the voltage drop over the LBS and phase L1. The voltage drop was measured when the actual temperature at the LBS matched the steady state temperature (at the LBS) for different applied currents (Table 4.2). A possible source of inaccuracy here is the problem of being able to measure the voltage drop at the exactly right temperature. The first challenge is the time it takes to observe the decreasing temperature and execute the measurements. The temperature decreased quicker when it was higher, which increases the possibility of the temperature not being exactly at steady state when the measurements was done. Another source of inaccuracy is the voltage drop measurements. The voltage drop values measured by the multimeter fluctuated to a degree (less than 1mV). The fluctuation was higher, the warmer the system was.

9.3 Thermal model and parameter values

Thermal model:

The thermal model is developed as a simplified model. Compared to other possible solutions, like creating a 3D model where all detail of the switchgear is included and drawn, this developed model has more simplifications and might be less accurate. Some of the simplifications are the exclusion of some devices inside the enclosure, a symmetric and homogenic device, other possible heat or cooling sources and specify direction of heat flow.

The thermal model is based on the general energy balance. The energy balance assumes a lumped system. In real life the switchgear is not a lumped system where only the input and output nodes represent the system. This simplifies the description of the system and excludes information like internal movements in the volume/system. The general thermal model itself (before any values are defined) is flexible and can be used on most switchgear systems.

The thermal model shows the temperature rise of one LBS and on one of the outside surface walls. The warmest point on the current path (and the system) was found to be one of the LBS on current path L1, but only the LBS on current path L1 and L2 was measured. To be able to get values from every aspect of the system for more accurate temperature overview, more sensors would have needed to be used. As described in [1], a temperature rise test on a MV switchgear with 134 sensors was executed. Instead for this thesis, the phases and the temperature change were assumed similar for several devices and on larger surface areas. This is based on the focus on this thesis, which is to estimate the temperature rise on the warmest location in the switchgear enclosure. A challenge is determining the location of the wall subsystem. In real life the heat transfers through all walls, the roof and the bottom of the enclosure flows at different rates, due to factors like the wall thickness and that warm air rises over colder air. When creating a thermal model to describe the heat transfer, it was chosen to use one of the side walls. But if any of the other walls was to be used instead, most of the parameter values must have been adjusted based on the result from 5.3.2. Only describing the heat transfer through the enclosure at one location, can lead to the misunderstanding that the heat transfer trough the enclosure walls, top and bottom are similar in all locations. It also disclude describing the actual heat transfer through these neglected walls, which can be necessary to know on a real system.

Resistance:

The resistance changes with temperature. In this thesis, the theoretical equation (Equation (2.4)) for resistance change was used to predict the resistance at warmer temperatures. This was compared to the calculated resistance from the measured voltage drop on the lab model. The comparison resulted in a deviation up to 24μΩ between the two methods. The solution was to adjust the theoretical equation to fit the measured values. This effects how the temperature rise of the system progresses in parameter calculations for the thermal model. This resulted in an equation which corresponds to the actual measured resistance. However, it is always possible with errors in the measurements, which would have changed the resistance increase and effect the temperature rise simulations. Since the resistance change is designed based on actual measurements, the equation is fixed to this system and must be adjusted for other systems.

Time constant and heat transfer coefficient:

The heat transfer coefficients and time constants of the LBS and wall was determined for each initial current (I = 400A, I = 500A and I = 630A). The time constants decreased for higher applied current and was between 90min and 70min at the LBS and 135min and 150min at the wall (Table 5.4). These values are retrieved from the steady state lab results and directly reflects the time it takes the temperature to reach 63.2% of the temperature increase to steady state. The values can therefore be considered accurate in the simulation when the associated currents are applied. The heat transfer coefficients are calculated based on the resistance, applied current, surface area and temperature deviation. Some inaccuracy can be present in these parameter values (like resistance measurements and surface area), but small enough to be neglected. The heat transfer coefficient for the steady state cases was between 10.6 W/m^2K and 13.2 W/m^2K for the LBS and between 12.6 W/m^2K and 15.4 W/m^2K at the wall. The heat transfer coefficient at the LBS is given to be within 10-17 W/m^2K in [33] when emission is closer to 0 than 1 (black body). This corresponds to the calculated values in this thesis where the heat transfer coefficient is 13.2 W/m^2K when nominal current is applied. The heat transfer coefficient at the wall is higher than expected. The values are higher than at the LBS for equal applied currents, but it seems more natural that the heat transfer is easier from the LBS to the surrounding air, than from the enclosure air to the outside surface wall. A higher heat transfer coefficient (for same applied current) indicates an “easier” heat transfer. [51]. A possible reason the heat transfer coefficients at the wall is higher than expected can be due to some error in the calculations or parameter values like cooling, emission or effective surface area. No reference values was found in published papers for comparison on a similar side wall.

Flexibility and use of the thermal model:

The thermal model parameters are determined specifically for this switchgear and for the chosen subsystems. This makes the developed thermal model and model parameters less flexible for other systems and might not give accurate results. The model also depends on values and parameters which (in this thesis) only is found by executing lab tests. It is therefore not possible to determine the model parameters with accuracy for a switchgear without doing some experiments. Even the formula for the resistance had to be adjusted to

this specific switchgear to get values fitted the system. However, if another switchgear system is wanted to be overloaded, the simplified thermal model can be adjusted to fit the system. The methods for lab experiments and calculations can be used to develop the thermal model to describe the temperature rise of another system.

Having simulations of the temperature rise of the switchgear is useful. The predictions will give an indication of the possible overload current and time for the system and can simulate final temperature/ temperature rise of the device. If an overload is needed for a short term, the model can predict if the system will be within the temperature limits or exceeds it. The amount of possible damage can then be considered whether the overload is worth it or not. The model can also be used to save time by not needing to perform hour long temperature rise test for each wanted overload situation.

9.4 Simulated thermal model vs. real temperature rise

Steady state simulation:

The accuracy of the calculated parameter values in this thesis is challenging to analyze without comparing it to the actual process. This is done when the simulation of the thermal model is plotted next to the real lab measurements. As seen from the real vs. simulated temperature rise of the different cases (Figure 8.1, Figure 8.2 and Figure 8.3), the thermal model gives similar plots as the real data in the steady state cases (no overload). There is still some deviation in the increase period, which indicates that the thermal models input parameter is not optimized to fit the data set at every time step. The initial and final temperatures is however equal in all steady state cases and the calculated average deviation is less than 10% (Table 8.1).

Simulation with overload:

Further, the thermal model was tested with overload cases to verify the results. First the model parameters found for the initial currents (I=400A, I=500A and I=630A) was used in the overload phases (no adjustment except changing the applied current. See section 8.2.1). This resulted in a less accurate temperature rise prediction in the overload period compared to the real data. The thermal model predicts a lower temperature in the overload period than the real system actually measured. If this model was used as a method to determine how long an overload could be (worst case scenario), the real system would have a steeper temperature rise to a higher final temperature than what the simulated model predicts. This could end up overheating and damaging the system. It was assumed the time constant was unideal in this solution and some adjustment was needed in the overload period. The inaccurate predication is most likely due to the thermal model being designed based on the steady state situations (I = 400A, 500A or 630A). Other possibilities are in the design and development of the thermal model parameters as described in the previous subchapter (9.3). This is unlikely since the model works well in the steady state cases.

Based on the overload simulations with no adjustments (except changing the current for the overload period), it was observed that the thermal time constant was not optimal for the overload periods. The most ideal solution would have been to preform temperature rise test until steady state at 700A, 800A and 850A. This is not possible due to the temperature limits

of the LBS. Another possibility is to develop a program to analyze and adjust specific parameters to optimize the temperature rise within given borders. Due to lack of time and the scope of this thesis a less complicated method was chosen. The time constant in the overload periods was manually adjusted until the temperature rise of the thermal model was as accurate to the real data as possible.

For the LBS and wall, the lower error between the real and simulated data with the new time constants (Table 8.6 and Table 8.7 compared to Table 8.2 and Table 8.3) indicates that the optimalization was needed and more accurate for the model. The time constants at the LBS followed the natural pattern with decreasing time constant for increasing overload current, but the effect of the different initial currents was not as expected as observed by the trendlines in Figure 8.22. This is most likely due to a combination of gathered the time constants only based on what's most ideal in each case and only adjusting the time constant parameter in the simulation. The time constant in the overload periods at the wall did also not follow the expected pattern (as shown in Figure 8.23). A possibility is the temperature rise is too small for the model to present the temperature increase well. Resulting in the time constant not being as expected, or not change in the case when initial current was 630A. Even with these challenges, the thermal model with adjusted time constant resulted in an average error less than 10% (Table 8.6 and Table 8.7). This indicates that the thermal model needs some adjustments in the overload phases to perform accurate simulations.

Possible overload time chart:

Figure 8.24 shows the possible overload times for different currents based on the simplified thermal model with the adjusted time constant pattern from section 868.2.3. The possible overload times corresponds to the result from the simulated adjusted thermal model and not the real laboratory test shown in section 7.4. Compared to the actual possible overload time from the lab measurements, the solution presented in section 8.3 gives not the same results. The chart allows for a higher overload current (up to 150A higher), than what is gathered from the lab experiments. This makes the chart risky to use for real systems since it in worst case scenario can seem like the system can handle a higher overload current compared to what was gathered from the measurements on the real system. This can lead to overheating and damage of the system. To be able to determine and create an overview of the actual possible overload times for different initial and overload currents it is needed to have more data, either from real laboratory tests or from a model where the slope of the overload current until steady state is known for all currents. However, the chart corresponds correctly to the developed thermal model simulations with the simplified time constant pattern (from section 868.2.3).

10 Conclusion and future work

This chapter includes the conclusion of the thesis and possible suggestion for future work.

10.1 Conclusion

The physical tests were executed at the high current lab at USN campus Porsgrunn on a MV metal enclosed switchgear. The temperature rise test was performed until steady state for the three initial current cases 400A, 500A and 630A. Further, overloaded tests were performed where the system was run until steady state with one of the three initial currents, before being overloaded with 700A, 800A or 850A. The longest overload possible is 3h when the initial current is 400A and later changed to 700A. The shortest overload time of the test cases is 10min when the initial current is 630A and changed to 850A.

Based on the gathered data, a thermal model was developed. The thermal time constant for the steady state cases was between 70min and 90min for the LBS subsystem and between 135min and 150min for the wall subsystem. The heat transfer coefficient for the steady state cases was determined to between 10.6 W/m^2K and 13.2 W/m^2K for the LBS, and between 12.6 W/m^2K and 15.4 W/m^2K at the wall subsystem.

The thermal model was implemented in Python 3.7 and simulates the predicted temperature rise at the LBS and outside wall. The real data from the temperature rise tests were exported to Python and plotted next to the predictions from the simulated thermal model. The average error between the real data and the simulated model when the system was run to steady state (no overload) was less than 10%.

For verification of the thermal model, 9 overload cases were simulated. The predicted temperature rise in each case (based on the thermal model) was plotted vs the real measured temperature rise. With no adjustments in the thermal model, the highest deviation was 21.5% at the wall. In these cases, the simulation of the thermal model predicts a lower maximum temperature than what the real temperature rise was in all cases. The next step was to manually adjust the time constant in the overload period for each case to reduce the deviation. This led to a deviation less than 10% in all cases.

A chart was developed to describe the possible overload current based on initial current and overload time. The chart is based on the thermal model with some simplifications. However, compared to the real lab measurements the chart overestimates the allowed currents with up to 150A.

Based on the thesis work, the thermal model is able to predict the temperature rise of the subsystems with some deviation. The thermal model is only designed for the specific MV switchgear at the lab. The method, lab work and procedures can be used on other similar systems, but the measurements and calculation of parameter values must be redone for the new switchgear. This includes dimensions of the switchgear and devices, resistances, heat transfer coefficients, thermal time constants, initial, final and room temperatures.

10.2 Future work

The first suggestion for future work regards the development of the thermal model. In this thesis, a simplified model was developed and implemented in Python 3.7. As described in section 2.6, a more detailed model is possible to create by using any of the mentioned software. This will result in a more detailed thermal model either for validation of the simplified model or for more detailed visual heat transfer process of the MV switchgear system.

The second possibility of future work is simulation and execution of temperature rise tests with more than one overload period in one test run. In a real system, it might be wanted for the switchgear to be able to be overloaded more than one time during one test run. As described in section 1.1, the switchgear does not necessary only run at rated current all the time. Creating simulations based on the thermal model and executing test runs when the current is adjusted several times (maybe following a normal switchgear operation) can be a possibility. This can be used to validate and optimize the thermal model and hopefully make the thermal model more useful in daily life or for normal operation.

It is also possible to analyze the cooling period for the system to be able to determine and predict the needed resting time for the system between several overload periods. This can be analyzed on the real lab model and included in the Python scripts. Further, this can be used to develop overview charts of possible loading scenarios.

In this thesis, the focus was on developing the thermal model, determining the parameter values and gathering needed theory to create the model. A possibility of future work on this model can be to optimize and analyze in more detail the input parameters. Especially the heat transfer coefficient or heat conductivity (heat transfer coefficient times area), heat capacity, thermal time constant and the resistance.

Since the thermal model is created based on one MV switchgear, the model is not designed for other systems. Future work can be to redo the procedures and adjust the input parameters to analyze how this solution work on other switchgear systems. It is also possible to analyze how the implementation and use of the thermal model needs to be adjusted for different switchgear systems and go deeper into surrounding factors outside the definition of the switchgear system. One example is the effect of room temperature regarding cooling.

References

[1] X. Dong and U. Kaltenborn, "DYNAMIC THERMAL SIMULATION OF GAS INSULATED SWITCHGEAR," in *Cired 21st International Conference on Electricity Distribution*, Frankfurt, 2011. [Online]. Availible: http://www.cired.net/publications/cired2011/part1/papers/CIRED2011_0495_final.pdf

[2] H. Kwak, "Thermal capacity and loading assessment for 24kV XLPE-insulated cables in air," Dept. Electro, IT and cybernetics. USN, Porsgrunn, 2021.

[3] *High-voltage switchgear and controlgear*, NEC IEC 62271-1 2017, 2017.

[4] X. Wang et al., "Precise Multi-Dimensional Temperature-rise Characterization of Switchgear based on Multi-Conditional Experiments and LPTN Model for High-Capacity Application," 2020. [Online]. Available: https://www.researchgate.net/publication/340486213_Precise_Multi-Dimensional_Temperature-rise_Characterization_of_Switchgear_based_on_Multi-Conditional_Experiments_and_LPTN_Model_for_High-Capacity_Application

[5] H. Xia et al., "Temperature Rise Test and Analysis of High Current Switchgear" in Distribution System," in *The Journal of Engineering*, 2018. [Online]. Available: https://www.researchgate.net/publication/328044840_Temperature_Rise_Test_and_Analysis_of_High_Current_Switchgear_in_Distribution_System

[6] M. Ruusunen , K. Leviska and P. Hietaharju, "A Dynamic Model for Indoor Temperature Prediction," in *energies*, Oulu, 2018. [Online]. Available: https://www.mdpi.com/1996-1073/11/6/1477

[7] Z. Yu et al., "Precise Multi-Dimensional Temperature-rise Characterization of Switchgear based on Multi-Conditional Experiments and LPTN Model for High-Capacity Application," 2020. [Online]. Available: https://www.researchgate.net/publication/340486213_Precise_Multi-Dimensional_Temperature-rise_Characterization_of_Switchgear_based_on_Multi-Conditional_Experiments_and_LPTN_Model_for_High-Capacity_Application.

[8] S. Øygarden, "Heat transfer mechanisms in MV load break switches," Dept. Electro, IT and cybernetics. USN, Porsgrunn, 2017.

[9] ASCO Power Technologies. "What Is a Switchgear?". https://www.ascopower.com/us/en/resources/articles/what-is-a-switchgear.jsp (accessed Jan. 10, 2022).

[10] EATON Powering Business Worldwide. "Switchgear: fundamentals of medium-voltage switchgear". https://www.eaton.com/us/en-us/products/medium-voltage-power-distribution-control-systems/switchgear/fundamentals-of-medium-voltage-switchgear.html (accessed Jan. 20, 2022).

[11] SINTEF. "New gases for GIS - long-term reliability and fundamental understanding of insulation properties". https://www.sintef.no/en/projects/2021/new-gases-for-gis-long-term-reliability-and-fundamental-understanding-of-insulation-properties/. (accessed Feb. 5, 2022).

[12] H. Breuer. "Alternatives for SF6 urgently sought". https://www.siemens-energy.com/global/en/news/magazine/2020/alternatives-for-sf6.html (accessed Feb. 17, 2022).

[13] ABB. "Air insulated switchgear - Medium Voltage". https://new.abb.com/medium-voltage/switchgear/air-insulated (accessed Jan.15, 2022).

[14] Electrical Installation wiki. "Ventilation in MV Substations". https://www.electrical-installation.org/enwiki/Ventilation_in_MV_Substations (accessed Feb. 8, 2022).

[15] Alfanar. "AIS - AIR INSULATED SWITCHGEAR". https://www.alfanar.com/AIS (accessed Jan. 15, 2022).

[16] ABB. "ZX0.2 gas-insulated switchgear (IEC)". https://new.abb.com/medium-voltage/switchgear/gas-insulated-switchgear/iec-gis-primar-distribution/ansi-iec-gas-insulated-primary-switchgear-zx0-2 (accessed Feb. 17, 2022).

[17] E. Fjeld, "EPE2419 Physics of Electrical Engineering", Lecture: "Electrical Resistance", University of South-Eastern Norway, 2021.

[18] E. Fjeld, "EPE2419 Physics of Electrical Power Engineering", Lecture: "Heat Generation", University of South-Eastern Norway, 2021.

[19] M. Kriegel et al., "Application and Benchmark of Multiphysics Simulation Tools for Temperature Rise Calculations," in *Cigre For power system expertise*, Paris, 2021.

[20] E. Fjeld, "EPE2419 Physics of Electrical Power Engineering", Lecture: "Electrical contacts", University of South-Eastern Norway, 2021.

[21] E. Fjeld, W. Rondeel, K. Vaagasaether, M. Saxegaard, P. Skryten and E. Attar "THERMAL DESIGN OF FUTURE MEDIUM VOLTAGE SWITCHGEAR," in *Cired 23rd International Conference on Electricity Distribution*, Lyon, 2015. [Online]. Available: https://openarchive.usn.no/usn-xmlui/bitstream/handle/11250/2438595/CIRED2015_1090_final.pdf?sequence=2&isAllowed=y

[22] R. Holm, *Electric Contacts Theory and Applications*,4th ed. Berlin, Germany: Springer, 2010.

[23] KENT INDUSTRIES INC, "The Importance Of Tightning Torque On Electrical Installations". https://kentstore.com/blog/the-importance-of-tightening-torque-on-electrical-installations/ (accessed Mar. 27, 2022).

[24] E. Fjeld, "EPE2419 Physics of Electrical Power Engineering", Lecture: "Stationary steady-state condition", University of South-Eastern Norway, 2021.

[25] E. Fjeld, "EPE2419 Physics of Electrical Power Engineering", Lecture: "Energy balance and heat transfer", University of South-Eastern Norway, 2021.

[26] Wikipedia. "Time constant". https://en.wikipedia.org/wiki/Time_constant (accessed Feb. 15, 2022).

[27] E. Fjeld, "EPE2419 Physics of Electrical Power Engineering", Lecture: "Electrical Resistance", University of South-Eastern Norway, 2021.

[28] X. Dong and U. Kaltenborn, "Dynamic thermal model simulation of gas insulated switchgear," in *21st International Conference on Electricity Distribution*, Frankfurt, 2011. [Online]. Available: http://www.cired.net/publications/cired2011/part1/papers/CIRED2011_0495_final.pdf

[29] Y. A. Cengel, *Heat Transfer; A practical Approach*, McGraw-Hill, 2002.

[30] T. Gløsmyr, "Influence of thermal radiation in MV switchgear," Dept. Electro, IT and cybernetics. USN, Porsgrunn, 2019.

[31] M. Szulborski et al., "Transient Thermal Analysis of NH000 gG 100A Fuse Link," in *energies*, Basel, 2021. [Online]. Available: https://www.researchgate.net/publication/349771801_Transient_Thermal_Analysis_of_NH000_gG_100A_Fuse_Link_Employing_Finite_Element_Method

[32] CORROSIONPEDIA. "Oxidized Surface". https://www.corrosionpedia.com/definition/843/oxidized-surface-steel (accesed Feb. 15, 2022).

[33] E. Fjeld, R. G.J. Wilhelm, A. Elham, S. Shailendra, "Estimate the Temperature Rise of Medium Voltage Metal Enclosed Switchgear by Simplified Heat Transfer Calculations," in *IEEE Transactions on Power Delivery*, 2020. [Online]. Available: https://openarchive.usn.no/usn-xmlui/bitstream/handle/11250/2756579/2020FjeldEstimate_POSTPRINT.pdf?sequence=5&isAllowed=y

[34] *A method of temperature-rise verification of low-voltage switchear abd controlgear assemblies by calculation*, NEC IEC 60890, 2014.

[35] COMSOL. "The COMSOL Product Suite". https://www.comsol.com/products. (accessed Mar. 17, 2022).

[36] O. Ulkir, I.Ertugrul, O. Girit and A. Ersoy. "Modeling and thermal analysis of micro beam using COMSOL multiphysics". https://www.researchgate.net/publication/348586290_Modeling_and_thermal_analysis_of_micro_beam_using_COMSOL_multiphysics (accessed Feb. 1, 2022).

[37] SIMSCALE. "Heat Transfer Simulation Software". https://www.simscale.com/heat-transfer-simulation/?utm_term=heat%20transfer%20simulation%20software&utm_source=adwords&utm_medium=ppc&utm_campaign=2020+-+RW+-+Search+-+Heat+Transfer&hsa_cam=11427732159&hsa_grp=111329859789&hsa_mt=b&hsa_src=g&hsa_ad=474432 (accessed Feb. 5, 2022).

[38] Ansys. "3D Design Product Design Solutions". https://www.ansys.com/products/3d-design (accessed Feb. 12, 2022).

[39] R. Adam, J. Heger, H. Lobl and S. Grossman, "ADAPTATION OF THE THERMAL NETWORK METHOD (TNM) FOR USE IN LOWVOLTAGE SWITCHGEAR AND CONTROLGEAR ASSEMBLIES," in *Cired 25th International Conference on Electrical Distribution*, Madrid, 2019. [Online]. Available: https://www.cired-repository.org/bitstream/handle/20.500.12455/613/CIRED%202019%20-%201862.pdf?sequence=1&isAllowed=y

[40] E. Csanyi. "What is a Load Break Switch?". https://electrical-engineering-portal.com/what-is-a-load-break-switch (accessed Feb. 10, 2022).

[41] S. Helland, "Power loss measurements in MV switchgear for Cigré-working group," Dept. Electro, IT and cybernetics. USN, Porsgrunn, 2018.

[42] RS. "Thermocouple Selection Guide". https://docs.rs-online.com/96d5/0900766b815e5302.pdf (accessed Mar. 21, 2022).

[43] P. B. Andersen. "Ohms lov". https://snl.no/Ohms_lov (accessed Feb. 15, 2022).

[44] E. Fjeld, "EPE2419 Physics of Electrical Power Engineering", Lecture: "Lab1: Resistance Measurements", University of South-Eastern Norway, 2019.

[45] A. Vahid, C. Gløsmyr, O. Dada, M. Akhlaq and L. Pham, "Report lab 1: Resistance measurements of MV switchgear," 2021.

[46] Z. Junmin and F. Hao, "Temperature Rise Comparison of Switchgear in SF6, N2, and Air," in *Universitas Ahmad Dahlan*, Beijing, 2013. [Online]. Available: https://www.gob.mx/cms/uploads/attachment/file/58945/Anexo_I.pdf

[47] E. Fjeld, W. Rondeel, K. Vaagsaether and E. Attar "INFLUENCE OF HEAT SOURCE LOCATION ON AIR TEMPERATURES IN SEALED MV SWITCHGEAR," in *Cired 24th International Conference on Electricity Distribution*, Glasgow, 2017. [Online]. Available: http://cired.net/publications/cired2017/pdfs/CIRED2017_0345_final.pdf

[48] Mech Content. "Thermal time constant in heat transfer: Definition, Unit, Formula [with Pdf]". https://mechcontent.com/thermal-time-constant/ (accessed Apr. 5. 2022).

[49] Wikipedia. "Lumped-element model". https://en.wikipedia.org/wiki/Lumped-element_model (accessed Apr. 4, 2022).

[50] B. Lie, "FM1015 Modelling of Dynamic System", Lecture: "Modeling of Dynamic System", University of South-Eastern Norway, 2019.

[51] P. H. Gill, "What is a Heat Transfer Coefficient". https://www.wise-geek.com/what-is-a-heat-transfer-coefficient.htm (accessed May. 13, 2022)

Appendices

Appendix A Task Description of Master Thesis

Appendix B Surface area calculations

Appendix C Effective surface area of switchgear enclosure

Appendix D Sensor overview

Appendix E Heat transfer calculation

Appendix F Time constant calculations

Appendix G Simulation vs real lab measurements

Appendix H Average deviation for overload cases

Appendix I Overload time for different currents

Appendix A

FMH606 Master's Thesis

Title: Thermal overloading of MV metal enclosed switchgear

USN supervisor: Elin Fjeld

External partner: ABB

Task background:
Electrification plays an important part in reducing the greenhouse gas emissions. Fast charging of high capacity batteries might represent an intermittent, high power demand on the electrical supply equipment. Depending on the time constant of the equipment, it might be able to handle a short time overload, without exceeding the temperature limits.

The MV switchgear located in the distribution transformer substations, is one example of equipment where one must make sure that the temperature rise does not exceeds limits set by the IEC, but where one might be able to utilize the time constant for a short time overload.

Task description:
The student should

- Perform a literature study on temporary overloading of metal enclosed switchgear.
- Perform temperature rise tests in the high current laboratory to determine heat transfer coefficients, time constants etc.
- Use the tests to make an initial, simplified thermal model of the switchgear that can be used to predict the allowable duration of a certain overload.

Student category: EPE

Is the task suitable for online students (not present at the campus)? No

Practical arrangements:
A 4-way air insulated switchgear unit is available at the USN lab for testing.

Supervision:
As a general rule, the student is entitled to 15-20 hours of supervision. This includes necessary time for the supervisor to prepare for supervision meetings (reading material to be discussed, etc).

Signatures:

Supervisor (date and signature): 31/1-22 Elin Fjeld

Student (write clearly in all capitalized letters): CECILIE DORTEA GLØSMYR

Student (date and signature): 31/1-22 Cecilie D. Glæsmyr

Appendix B

Surface area calculations of switchgear enclosure

The table below shows the dimensions measured for the switchgear enclosure.

Dimension	Measurement [m]
Width w	0.52
Length l	1.28
Switchgear height H_{sw}	0.85

The switchgear enclosure is the upper part of the entire enclosure where the current path is located. The lower part, which is empty for this specific switchgear, is not included as described in section 3.1.1. The calculated surface area is used in the thermal model. The calculation is shown below.

$$A_{surf,sw} = 2\,[(l_{sw} * w_{sw}) + (l_{sw} * H_{sw}) + (H_{sw} * w_{sw})]$$

$$A_{surf,sw} = 2\,[(1.28 * 0.52) + (1.28 * 0.85) + (0.85 * 0.52)] = 4.39m^2$$

The surface area of the switchgear enclosure is approximately 4.39m^2.

Surface area calculations of LBS

The dimensions measured for one LBS are given in the table below.

Dimension	Measurement [m]
Width middle part w_m	0.005
Length middle part l_m	0.04
Height middle part H_m	0.13
Width upper and lower part $w_{u\&l}$	0.0024
Length upper and lower part $l_{u\&l}$	0.027
Height upper and lower part $H_{m\&l}$	0.018

The surface area of the LBS is calculated by dividing the device into three different pieces based on its shape. The upper/lower part and the middle part. The surface area is calculated for each of the pieces and added together to get the total surface area. The surface area for both the middle and upper/lower part can then be calculated with use of the surface area equation for a rectangle, excluding the overlapping areas where the pieces connect (one of the $l * w$). The calculations are shown below.

Surface area LBS middle part:

$$A_{surf,LBS,m} = \left(l_{LBS,m} * w_{LBS,m}\right) + 2\left(l_{LBS,m} * H_{LBS,m}\right) + 2\left(H_{LBS,m} * w_{LBS,m}\right)$$

$$A_{surf,LBS,m} = (0.04 * 0.005) + 2(0.04 * 0.13) + 2(0.13 * 0.005) = 0.0119m^2$$

Surface area LBS upper and lower part:

$$A_{surf,LBS,u\&l} = \left(l_{LBS,u\&l} * w_{LBS,u\&l}\right) + 2\left(l_{LBS,u\&l} * H_{LBS,u\&l}\right) + 2\left(H_{LBS,u\&l} * w_{LBS,u\&l}\right)]$$

$$A_{surf,LBS,u\&l} = (0.027 * 0.024) + 2(0.027 * 0.018) + 2(0.018 * 0.024) = 0.0031m^2$$

Total surface area of one LBS:

$$A_{surf,LBS} = A_{surf,LBS,m} + A_{surf,LBS,u\&l}$$

$$A_{surf,LBS} = 0.0119 + 0.0031 \approx 0.015m^2$$

The surface area of one LBS is approximately $0.015m^2$.

Surface area calculations of busbar

Measured dimensions are shown below.

Dimension	Measurement [m]
Width middle part w_{busbar}	0.037
Length middle part l_{busbar}	0.165
Height middle part H_{busbar}	0.005

Surface area of busbar:

$$A_{surf,busbar} = 2(l_{busbar} * w_{busbar}) + 2(l_{busbar} * H_{busbar}) + 2(H_{busbar} * w_{busbar})$$

$$A_{surf,busbar} = 2(0.165 * 0.037) + 2(0.165 * 0.005) + 2(0.005 * 0.037) = 0.01423m^2$$

Surface area of the busbar is approximately 0.015m^2.

Surface area calculations of current path

Table below shows the dimensions measured for the current path. The radius is similar for all phases L1, L2 and L3.

Dimension	Measurement [m]
Radius	0.01
Height phase L1 H_{L1} (one leg)	0.82
Height phase L2 H_{L2} (one leg)	0.77
Height phase L3 H_{L3} (one leg)	0.79

To calculate the surface area for the total current path, the surface area of each of the three phases is first calculated individual. Each phase is divided into two legs (cylinder shaped), 2 LBS and one busbar for the calculations. Only the length of the legs varies between the phases as shown in the table above. Within one phase the length of the legs is equal.

The surface area of one leg is calculated as:

$$A_{surf,cp,legs} = 2\pi r^2 + 2\pi rH$$

For phase L1:

$$A_{surf,cp\,L1} = 2\pi r^2 + 2\pi rH_{L1}$$

$$A_{surf,cp\,L1,1\,leg} = 2\pi(0.01)^2 + 2\pi * 0.01 * 0.82 = 0.052m^2$$

For phase L2:

$$A_{surf,cp\,L2} = 2\pi r^2 + 2\pi rH_{L3}$$

$$A_{surf,cp\,L2,1\,leg} = 2\pi(0.01)^2 + 2\pi * 0.01 * 0.77 = 0.049m^2$$

For phase L3:

$$A_{surf,cp\,L3} = 2\pi r^2 + 2\pi rH_{L3}$$

$$A_{surf,cp\,L3,1\,leg} = 2\pi(0.01)^2 + 2\pi * 0.01 * 0.79 = 0.050m^2$$

The surface area of one phase is:

$$A_{surf,cp\,L} = 2(A_{surf,cp\,L,1\,leg}) + 2\left(A_{surf,LBS}\right) + A_{surf,busbar}$$

Where:

$$A_{surf,LBS} = 0.015m^2$$

$$A_{surf,busbar} = 0.11m^2$$

For phase L1:

$$A_{surf,cp\,L} = 2(0.052m^2) + 2(0.015m^2) + 0.11m^2 = 0.244m^2$$

For phase L2:

$$A_{surf,cp\,L} = 2(0.049m^2) + 2(0.015m^2) + 0.11m^2 = 0.238m^2$$

For phase L3:

$$A_{surf,cp\,L} = 2(0.050m^2) + 2(0.015m^2) + 0.11m^2 = 0.24m^2$$

The total surface area of the current path (all phases) is:

$$A_{surf,cp\,total} = A_{surf,cp,L1} + A_{surf,cp,L2} + A_{surf,cp,L3}$$

$$A_{surf,cp\,total} = 0.244m^2 + 0.238m^2 + 0.24m^2 = 0.72m^2$$

The total surface area of the total current path is approximately 0.72m^2.

Appendix C

Effective surface area of switchgear enclosure

The effective surface area of the switchgear is calculated by the Python script below.

```
#Calculate effective surface area
l=1.28
h=0.845
w=0.52

#Actual surface area
A_back = (l*h)
A_top = (l*w)
A_front = (l*h)
A_side = (w*h)
A_bottom = (l*w)

#Effective surface area IEC
A_back_IEC = (l*h)*0.5
A_top_IEC = (l*w)*1.4
A_front_IEC = (l*h)*0.9
A_side_IEC = (w*h)*0.5
A_bottom_IEC = (l*w)*0

Sum_A_actual = A_back + A_top + A_front + A_side +A_side + A_top
Sum_A_IEC = A_back_IEC + A_top_IEC + A_front_IEC + A_side_IEC + A_side_IEC + A_top_IEC

#Actual surface area
print ('Actual surface area back/ front wall:',"%.2f" % A_front,'m2')
print ('Actual surface area top/bottom wall:',"%.2f" % A_top,'m2')
print ('Actual surface area side wall:'," %.2f" % A_side,'m2')
print ('Actual surface area'," %.2f" % Sum_A_actual,'m2')

print ("")

#Effective surface area
print ('Effective surface area back/ front wall:'," %.2f" %A_front_IEC,'m2')
print ('Effective surface area top/bottom wall:', " %.2f" %A_top_IEC,'m2')
print ('Effective surface area side wall:'," %.2f" % A_side_IEC,'m2')
print ('Effective surface area'," %.2f" % Sum_A_IEC,'m2')
```

The script prints:

Actual surface area back/ front wall: 1.08 m2
Actual surface area top/bottom wall: 0.67 m2
Actual surface area side wall: 0.44 m2
Actual surface area 4.37 m2

Effective surface area back/ front wall: 0.97 m2
Effective surface area top/bottom wall: 0.93 m2
Effective surface area side wall: 0.22 m2
Effective surface area 3.82 m2

Appendix D

Sensor overview

Sensor overview for thermocouples located on the current path inside the switchgear enclosure, the surrounding air and one on the outside surface walls.

Sensor nr. (Logging)	Description	Phase	Module
301	Busbar bolted connection Ag/Cu	L1	C2
103	Open/close contact Ag/Ag	L1	C2
302	Rotating contact Ag/Ag	L1	C2
102	Lower LBS bolted connection Cu/Ag	L1	C2
107	Bushing bolted connection Cu/Cu	L1	C2
303	Busbar bolted connection Ag/Cu	L1	C3
111	Open/close contact Ag/Ag (left side)	L1	C3
116	Rotating contact Cu/Ag - left	L1	C3
114	Lower LBS bolted connection Cu/Ag	L1	C3
112	Bushing bolted connection Cu/Cu	L1	C3
108	Rotating contact Ag/Ag	L2	C2
304 / 303	Open/close contact Ag/Ag	L2	C2
309	Room temperature	-	-
115	Air near top	-	-
104	Air midt height (LBS height)	-	-
305	Air right wall	-	-
306	Air left wall	-	-
307	Air lower	-	-
308	Air middle	-	-
310	Outside wall, right side	-	-

The sensor overview for location of thermocouple for measuring the temperature at all outside surface walls is shown in the following figures and table.

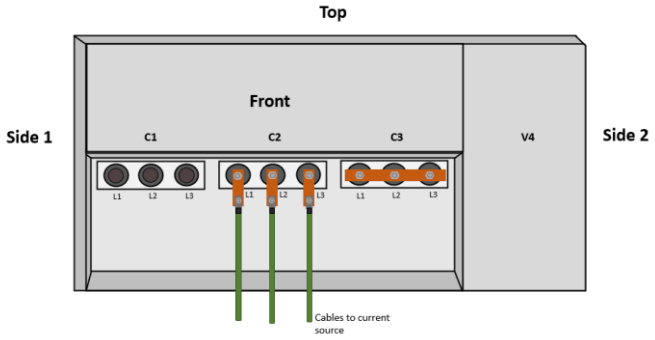

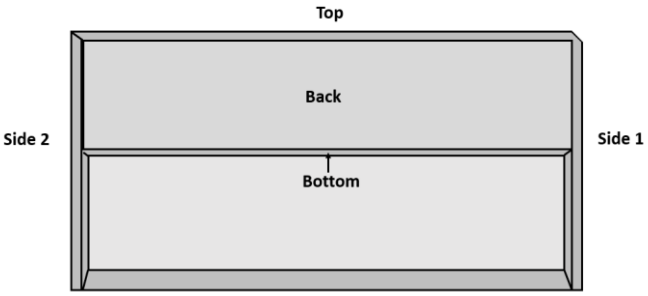

Sensor nr. (Logging)	Description	Phase	Module
101	Top	-	-
102	Side wall left	-	-
103	Side wall right	-	-
104	Bottom	-	-
107	Front	-	-
108	Back	-	-
109	LBS	L1	C2

Appendix E

Heat transfer calculation

Heat transfer calculations for applied current at 400A, 500A and 630A is shown in the following scripts. The temperatures are gathered from real measurements, the surface areas are measured and calculated in previous appendix and the resistance are determined in section 4.3.

Heat transfer coefficient when I = 400A:

```
#Heat transfer coefficient
T_max_LBS = 48.4
T_max_wall = 21.8
T_room = 19.5
A_surf_wall = 3.82  #Surface area enclosure
A_surf_LBS = 0.015  #Surface area of LBS
R_cp = 3*(231*10**-6)  #Warm resistance for 3*phase L1
R_LBS = (28.7*10**-6)  #Warm resistance for LBS
I = 400

delta_T_LBS = T_max_LBS - T_room
delta_T_wall = T_max_wall - T_room
P_in_cp = R_cp*(I)**2
P_in_LBS = R_LBS*(I)**2

h_LBS = P_in_LBS / (A_surf_LBS*delta_T_LBS)
h_wall = P_in_cp/(A_surf_wall*delta_T_wall)

print ("h (LBS): ",h_LBS)
print ("h (outside wall): ",h_wall)
```

The script prints:

h (LBS): 10.59284890426759
h (outside wall): 12.62007739585704

Heat transfer coefficient when I = 500A:

```
#Heat transfer coefficient
T_max_LBS = 63.3
T_max_wall = 24
T_room = 20.4
A_surf_wall = 3.82    #Surface area enclosure
A_surf_LBS = 0.015   #Surface area of LBS
R_cp = 3*(245*10**-6)  #Warm resistance for 3*phase L1
R_LBS = (29.2*10**-6)  #Warm resistance for LBS
I = 500

delta_T_LBS = T_max_LBS - T_room
delta_T_wall = T_max_wall - T_room
P_in_wall = R_cp*(I)**2
P_in_LBS = R_LBS*(I)**2

h_LBS = P_in_LBS / (A_surf_LBS*delta_T_LBS)
h_wall = P_in_wall/(A_surf_wall*delta_T_wall)

print ("h (LBS): ",h_LBS)
print ("h (outside wall): ",h_wall)
```

The script prints:

h (LBS): 11.344211344211345
h (outside wall): 13.361692844677133

Heat transfer coefficient when I = 630A (nominal current):

```
#Heat transfer coefficient
T_max_LBS = 86.7
T_max_wall = 26.3
T_room = 20.4
A_wall = 3.82       #Surface area enclosure
A_surf_LBS = 0.015  #Surface area of LBS
R_cp = 3*(265*10**-6)  #Warm resistance for 3*phase L1
R_LBS = (30.6*10**-6)   #Warm resistance for LBS
I = 630

delta_T_LBS = T_max_LBS - T_room
delta_T_wall = T_max_wall - T_room
P_in_wall = R_cp*(I)**2
P_in_LBS = R_LBS*(I)**2

h_LBS = P_in_LBS / (A_surf_LBS*delta_T_LBS)
h_wall = P_in_wall/(A_wall*delta_T_wall)

print ("h (LBS): ",h_LBS)
print ("h (outside wall): ",h_wall)
```

The script prints:

h (LBS): 13.16215384615384
h (outside wall): 15.363189280326555

Appendix F

Time constant when I = 400A

The time constant when I = 400A is calculated below for the LBS and the outside surface wall. The method is described in section 5.3.3.

For current path / LBS:

$$T_{\tau,LBS} = \left((48.4℃ - 19.8℃) * 63.2\%\right) + 19.8℃ = 38.9℃ \approx 39℃$$

For surface wall:

$$T_{\tau,wall} = \left((26.3℃ - 19.8℃) * 63.2\%\right) + 19.8℃ = 23.9℃ \approx 24℃$$

The time constant can visually be found at these temperatures. The time constants for the LBS and outside surface wall are shown respectively in the following figures. The results of the time constant calculations are shown in the table below.

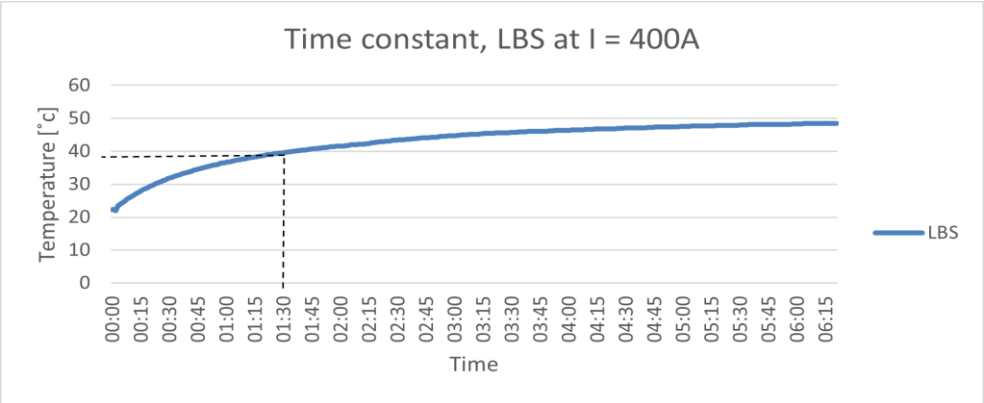

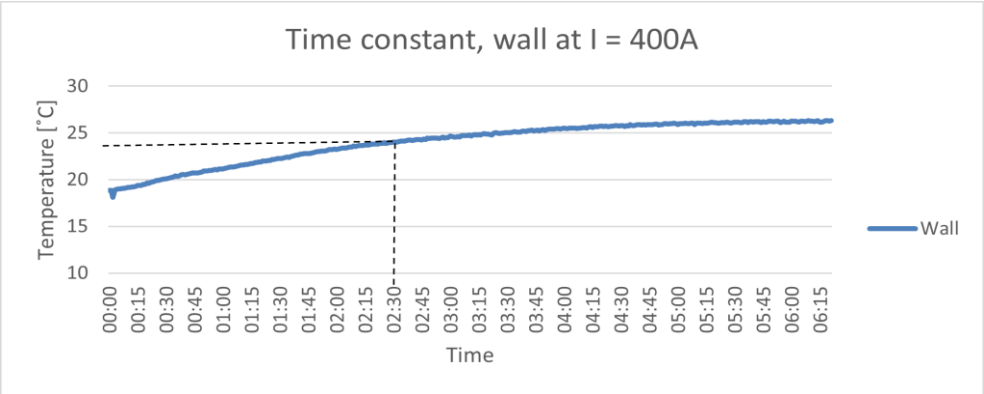

	LBS	Outside wall
Temperature at time constant [˚C]	39	24
Time constant [min]	90	150

Time constant when I = 500A

The time constant when I = 500A is calculated by the method described in section 5.3.3 for the LBS and the outside surface wall.

For LBS:

$$T_{\tau,LBS} = \left((63.3^{\circ}\mathrm{C} - 20.9^{\circ}\mathrm{C}) * 63.2\%\right) + 20.9^{\circ}\mathrm{C} = 47.7^{\circ}\mathrm{C} \approx 48^{\circ}\mathrm{C}$$

For surface wall:

$$T_{\tau,wall} = \left((24.7^{\circ}\mathrm{C} - 20.9^{\circ}\mathrm{C}) * 63.2\%\right) + 20.9^{\circ}\mathrm{C} = 23.3^{\circ}\mathrm{C} \approx 23^{\circ}\mathrm{C}$$

The figures below show the plots for the temperature rise for the LBS and outside wall. The time constant can be found at 63.2% of the temperature increase, which is at the calculated temperatures above. The found time constants are shown in the following table.

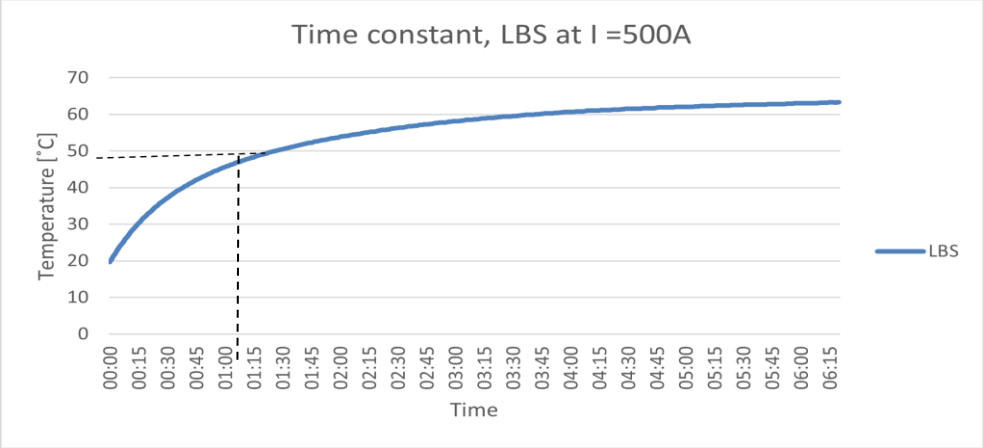

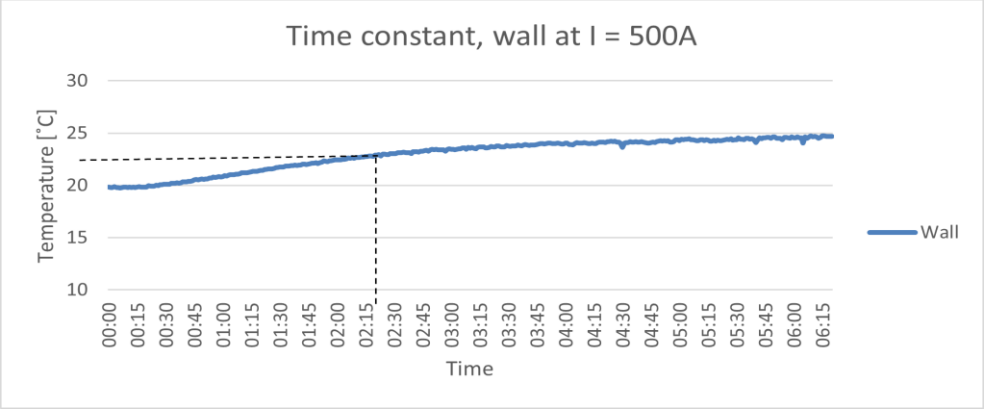

	LBS	Outside wall
Temperature at time constant [˚C]	48	23
Time constant [min]	80	140

Appendix G

Real vs. simulated temperature rise

Temperature rise of the real data and simulated thermal model is plotted for the different applied currents (400A, 500A and 630A) until steady state. The temperature at the LBS and outside wall is plotted.

Temperature rise with I = 400A until steady state:

```
import numpy as np
import matplotlib.pyplot as plt

I = 400
h_LBS = 10.6    #heat transfer coefficient
h_wall = 12.6   #heat transfer coefficient
alpha_LBS = 0.0021
alpha_wall = 0.00305
R_factor_LBS = -0.9*10**-6
R_factor_wall = -11*10**-6
tau_LBS = 90    #time constant
tau_wall = 150  #time constant
x_LBS = 2.1
x_wall = 0.6
A_LBS = 0.015
A_wall = 0.22
A_surf = 0.725

hA_LBS = h_LBS*A_surf
hA_wall = h_wall*A_surf
C_LBS = tau_LBS*A_surf*h_LBS
C_wall = tau_wall*A_surf*h_wall

a = 0.0; b = 400   #running time
d = 382
N = 50
dt = ((b-a)/N)
dt_1 = dt/330

#timespan
time = np.linspace(a,b,N+1)
time_real = np.linspace(a,d,d-1)

#Empty arrays
T_LBS = np.zeros(N+1)
T_real_LBS = np.zeros(b)
R_LBS = np.zeros(N+1)
P_LBS = np.zeros(N+1)

T_wall = np.zeros(N+1)
T_real_wall = np.zeros(b)
R_wall = np.zeros(N+1)
P_wall = np.zeros(N+1)

for n in range(N):
    #LBS
    T_0_LBS = 22.273
    T_LBS[0] = T_0_LBS
    T_max_LBS = 48.43

    R_cold_LBS = 28.1*10**-6
    R_LBS[0] =  R_cold_LBS
    R_LBS[n] = (R_cold_LBS*(1+(alpha_LBS*(T_LBS[n-1]-T_0_LBS))))+R_factor_LBS
```

```
    P_LBS[n] = R_LBS[n]*I*I
    T_LBS[n] = (T_LBS[n-1]+(dt_1/C_LBS)*P_LBS[n]-hA_LBS*(T_LBS[n-1]-T_LBS[0]))+x_LBS

    #Enclosure wall
    T_0_wall = 18.87
    T_wall[0] = T_0_wall
    T_max_wall = 26.33

    R_cold_wall = 229.2*10**-6
    R_wall[0] =  R_cold_wall
    R_wall[n] = (R_cold_wall*(1+(alpha_wall*(T_wall[n-1]-T_0_wall))))+R_factor_wall

    P_wall[n] = R_wall[n]*I*I
    T_wall[n] = (T_wall[n-1]+(dt_1/C_wall)*P_wall[n]-hA_wall*(T_wall[n-1]-T_wall[0]))+x

#Plot real vs simulation
import pandas as pd
T_real_LBS = pd.read_excel (r'C:\Users\ceglo\Documents\1_Spring 2022\Tests\LBS_Python\4
T_real_wall = pd.read_excel (r'C:\Users\ceglo\Documents\1_Spring 2022\Tests\Wall_Pythor

#Get to 1dim array for LBS
T_real_data_LBS = pd.read_excel (r'C:\Users\ceglo\Documents\1_Spring 2022\Tests\LBS_Pyt
T_real_prep_LBS = T_real_data_LBS.values
T_real_1dim_LBS =T_real_prep_LBS[:,0]

#Get to 1dim array for outside wall
T_real_data_wall = pd.read_excel (r'C:\Users\ceglo\Documents\1_Spring 2022\Tests\Wall_F
T_real_prep_wall = T_real_data_wall.values
T_real_1dim_wall =T_real_prep_wall[:,0]

#Calc average error
def calc_average_error(temp_sim, temp_real_1dim):
    mean_sim = np.mean(np.abs(temp_sim))
    mean_real = np.mean(np.abs(temp_real_1dim))
    mean_error = np.abs(mean_real-mean_sim)
    return mean_error

av_error_LBS = calc_average_error(T_LBS,T_real_1dim_LBS)
print ("Average error for LBS [degree C]:","%.2f" % av_error_LBS)

av_error_wall = calc_average_error(T_wall,T_real_1dim_wall)
print ("Average error for outside wall [degree C]:","%.2f" % av_error_wall)

#Plot
fig = plt.figure()
l1 = plt.plot(time, T_LBS, 'b', label = "simulated LBS")
l2 = plt.plot(time_real, T_real_LBS, 'b--', label = "real LBS")
l3 = plt.plot(time, T_wall, 'r', label = "simulated wall")
l4 = plt.plot(time_real, T_real_wall, 'r--', label = "real wall")
plt.grid('on')
plt.title('Simulated temperature rise at LBS and enclosure wall. I = 400A')
plt.legend(loc = 'upper left')
plt.xlabel('Min' )
plt.ylabel('Temp [Degree C]')
plt.axis([0,380,0,120])
plt.show()
```

Temperature rise with I = 500A until steady state:

```
import numpy as np
import matplotlib.pyplot as plt

I = 500
h_LBS = 11.3    #heat transfer coefficient
h_wall = 13.4   #heat transfer coefficient
alpha_LBS = 0.0021
alpha_wall = 0.00305
R_factor_LBS = -0.9*10**-6
R_factor_wall = -11*10**-6
tau_LBS = 80    #time constant
tau_wall = 140  #time constant
x_LBS = 3.59
x_wall = 0.3
A_LBS = 0.015
A_wall = 0.22
A_surf = 0.725

hA_LBS = h_LBS*A_surf
hA_wall = h_wall*A_surf
C_LBS = tau_LBS*A_surf*h_LBS
C_wall = tau_wall*A_surf*h_wall

a = 0.0; b = 400   #running time, min
d = 381
N = 50
dt = ((b-a)/N)
dt_1 = dt/200

#Timespan for this plot
time = np.linspace(a,b,N+1)
time_real = np.linspace(a,d,d-1)

T_LBS = np.zeros(N+1)
T_real_LBS = np.zeros(d)
P_LBS = np.zeros(N+1)
R_LBS = np.zeros(N+1)

T_wall = np.zeros(N+1)
T_real_wall = np.zeros(d)
P_wall = np.zeros(N+1)
R_wall = np.zeros(N+1)

for n in range(N):
    #LBS
    T_0_LBS = 19.7
    T_LBS[0] = T_0_LBS
    T_max_LBS = 63.32

    R_cold_LBS = 28.1*10**-6
    R_LBS[0] =  R_cold_LBS
    R_LBS[n] = (R_cold_LBS*(1+(alpha_LBS*(T_LBS[n-1]-T_0_LBS))))+R_factor_LBS
```

```
    P_LBS[n] = R_LBS[n]*I*I
    T_LBS[n] = (T_LBS[n-1]+(dt_1/C_LBS)*P_LBS[n]-hA_LBS*(T_LBS[n-1]-T_LBS[0]))+ x_LBS

    #Enclosure wall
    T_0_wall = 19.84
    T_wall[0] = T_0_wall
    T_max_wall = 24.69

    R_cold_wall = 229.2*10**-6
    R_wall[0] =  R_cold_wall
    R_wall[n] = (R_cold_wall*(1+(alpha_wall*(T_wall[n-1]-T_0_wall))))+R_factor_wall

    P_wall[n] = R_wall[n]*I*I
    T_wall[n] = (T_wall[n-1]+(dt_1/C_wall)*P_wall[n]-hA_wall*(T_wall[n-1]-T_wall[0]))+

#Plot real vs simulation
import pandas as pd
T_real_LBS = pd.read_excel (r'C:\Users\ceglo\Documents\1_Spring 2022\Tests\LBS_Python\S
T_real_wall = pd.read_excel (r'C:\Users\ceglo\Documents\1_Spring 2022\Tests\Wall_Pythor

#Get to 1dim array for LBS
T_real_data_LBS = pd.read_excel (r'C:\Users\ceglo\Documents\1_Spring 2022\Tests\LBS_Pyt
T_real_prep_LBS = T_real_data_LBS.values
T_real_1dim_LBS =T_real_prep_LBS[:,0]

#Get to 1dim array for outside wall
T_real_data_wall = pd.read_excel (r'C:\Users\ceglo\Documents\1_Spring 2022\Tests\Wall_P
T_real_prep_wall = T_real_data_wall.values
T_real_1dim_wall =T_real_prep_wall[:,0]

#Calc average error
def calc_average_error(temp_sim, temp_real_1dim):
    mean_sim = np.mean(np.abs(temp_sim))
    mean_real = np.mean(np.abs(temp_real_1dim))
    mean_error = np.abs(mean_real-mean_sim)
    return mean_error

av_error_LBS = calc_average_error(T_LBS,T_real_1dim_LBS)
print ("Average error for LBS [degree C]:","%.2f" % av_error_LBS)

av_error_wall = calc_average_error(T_wall,T_real_1dim_wall)
print ("Average error for outside wall [degree C]:","%.2f" % av_error_wall)

fig = plt.figure()
l1 = plt.plot(time, T_LBS, 'b', label = "simulated LBS")
l2 = plt.plot(time_real, T_real_LBS, 'b--', label = "real LBS")
l3 = plt.plot(time, T_wall, 'r', label = "simulated wall")
l4 = plt.plot(time_real, T_real_wall, 'r--', label = "real wall")
plt.grid('on')
plt.legend(loc = 'upper left')
plt.title('Simulated temperature rise at LBS and enclosure wall. I = 500A')
plt.xlabel('Min' )
plt.ylabel('Temp [Degree C]')
plt.axis([0,380,0,120])
plt.show()
```

Temperature rise with I = 630A until steady state:

```
import numpy as np
import matplotlib.pyplot as plt

I = 630
h_LBS = 13.2   #heat transfer coefficient
h_wall = 15.4  #heat transfer coefficient
tau_LBS = 70    #time constant
tau_wall = 135  #time constant
alpha_LBS = 0.0021
alpha_wall = 0.00305
R_factor_LBS = -0.9*10**-6
R_factor_wall = -11*10**-6
x_LBS = 6.1
x_wall = 0.05
A_LBS = 0.015
A_wall = 0.22
A_surf = 0.725

C_LBS = tau_LBS*A_surf*h_LBS
C_wall = tau_wall*A_surf*h_wall
hA_LBS = h_LBS*A_surf
hA_wall = h_wall*A_surf

a = 0.0; b = 400 # running time
N = 50
dt = ((b-a)/N)
dt_1 = dt/135

#Timespan
time = np.linspace(a,b,N+1)
time_real = np.linspace(a,b,b-1)

#Empty arrays
T_LBS = np.zeros(N+1)
T_real_LBS = np.zeros(b)
P_LBS = np.zeros(N+1)
R_LBS = np.zeros(N+1)

T_wall = np.zeros(N+1)
T_real_wall = np.zeros(b)
P_wall = np.zeros(N+1)
R_wall = np.zeros(N+1)

for n in range(N):
    #LBS
    T_0_LBS = 21.1
    T_LBS[0] = T_0_LBS
    T_max_LBS = 86.7

    R_cold_LBS = 28.1*10**-6
    R_LBS[0] =  R_cold_LBS
    R_LBS[n] = (R_cold_LBS*(1+(alpha_LBS*(T_LBS[n-1]-T_0_LBS))))+R_factor_LBS
```

```
    P_LBS[n] = R_LBS[n]*I*I
    T_LBS[n] = (T_LBS[n-1]+(dt_1/C_LBS)*P_LBS[n]-hA_LBS*(T_LBS[n-1]-T_LBS[0]))+x_LBS

    #Wall
    T_0_wall = 19.43
    T_wall[0] = T_0_wall
    T_max_wall = 47.99

    R_cold_wall = 229.2*10**-6
    R_wall[0] =  R_cold_wall
    R_wall[n] = (R_cold_wall*(1+(alpha_wall*(T_wall[n-1]-T_0_wall))))+R_factor_wall

    P_wall[n] = R_wall[n]*I*I
    T_wall[n] = (T_wall[n-1]+(dt_1/C_LBS)*P_wall[n]-hA_wall*(T_wall[n-1]-T_wall[0]))+x_

#Plot real vs simulation
import pandas as pd
T_real_LBS = pd.read_excel (r'C:\Users\ceglo\Documents\1_Spring 2022\Tests\LBS_Python\6
T_real_wall = pd.read_excel (r'C:\Users\ceglo\Documents\1_Spring 2022\Tests\Wall_Python

#Get to 1dim array for LBS
T_real_data_LBS = pd.read_excel (r'C:\Users\ceglo\Documents\1_Spring 2022\Tests\LBS_Pyt
T_real_prep_LBS = T_real_data_LBS.values
T_real_1dim_LBS =T_real_prep_LBS[:,0]

#Get to 1dim array for outside wall
T_real_data_wall = pd.read_excel (r'C:\Users\ceglo\Documents\1_Spring 2022\Tests\Wall_P
T_real_prep_wall = T_real_data_wall.values
T_real_1dim_wall =T_real_prep_wall[:,0]

#Calc average error
def calc_average_error(temp_sim, temp_real_1dim):
    mean_sim = np.mean(np.abs(temp_sim))
    mean_real = np.mean(np.abs(temp_real_1dim))
    mean_error = np.abs(mean_real-mean_sim)
    return mean_error

av_error_LBS = calc_average_error(T_LBS,T_real_1dim_LBS)
print ("Average error for LBS [degree C]:","%.2f" % av_error_LBS)

av_error_wall = calc_average_error(T_wall,T_real_1dim_wall)
print ("Average error for outside wall [degree C]:","%.2f" % av_error_wall)

fig = plt.figure()
l1 = plt.plot(time, T_LBS, 'b', label = "simulated LBS")
l2 = plt.plot(time_real, T_real_LBS, 'b--', label = "real LBS")
l3 = plt.plot(time, T_wall, 'r', label = "simulated wall")
l4 = plt.plot(time_real, T_real_wall, 'r--', label = "real wall")
plt.legend(loc = 'upper left')
plt.title('Simulated temperature rise at LBS and eclosure wall. I = 630A')
plt.xlabel('Min' )
plt.ylabel('Temp [Degree C]')
plt.axis([0,380,0,120])
plt.grid('on')
plt.show()
```

Real vs. simulated temperature rise for I = 400A with overload

I = 400A and adjusted to 700A at a given time:

```
import numpy as np
import matplotlib.pyplot as plt

alpha_LBS = 0.0021
alpha_wall = 0.00305
R_factor_LBS = -0.9*10**-6
R_factor_wall = -11*10**-6
h_LBS = 10.6
h_wall = 12.6
x_LBS = 0.7
x_wall = 0.05
A_surf = 0.725
A_wall = 0.22
A_LBS = 0.015

hA_LBS = h_LBS*A_surf
hA_wall = h_wall*A_surf

a = 0.0; b = 854 # running time
N = 100
dt = ((b-a)/N)
dt_1 = (dt/150)

#Timespan
time = np.linspace(a,b,N+1)
time_real = np.linspace(a,b,b-1)

#Empty arrays
T_LBS = np.zeros(N+1)
T_real_LBS = np.zeros(b)
R_LBS = np.zeros(N+1)
P_LBS = np.zeros(N+1)

T_wall = np.zeros(N+1)
T_real_wall = np.zeros(b)
R_wall = np.zeros(N+1)
P_wall = np.zeros(N+1)

for n in range(N):
    #LBS
    T_0_LBS = 19.7
    T_LBS[0] = T_0_LBS
    T_max_LBS = 100.1

    #Wall
    T_0_wall = 18.3
    T_wall[0] = T_0_wall
    T_max_wall = 25.4

    #Changing current
    I_1 = 400
    I_2 = 700
    I_off = 0
```

```
    if (n < 40):
        I = I_1
        tau_LBS = 90
        tau_wall = 150
    elif (n > 41 and n < 84 ):
        I = I_2
        tau_LBS = 90
        tau_wall = 150
    elif (n > 85):
        I = I_off
        tau_LBS = 90
        tau_wall = 150

    C_LBS = tau_LBS*A_LBS*h_LBS
    C_wall = tau_wall*A_wall*h_wall

    #LBS
    R_cold_LBS = 28.1*10**-6
    R_LBS[0] =  R_cold_LBS
    R_LBS[n] = (R_cold_LBS*(1+(alpha_LBS*(T_LBS[n-1]-T_0_LBS))))+R_factor_LBS

    P_LBS[n] = R_LBS[n]*I*I
    T_LBS[n] = (T_LBS[n-1]+(dt_1/C_LBS)*P_LBS[n]-hA_LBS*(T_LBS[n-1]-T_LBS[0]))+x_LBS

    #Wall
    R_cold_wall = 229.2*10**-6
    R_wall[0] =  R_cold_wall
    R_wall[n] = (R_cold_wall*(1+(alpha_wall*(T_wall[n-1]-T_0_wall))))+R_factor_wall

    P_wall[n] = R_wall[n]*I*I
    T_wall[n] = (T_wall[n-1]+(dt_1/C_wall)*P_wall[n]-hA_wall*(T_wall[n-1]-T_wall[0]))+

#Plot real vs simulation
import pandas as pd
T_real_LBS = pd.read_excel (r'C:\Users\ceglo\Documents\1_Spring 2022\Tests\LBS_Python\
T_real_wall = pd.read_excel (r'C:\Users\ceglo\Documents\1_Spring 2022\Tests\Wall_Pythor

#Get to 1dim array for LBS
T_real_data_LBS = pd.read_excel (r'C:\Users\ceglo\Documents\1_Spring 2022\Tests\LBS_Pyt
T_real_prep_LBS = T_real_data_LBS.values
T_real_1dim_LBS =T_real_prep_LBS[:,0]

#Get to 1dim array for outside wall
T_real_data_wall = pd.read_excel (r'C:\Users\ceglo\Documents\1_Spring 2022\Tests\Wall_F
T_real_prep_wall = T_real_data_wall.values
T_real_1dim_wall =T_real_prep_wall[:,0]

#Calc average error
def calc_average_error(temp_sim, temp_real_1dim):
    mean_sim = np.mean(np.abs(temp_sim))
    mean_real = np.mean(np.abs(temp_real_1dim))
    mean_error = np.abs(mean_real-mean_sim)
    return mean_error

av_error_LBS = calc_average_error(T_LBS,T_real_1dim_LBS)
print ("Average error for LBS [degree C]:","%.2f" % av_error_LBS)

av_error_wall = calc_average_error(T_wall,T_real_1dim_wall)
print ("Average error for outside wall [degree C]:","%.2f" % av_error_wall)
fig = plt.figure()
l1 = plt.plot(time, T_LBS, 'b', label = "simulated LBS")
l2 = plt.plot(time_real, T_real_LBS, 'b--', label = "real LBS")
l3 = plt.plot(time, T_wall, 'r', label = "simulated wall")
l4 = plt.plot(time_real, T_real_wall, 'r--', label = "real wall")
plt.grid('on')
plt.title('Sim vs real. I = 400A and later overloaded to be I = 700A')
plt.legend(loc = 'upper left')
plt.xlabel('Min' )
plt.ylabel('Temp [Degree C]')
plt.axis([0,830,0,130])
plt.show()
```

I = 400A and adjusted to 800A at a given time:

```
import numpy as np
import matplotlib.pyplot as plt

alpha_LBS = 0.0021
alpha_wall = 0.00305
R_factor_LBS = -0.9*10**-6
R_factor_wall = -11*10**-6
h_LBS = 10.6
h_wall = 12.6
x_LBS = 1
x_wall = 0.3
A_surf = 0.725
A_wall = 0.22
A_LBS = 0.015

hA_LBS = h_LBS*A_surf
hA_wall = h_wall*A_surf

a = 0.0; b = 651 # running time
N = 100
dt = ((b-a)/N)
dt_1 = (dt/150)

#Timespan
time = np.linspace(a,b,N+1)
time_real = np.linspace(a,b,b-1)

#Empty arrays
T_LBS = np.zeros(N+1)
T_real_LBS = np.zeros(b)
R_LBS = np.zeros(N+1)
P_LBS = np.zeros(N+1)

T_wall = np.zeros(N+1)
T_real_wall = np.zeros(b)
R_wall = np.zeros(N+1)
P_wall = np.zeros(N+1)

for n in range(N):
    #LBS
    T_0_LBS = 21.3
    T_LBS[0] = T_0_LBS
    T_max_LBS = 110

    #Wall
    T_0_wall = 20.2
    T_wall[0] = T_0_wall
    T_max_wall = 30.7

    #Changing current
    I_1 = 400
    I_2 = 800
    I_off = 0

    if (n < 62):
        I = I_1
        tau_LBS = 90
        tau_wall = 150
    elif (n > 63 and n < 77 ):
        I = I_2
        tau_LBS = 90
        tau_wall = 150
    elif (n > 78):
        I = I_off
        tau_LBS = 90
        tau_wall = 150
```

```
    U_LBS = h_LBS*A_surf
    U_wall = h_wall*A_surf

    C_LBS = tau_LBS*A_LBS*h_LBS
    C_wall = tau_wall*A_wall*h_wall

    #LBS
    R_cold_LBS = 28.1*10**-6
    R_LBS[0] =  R_cold_LBS
    R_LBS[n] = (R_cold_LBS*(1+(alpha_LBS*(T_LBS[n-1]-T_0_LBS))))+R_factor_LBS

    P_LBS[n] = R_LBS[n]*I*I
    T_LBS[n] = (T_LBS[n-1]+(dt_1/C_LBS)*P_LBS[n]-hA_LBS*(T_LBS[n-1]-T_LBS[0]))+x_LBS

    #Wall
    R_cold_wall = 229.2*10**-6
    R_wall[0] =  R_cold_wall
    R_wall[n] = (R_cold_wall*(1+(alpha_wall*(T_wall[n-1]-T_0_wall))))+R_factor_wall

    P_wall[n] = R_wall[n]*I*I
    T_wall[n] = (T_wall[n-1]+(dt_1/C_LBS)*P_wall[n]-hA_wall*(T_wall[n-1]-T_wall[0]))+x_

#Plot real vs simulation
import pandas as pd
T_real_LBS = pd.read_excel (r'C:\Users\ceglo\Documents\1_Spring 2022\Tests\LBS_Python\4
T_real_wall = pd.read_excel (r'C:\Users\ceglo\Documents\1_Spring 2022\Tests\Wall_Pythor

#Get to 1dim array for LBS
T_real_data_LBS = pd.read_excel (r'C:\Users\ceglo\Documents\1_Spring 2022\Tests\LBS_Pyt
T_real_prep_LBS = T_real_data_LBS.values
T_real_1dim_LBS =T_real_prep_LBS[:,0]

#Get to 1dim array for outside wall
T_real_data_wall = pd.read_excel (r'C:\Users\ceglo\Documents\1_Spring 2022\Tests\Wall_F
T_real_prep_wall = T_real_data_wall.values
T_real_1dim_wall =T_real_prep_wall[:,0]

#Calc average error
def calc_average_error(temp_sim, temp_real_1dim):
    mean_sim = np.mean(np.abs(temp_sim))
    mean_real = np.mean(np.abs(temp_real_1dim))
    mean_error = np.abs(mean_real-mean_sim)
    return mean_error

av_error_LBS = calc_average_error(T_LBS,T_real_1dim_LBS)
print ("Average error for LBS [degree C]:","%.2f" % av_error_LBS)

av_error_wall = calc_average_error(T_wall,T_real_1dim_wall)
print ("Average error for outside wall [degree C]:","%.2f" % av_error_wall)

fig = plt.figure()
l1 = plt.plot(time, T_LBS, 'b', label = "simulated LBS")
l2 = plt.plot(time_real, T_real_LBS, 'b--', label = "real LBS")
l3 = plt.plot(time, T_wall, 'r', label = "simulated wall")
l4 = plt.plot(time_real, T_real_wall, 'r--', label = "real wall")
plt.grid('on')
plt.title('Sim vs real. I = 400A and later overloaded to be I = 800A')
plt.legend(loc = 'upper left')
plt.xlabel('Min' )
plt.ylabel('Temp [Degree C]')
plt.axis([0,640,0,120])
plt.show()
```

I = 400A and adjusted to 850A at a given time:

```
import numpy as np
import matplotlib.pyplot as plt

alpha_LBS = 0.0021
alpha_wall = 0.00305
R_factor_LBS = -0.9*10**-6
R_factor_wall = -11*10**-6
h_LBS = 10.6
h_wall = 12.6
x_LBS = 1.3
x_wall = 0.05
A_surf = 0.725
A_wall = 0.22
A_LBS = 0.015

hA_LBS = h_LBS*A_surf
hA_wall = h_wall*A_surf

a = 0.0; b = 525 # running time
N = 100
dt = ((b-a)/N)
dt_1 = (dt/150)

#Timespan
time = np.linspace(a,b,N+1)
time_real = np.linspace(a,b,b-1)

#Empty arrays
T_LBS = np.zeros(N+1)
T_real_LBS = np.zeros(b)
R_LBS = np.zeros(N+1)
P_LBS = np.zeros(N+1)

T_wall = np.zeros(N+1)
T_real_wall = np.zeros(b)
R_wall = np.zeros(N+1)
P_wall = np.zeros(N+1)

for n in range(N):
    #LBS
    T_0_LBS = 19.1
    T_LBS[0] = T_0_LBS
    T_max_LBS = 110.2

    #Wall
    T_0_wall = 20.5
    T_wall[0] = T_0_wall
    T_max_wall = 28

    #Changing current
    I_1 = 400
    I_2 = 850
    I_off = 0

    if (n < 64):
        I = I_1
        tau_LBS = 90
        tau_wall = 150
    elif (n > 65 and n < 78):
        I = I_2
        tau_LBS = 90
        tau_wall = 150
    elif (n > 79):
        I = I_off
        tau_LBS = 90
        tau_wall = 150
```

```
    hA_LBS = h_LBS*A_surf
    hA_wall = h_wall*A_surf

    C_LBS = tau_LBS*A_LBS*h_LBS
    C_wall = tau_wall*A_wall*h_wall

    R_cold_LBS = 28.1*10**-6
    R_LBS[0] =  R_cold_LBS
    R_LBS[n] = (R_cold_LBS*(1+(alpha_LBS*(T_LBS[n-1]-T_0_LBS))))+R_factor_LBS

    P_LBS[n] = R_LBS[n]*I*I
    T_LBS[n] = (T_LBS[n-1]+(dt_1/C_LBS)*P_LBS[n]-hA_LBS*(T_LBS[n-1]-T_LBS[0]))+x_LBS

    R_cold_wall = 229.2*10**-6
    R_wall[0] =  R_cold_wall
    R_wall[n] = (R_cold_wall*(1+(alpha_wall*(T_wall[n-1]-T_0_wall))))+R_factor_wall

    P_wall[n] = R_wall[n]*I*I
    T_wall[n] = (T_wall[n-1]+(dt_1/C_wall)*P_wall[n]-hA_wall*(T_wall[n-1]-T_wall[0]))+x

#Plot real vs simulation
import pandas as pd
T_real_LBS = pd.read_excel (r'C:\Users\ceglo\Documents\1_Spring 2022\Tests\LBS_Python\4
T_real_wall = pd.read_excel (r'C:\Users\ceglo\Documents\1_Spring 2022\Tests\Wall_Python

#Get to 1dim array for LBS
T_real_data_LBS = pd.read_excel (r'C:\Users\ceglo\Documents\1_Spring 2022\Tests\LBS_Pyt
T_real_prep_LBS = T_real_data_LBS.values
T_real_1dim_LBS =T_real_prep_LBS[:,0]

#Get to 1dim array for outside wall
T_real_data_wall = pd.read_excel (r'C:\Users\ceglo\Documents\1_Spring 2022\Tests\Wall_P
T_real_prep_wall = T_real_data_wall.values
T_real_1dim_wall =T_real_prep_wall[:,0]

#Calc average error
def calc_average_error(temp_sim, temp_real_1dim):
    mean_sim = np.mean(np.abs(temp_sim))
    mean_real = np.mean(np.abs(temp_real_1dim))
    mean_error = np.abs(mean_real-mean_sim)
    return mean_error

av_error_LBS = calc_average_error(T_LBS,T_real_1dim_LBS)
print ("Average error for LBS [degree C]:","%.2f" % av_error_LBS)

av_error_wall = calc_average_error(T_wall,T_real_1dim_wall)
print ("Average error for outside wall [degree C]:","%.2f" % av_error_wall)

fig = plt.figure()
l1 = plt.plot(time, T_LBS, 'b', label = "simulated LBS")
l2 = plt.plot(time_real, T_real_LBS, 'b--', label = "real LBS")
l3 = plt.plot(time, T_wall, 'r', label = "simulated wall")
l4 = plt.plot(time_real, T_real_wall, 'r--', label = "real wall")
plt.grid('on')
plt.title('Sim vs real. I = 400A and later overloaded to be I = 850A')
plt.legend(loc = 'upper left')
plt.xlabel('Min' )
plt.ylabel('Temp [Degree C]')
plt.axis([0,510,0,120])
plt.show()
```

Real vs. simulated temperature rise for I = 500A with overload

I = 500A and adjusted to 700A at a given time:

```
import numpy as np
import matplotlib.pyplot as plt

alpha_LBS = 0.0021
alpha wall = 0.00305
R_factor_LBS = -0.9*10**-6
R factor wall = -11*10**-6
h_LBS = 11.3
h wall = 13.4
x_LBS = 1.1
x wall = -0.3
A_surf = 0.725
A wall = 0.22
A_LBS = 0.015

a = 0.0; b = 821 # running time
N = 100
dt = ((b-a)/N)
dt_1 = (dt/150)

hA LBS = h LBS*A surf
hA_wall = h_wall*A_surf

#Timespan
time = np.linspace(a,b,N+1)
time_real = np.linspace(a,b,b-1)

#Empty arrays
T_LBS = np.zeros(N+1)
T_real_LBS = np.zeros(b)
R_LBS = np.zeros(N+1)
P_LBS = np.zeros(N+1)

T_wall = np.zeros(N+1)
T_real_wall = np.zeros(b)
R_wall = np.zeros(N+1)
P_wall = np.zeros(N+1)

for n in range(N):
    #LBS
    T_0_LBS = 18.8
    T_LBS[0] = T_0_LBS
    T_max_LBS = 101.3

    #Wall
    T_0_wall = 18.7
    T_wall[0] = T_0_wall
    T_max_wall = 28.3

    #Changing current
    I_1 = 500
    I_2 = 700
    I_off = 0
     if (n < 45):
         I = I_1
         tau_LBS = 80
         tau_wall = 140
     elif (n > 46 and n < 84 ):
         I = I_2
         tau_LBS = 80
         tau_wall = 140
```

```
    elif (n > 85):
        I = I_off
        tau_LBS = 80
        tau_wall = 140

    U_LBS = h_LBS*A_surf
    U_wall = h_wall*A_surf

    C_LBS = tau_LBS*A_LBS*h_LBS
    C_wall = tau_wall*A_wall*h_wall

    #LBS
    R_cold_LBS = 28.1*10**-6
    R_LBS[0] =  R_cold_LBS
    R_LBS[n] = (R_cold_LBS*(1+(alpha_LBS*(T_LBS[n-1]-T_0_LBS))))+R_factor_LBS

    P_LBS[n] = R_LBS[n]*I*I
    T_LBS[n] = (T_LBS[n-1]+(dt_1/C_LBS)*P_LBS[n]-hA_LBS*(T_LBS[n-1]-T_LBS[0]))+x_LBS

    #Wall
    R_cold_wall = 229.2*10**-6
    R_wall[0] =  R_cold_wall
    R_wall[n] = (R_cold_wall*(1+(alpha_wall*(T_wall[n-1]-T_0_wall))))+R_factor_LBS

    P_wall[n] = R_wall[n]*I*I
    T_wall[n] = (T_wall[n-1]+(dt_1/C_wall)*P_wall[n]-hA_wall*(T_wall[n-1]-T_wall[0]))+x

#Plot real vs simulation
import pandas as pd
T_real_LBS = pd.read_excel (r'C:\Users\ceglo\Documents\1_Spring 2022\Tests\LBS_Python\
T_real_wall = pd.read_excel (r'C:\Users\ceglo\Documents\1_Spring 2022\Tests\Wall_Pythor

#Get to 1dim array for LBS
T_real_data_LBS = pd.read_excel (r'C:\Users\ceglo\Documents\1_Spring 2022\Tests\LBS_Py
T_real_prep_LBS = T_real_data_LBS.values
T_real_1dim_LBS =T_real_prep_LBS[:,0]

#Get to 1dim array for outside wall
T_real_data_wall = pd.read_excel (r'C:\Users\ceglo\Documents\1_Spring 2022\Tests\Wall_F
T_real_prep_wall = T_real_data_wall.values
T_real_1dim_wall =T_real_prep_wall[:,0]

#Calc average error
def calc_average_error(temp_sim, temp_real_1dim):
    mean_sim = np.mean(np.abs(temp_sim))
    mean_real = np.mean(np.abs(temp_real_1dim))
    mean_error = np.abs(mean_real-mean_sim)
    return mean_error

av_error_LBS = calc_average_error(T_LBS,T_real_1dim_LBS)
print ("Average error for LBS [degree C]:","%.2f" % av_error_LBS)

av_error_wall = calc_average_error(T_wall,T_real_1dim_wall)
print ("Average error for outside wall [degree C]:","%.2f" % av_error_wall)

fig = plt.figure()
l1 = plt.plot(time, T_LBS, 'b', label = "simulated LBS")
l2 = plt.plot(time_real, T_real_LBS, 'b--', label = "real LBS")
l3 = plt.plot(time, T_wall, 'r', label = "simulated wall")
l4 = plt.plot(time_real, T_real_wall, 'r--', label = "real wall")
plt.grid('on')
plt.title('Sim vs real. I = 500A and later overloaded to I = 700A.')
plt.legend(loc = 'upper left')
plt.xlabel('Min' )
plt.ylabel('Temp [Degree C]')
plt.axis([0,800,0,130])
plt.show()
```

I = 500A and adjusted to 800A at a given time:

```
import numpy as np
import matplotlib.pyplot as plt

alpha_LBS = 0.0021
alpha_wall = 0.00305
R_factor_LBS = -0.9*10**-6
R_factor_wall = -11*10**-6
h_LBS = 11.3
h_wall = 13.4
x_LBS = 0.1
x_wall = 0.1
A_surf = 0.725
A_wall = 0.22
A_LBS = 0.015

a = 0.0; b = 584 # running time
N = 100
dt = ((b-a)/N)
dt_1 = (dt/150)

hA_LBS = h_LBS*A_surf
hA_wall = h_wall*A_surf

#Timespan
time = np.linspace(a,b,N+1)
time_real = np.linspace(a,b,b-1)

#Empty arrays
T_LBS = np.zeros(N+1)
T_real_LBS = np.zeros(b)
R_LBS = np.zeros(N+1)
P_LBS = np.zeros(N+1)

T_wall = np.zeros(N+1)
T_real_wall = np.zeros(b)
R_wall = np.zeros(N+1)
P_wall = np.zeros(N+1)

for n in range(N):
    #LBS
    T_0_LBS = 19.8
    T_LBS[0] = T_0_LBS
    T_max_LBS = 110

    #Wall
    T_0_wall = 19.5
    T_wall[0] = T_0_wall
    T_max_wall = 27.1

    #Changing current
    I_1 = 500
    I_2 = 800
    I_off = 0

    if (n < 64):
        I = I_1
        tau_LBS = 80
        tau_wall = 140
    elif (n > 65 and n < 80 ):
        I = I_2
        tau_LBS = 80
        tau_wall = 140
    elif (n > 81):
        I = I_off
        tau_LBS = 80
        tau_wall = 140
```

```
    C_LBS = tau_LBS*A_LBS*h_LBS
    C_wall = tau_wall*A_wall*h_wall

    #LBS
    R_cold_LBS = 28.1*10**-6 #229.2*10**-6
    R_LBS[0] =  R_cold_LBS
    R_LBS[n] = (R_cold_LBS*(1+(alpha_LBS*(T_LBS[n-1]-T_0_LBS))))+R_factor_LBS

    P_LBS[n] = R_LBS[n]*I*I
    T_LBS[n] = (T_LBS[n-1]+(dt_1/C_LBS)*P_LBS[n]-hA_LBS*(T_LBS[n-1]-T_LBS[0]))+x_LBS

    #Wall
    R_cold_wall = 229.2*10**-6#28.1*10**-6
    R_wall[0] =  R_cold_wall
    R_wall[n] = (R_cold_wall*(1+(alpha_wall*(T_wall[n-1]-T_0_wall))))+R_factor_wall

    P_wall[n] = R_wall[n]*I*I
    T_wall[n] = (T_wall[n-1]+(dt_1/C_wall)*P_wall[n]-hA_wall*(T_wall[n-1]-T_wall[0]))+x

#Plot real vs simulation
import pandas as pd
T_real_LBS = pd.read_excel (r'C:\Users\ceglo\Documents\1_Spring 2022\Tests\LBS_Python\S
T_real_wall = pd.read_excel (r'C:\Users\ceglo\Documents\1_Spring 2022\Tests\Wall_Python

#Get to 1dim array for LBS
T_real_data_LBS = pd.read_excel (r'C:\Users\ceglo\Documents\1_Spring 2022\Tests\LBS_Pyt
T_real_prep_LBS = T_real_data_LBS.values
T_real_1dim_LBS =T_real_prep_LBS[:,0]

#Get to 1dim array for outside wall
T_real_data_wall = pd.read_excel (r'C:\Users\ceglo\Documents\1_Spring 2022\Tests\Wall_P
T_real_prep_wall = T_real_data_wall.values
T_real_1dim_wall =T_real_prep_wall[:,0]

#Calc average error
def calc_average_error(temp_sim, temp_real_1dim):
    mean_sim = np.mean(np.abs(temp_sim))
    mean_real = np.mean(np.abs(temp_real_1dim))
    mean_error = np.abs(mean_real-mean_sim)
    return mean_error

av_error_LBS = calc_average_error(T_LBS,T_real_1dim_LBS)
print ("Average error for LBS [degree C]:","%.2f" % av_error_LBS)

av_error_wall = calc_average_error(T_wall,T_real_1dim_wall)
print ("Average error for outside wall [degree C]:","%.2f" % av_error_wall)


fig = plt.figure()
l1 = plt.plot(time, T_LBS, 'b', label = "simulated LBS")
l2 = plt.plot(time_real, T_real_LBS, 'b--', label = "real LBS")
l3 = plt.plot(time, T_wall, 'r', label = "simulated wall")
l4 = plt.plot(time_real, T_real_wall, 'r--', label = "real wall")
plt.grid('on')
plt.title('Sim vs real. I = 500A and later overloaded to I = 800A.')
plt.legend(loc = 'upper left')
plt.xlabel('Min' )
plt.ylabel('Temp [Degree C]')
plt.axis([0,550,0,130])
plt.show()
```

I = 500A and adjusted to 850A at a given time:

```
import numpy as np
import matplotlib.pyplot as plt

alpha_LBS = 0.0021
alpha_wall = 0.00305
R_factor_LBS = -0.9*10**-6
R_factor_wall = -11*10**-6
h_LBS = 11.3
h_wall = 13.4
x_LBS = 1.9
x_wall = 0.3
A_surf = 0.725
A_wall = 0.22
A_LBS = 0.015

hA_LBS = h_LBS*A_surf
hA_wall = h_wall*A_surf

a = 0.0; b = 550 # running time
N = 100
dt = ((b-a)/N)
dt_1 = (dt/150)

#Timespan
time = np.linspace(a,b,N+1)
time_real = np.linspace(a,b,b-1)

#Empty arrays
T_LBS = np.zeros(N+1)
T_real_LBS = np.zeros(b)
R_LBS = np.zeros(N+1)
P_LBS = np.zeros(N+1)

T_wall = np.zeros(N+1)
T_real_wall = np.zeros(b)
R_wall = np.zeros(N+1)
P_wall = np.zeros(N+1)

for n in range(N):
    #LBS
    T_0_LBS = 19.7
    T_LBS[0] = T_0_LBS
    T_max_LBS = 110

    #Wall -update
    T_0_wall = 18.9
    T_wall[0] = T_0_wall
    T_max_wall = 28.1

    #Changing current
    I_1 = 500
    I_2 = 850
    I_off = 0

    if (n < 65):
        I = I_1
        tau_LBS = 80
        tau_wall = 140
    elif (n > 67 and n < 76 ):
        I = I_2
        tau_LBS = 80
        tau_wall = 140
    elif (n > 77):
        I = I_off
        tau_LBS = 80
        tau_wall = 140
```

```
    C_LBS = tau_LBS*A_LBS*h_LBS
    C_wall = tau_wall*A_wall*h_wall

    #LBS
    R_cold_LBS = 28.1*10**-6
    R_LBS[0] =  R_cold_LBS
    R_LBS[n] = (R_cold_LBS*(1+(alpha_LBS*(T_LBS[n-1]-T_0_LBS))))+R_factor_LBS

    P_LBS[n] = R_LBS[n]*I*I
    T_LBS[n] = (T_LBS[n-1]+(dt_1/C_LBS)*P_LBS[n]-hA_LBS*(T_LBS[n-1]-T_LBS[0]))+x_LBS

    #Wall
    R_cold_wall = 229.2*10**-6
    R_wall[0] =  R_cold_wall
    R_wall[n] = (R_cold_wall*(1+(alpha_wall*(T_wall[n-1]-T_0_wall))))+R_factor_wall

    P_wall[n] = R_wall[n]*I*I
    T_wall[n] = (T_wall[n-1]+(dt_1/C_wall)*P_wall[n]-hA_wall*(T_wall[n-1]-T_wall[0]))+

#Plot real vs simulation
import pandas as pd
T_real_LBS = pd.read_excel (r'C:\Users\ceglo\Documents\1_Spring 2022\Tests\LBS_Python\
T_real_wall = pd.read_excel (r'C:\Users\ceglo\Documents\1_Spring 2022\Tests\Wall_Pytho

#Get to 1dim array for LBS
T_real_data_LBS = pd.read_excel (r'C:\Users\ceglo\Documents\1_Spring 2022\Tests\LBS_Py
T_real_prep_LBS = T_real_data_LBS.values
T_real_1dim_LBS =T_real_prep_LBS[:,0]

#Get to 1dim array for outside wall
T_real_data_wall = pd.read_excel (r'C:\Users\ceglo\Documents\1_Spring 2022\Tests\Wall_
T_real_prep_wall = T_real_data_wall.values
T_real_1dim_wall =T_real_prep_wall[:,0]

#Calc average error
def calc_average_error(temp_sim, temp_real_1dim):
    mean_sim = np.mean(np.abs(temp_sim))
    mean_real = np.mean(np.abs(temp_real_1dim))
    mean_error = np.abs(mean_real-mean_sim)
    return mean_error

av_error_LBS = calc_average_error(T_LBS,T_real_1dim_LBS)
print ("Average error for LBS [degree C]:","%.2f" % av_error_LBS)

av_error_wall = calc_average_error(T_wall,T_real_1dim_wall)
print ("Average error for outside wall [degree C]:","%.2f" % av_error_wall)


fig = plt.figure()
l1 = plt.plot(time, T_LBS, 'b', label = "simulated LBS")
l2 = plt.plot(time_real, T_real_LBS, 'b--', label = "real LBS")
l3 = plt.plot(time, T_wall, 'r', label = "simulated wall")
l4 = plt.plot(time_real, T_real_wall, 'r--', label = "real wall")
plt.grid('on')
plt.title('Sim vs real. I = 500A and later overloaded to I = 850A.')
plt.legend(loc = 'upper left')
plt.xlabel('Min' )
plt.ylabel('Temp [Degree C]')
plt.axis([0,540,0,130])
plt.show()
```

Real vs. simulated temperature rise for I = 630A with overload

I = 630A and adjusted to 700A at a given time:

```
import numpy as np
import matplotlib.pyplot as plt

alpha_LBS = 0.0021
alpha_wall = 0.00305
R_factor_LBS = -0.9*10**-6
R_factor_wall = -11*10**-6
h_LBS = 13.2
h_wall = 15.4
x_LBS = 2.1
x_wall = 0.8
A_surf = 0.725
A_wall = 0.22
A_LBS = 0.015

hA_LBS = h_LBS*A_surf
hA_wall = h_wall*A_surf

a = 0.0; b = 841 # running time
N = 100
dt = ((b-a)/N)
dt_1 = (dt/150)

#Timespan
time = np.linspace(a,b,N+1)
time_real = np.linspace(a,b,b-1)

#Empty arrays
T_LBS = np.zeros(N+1)
T_real_LBS = np.zeros(b)
P_LBS = np.zeros(N+1)
R_LBS = np.zeros(N+1)

T_wall = np.zeros(N+1)
T_real_wall = np.zeros(b)
P_wall = np.zeros(N+1)
R_wall = np.zeros(N+1)

for n in range(N):
    #LBS
    T_0_LBS = 21.1
    T_LBS[0] = T_0_LBS
    T_max_LBS = 100

    #Wall
    T_0_wall = 18.52
    T_wall[0] = T_0_wall
    T_max_wall = 31

    #Changing current
    I_1 = 630
    I_2 = 700
    I_off = 0

     if (n < 40):
         I = I_1
         tau_LBS = 70
         tau_wall = 135
     elif (n > 52 and n < 82 ):
         I = I_2
         tau_LBS = 70
         tau_wall = 135
```

```
    elif (n > 83):
        I = I_off
        tau_LBS = 70
        tau_wall = 135

    C_LBS = tau_LBS*A_LBS*h_LBS
    C_wall = tau_wall*A_wall*h_wall

    #LBS
    R_cold_LBS = 28.1*10**-6
    R_LBS[0] =  R_cold_LBS
    R_LBS[n] = (R_cold_LBS*(1+(alpha_LBS*(T_LBS[n-1]-T_0_LBS))))+R_factor_LBS

    P_LBS[n] = R_LBS[n]*I*I
    T_LBS[n] = (T_LBS[n-1]+(dt_1/C_LBS)*P_LBS[n]-hA_LBS*(T_LBS[n-1]-T_LBS[0]))+x_LBS

    #Wall
    R_cold_wall = 229.2*10**-6
    R_wall[0] =  R_cold_wall
    R_wall[n] = (R_cold_wall*(1+(alpha_wall*(T_wall[n-1]-T_0_wall))))+R_factor_wall

    P_wall[n] = R_wall[n]*I*I
    T_wall[n] = (T_wall[n-1]+(dt_1/C_LBS)*P_wall[n]-hA_wall*(T_wall[n-1]-T_wall[0]))+x_

#Plot real vs simulation
import pandas as pd
T_real_LBS = pd.read_excel (r'C:\Users\ceglo\Documents\1_Spring 2022\Tests\LBS_Python\
T_real_wall = pd.read_excel (r'C:\Users\ceglo\Documents\1_Spring 2022\Tests\Wall_Pytho

#Get to 1dim array for LBS
T_real_data_LBS = pd.read_excel (r'C:\Users\ceglo\Documents\1_Spring 2022\Tests\LBS_Py
T_real_prep_LBS = T_real_data_LBS.values
T_real_1dim_LBS =T_real_prep_LBS[:,0]

#Get to 1dim array for outside wall
T_real_data_wall = pd.read_excel (r'C:\Users\ceglo\Documents\1_Spring 2022\Tests\Wall_
T_real_prep_wall = T_real_data_wall.values
T_real_1dim_wall =T_real_prep_wall[:,0]

#Calc average error
def calc_average_error(temp_sim, temp_real_1dim):
    mean_sim = np.mean(np.abs(temp_sim))
    mean_real = np.mean(np.abs(temp_real_1dim))
    mean_error = np.abs(mean_real-mean_sim)
    return mean_error

av_error_LBS = calc_average_error(T_LBS,T_real_1dim_LBS)
print ("Average error for LBS [degree C]:","%.2f" % av_error_LBS)

av_error_wall = calc_average_error(T_wall,T_real_1dim_wall)
print ("Average error for outside wall [degree C]:","%.2f" % av_error_wall)

fig = plt.figure()
l1 = plt.plot(time, T_LBS, 'b', label = "simulated LBS")
l2 = plt.plot(time_real, T_real_LBS, 'b--', label = "real LBS")
l3 = plt.plot(time, T_wall, 'r', label = "simulated wall")
l4 = plt.plot(time_real, T_real_wall, 'r--', label = "real wall")
plt.legend(loc = 'upper left')
plt.title('Sim vs real. I = 630A and later overloaded to I = 700A.')
plt.xlabel('Min' )
plt.ylabel('Temp [Degree C]')
plt.axis([0,820,0,120])
plt.grid('on')
plt.show()
```

I = 630A and adjusted to 800A at a given time:

```
import numpy as np
import matplotlib.pyplot as plt

alpha_LBS = 0.0021
alpha_wall = 0.00305
R_factor_LBS = -0.9*10**-6
R_factor_wall = -11*10**-6
h_LBS = 13.2
h_wall = 15.4
x_LBS = 1.8
x_wall = 0.4
A_surf = 0.725
A_wall = 0.22
A_LBS = 0.015

hA_LBS = h_LBS*A_surf
hA_wall = h_wall*A_surf

a = 0.0; b = 559 # running time
N = 65
dt = ((b-a)/N)
dt_1 = (dt/141)

#Timespan
time = np.linspace(a,b,N+1)
time_real = np.linspace(a,b,b-1)

#Empty arrays
T_LBS = np.zeros(N+1)
T_real_LBS = np.zeros(b)
P_LBS = np.zeros(N+1)
R_LBS = np.zeros(N+1)

T_wall = np.zeros(N+1)
T_real_wall = np.zeros(b)
P_wall = np.zeros(N+1)
R_wall = np.zeros(N+1)

for n in range(N):
    #LBS
    T_0_LBS = 21.1
    T_LBS[0] = T_0_LBS
    T_max_LBS = 110

    #Wall
    T_0_wall = 19.3
    T_wall[0] = T_0_wall
    T_max_wall = 24.3

    #Changing current
    I_1 = 630
    I_2 = 800
    I_off = 0

     if (n < 46):
         I = I_1
         tau_LBS = 70
         tau_wall = 135
     elif (n > 47 and n < 51):
         I = I_2
         tau_LBS = 70
         tau_wall = 135
     elif (n > 52):
         I = I_off
         tau_LBS = 70
         tau_wall = 135
```

```
    C_LBS = tau_LBS*A_LBS*h_LBS
    C_wall = tau_wall*A_wall*h_wall

    #LBS
    R_cold_LBS = 28.1*10**-6
    R_LBS[0] =  R_cold_LBS
    R_LBS[n] = (R_cold_LBS*(1+(alpha_LBS*(T_LBS[n-1]-T_0_LBS))))+R_factor_LBS

    P_LBS[n] = R_LBS[n]*I**2
    T_LBS[n] = (T_LBS[n-1]+(dt_1/C_LBS)*P_LBS[n]-hA_LBS*(T_LBS[n-1]-T_LBS[0]))+x_LBS

    #Wall
    R_cold_wall = 229.2*10**-6
    R_wall[0] =  R_cold_wall
    R_wall[n] = (R_cold_wall*(1+(alpha_wall*(T_wall[n-1]-T_0_wall))))+R_factor_wall

    P_wall[n] = R_wall[n]*I**2
    T_wall[n] = (T_wall[n-1]+(dt_1/C_LBS)*P_wall[n]-hA_wall*(T_wall[n-1]-T_wall[0]))+x_

#Plot real vs simulation
import pandas as pd
T_real_LBS = pd.read_excel (r'C:\Users\ceglo\Documents\1_Spring 2022\Tests\LBS_Python\(
T_real_wall = pd.read_excel (r'C:\Users\ceglo\Documents\1_Spring 2022\Tests\Wall_Pythor

#Get to 1dim array for LBS
T_real_data_LBS = pd.read_excel (r'C:\Users\ceglo\Documents\1_Spring 2022\Tests\LBS_Pyt
T_real_prep_LBS = T_real_data_LBS.values
T_real_1dim_LBS =T_real_prep_LBS[:,0]

#Get to 1dim array for outside wall
T_real_data_wall = pd.read_excel (r'C:\Users\ceglo\Documents\1_Spring 2022\Tests\Wall_F
T_real_prep_wall = T_real_data_wall.values
T_real_1dim_wall =T_real_prep_wall[:,0]

#Calc average error
def calc_average_error(temp_sim, temp_real_1dim):
    mean_sim = np.mean(np.abs(temp_sim))
    mean_real = np.mean(np.abs(temp_real_1dim))
    mean_error = np.abs(mean_real-mean_sim)
    return mean_error

av_error_LBS = calc_average_error(T_LBS,T_real_1dim_LBS)
print ("Average error for LBS [degree C]:","%.2f" % av_error_LBS)

av_error_wall = calc_average_error(T_wall,T_real_1dim_wall)
print ("Average error for outside wall [degree C]:","%.2f" % av_error_wall)


fig = plt.figure()
l1 = plt.plot(time, T_LBS, 'b', label = "simulated LBS")
l2 = plt.plot(time_real, T_real_LBS, 'b--', label = "real LBS")
l3 = plt.plot(time, T_wall, 'r', label = "simulated wall")
l4 = plt.plot(time_real, T_real_wall, 'r--', label = "real wall")
plt.legend(loc = 'upper left')
plt.title('Sim vs real. I = 630A and later overloaded to I = 800A.')
plt.xlabel('Min' )
plt.ylabel('Temp [Degree C]')
plt.axis([0,530,0,120])
plt.grid('on')
plt.show()
```

I = 630A and adjusted to 850A at a given time:

```
import numpy as np
import matplotlib.pyplot as plt

alpha_LBS = 0.0021
alpha_wall = 0.00305
R_factor_LBS = -0.9*10**-6
R_factor_wall = -11*10**-6
h_LBS = 13.2
h_wall = 15.4
x_LBS = 2
x_wall = -0.1
A_surf = 0.725
A_wall = 0.22
A_LBS = 0.015

hA_LBS = h_LBS*A_surf
hA_wall = h_wall*A_surf

a = 0.0; b = 525 # running time
N = 65
dt = ((b-a)/N)
dt_1 = (dt/141)

#Timespan
time = np.linspace(a,b,N+1)
time_real = np.linspace(a,b,b-1)

#Empty arrays
T_LBS = np.zeros(N+1)
T_real_LBS = np.zeros(b)
P_LBS = np.zeros(N+1)
R_LBS = np.zeros(N+1)

T_wall = np.zeros(N+1)
T_real_wall = np.zeros(b)
P_wall = np.zeros(N+1)
R_wall = np.zeros(N+1)

for n in range(N):
    #LBS
    T_0_LBS = 21.1
    T_LBS[0] = T_0_LBS
    T_max_LBS = 109.9

    #Wall
    T_0_wall = 20.1
    T_wall[0] = T_0_wall
    T_max_wall = 28

    #Current
    I_1 = 630
    I_2 = 850
    I_off = 0

     if (n < 46):
         I = I_1
         tau_LBS = 70
         tau_wall = 135
     elif (n > 47 and n < 50):
         I = I_2
         tau_LBS = 70
         tau_wall = 135
     elif (n > 51):
         I = I_off
         tau_LBS = 70
         tau_wall = 135
```

```
    C_LBS = tau_LBS*A_LBS*h_LBS
    C_wall = tau_wall*A_wall*h_wall

    #LBS
    R_cold_LBS = 28.11*10**-6
    R_LBS[0] =  R_cold_LBS
    R_LBS[n] = (R_cold_LBS*(1+(alpha_LBS*(T_LBS[n-1]-T_0_LBS))))+R_factor_LBS

    P_LBS[n] = R_LBS[n]*I**2
    T_LBS[n] = (T_LBS[n-1]+(dt_1/C_LBS)*P_LBS[n]-hA_LBS*(T_LBS[n-1]-T_LBS[0]))+x_LBS

    #Wall
    R_cold_wall = 229.2*10**-6
    R_wall[0] =  R_cold_wall
    R_wall[n] = (R_cold_wall*(1+(alpha_wall*(T_wall[n-1]-T_0_wall))))+R_factor_wall

    P_wall[n] = R_wall[n]*I**2
    T_wall[n] = (T_wall[n-1]+(dt_1/C_wall)*P_wall[n]-hA_wall*(T_wall[n-1]-T_wall[0]))+

#Plot real vs simulation
import pandas as pd
T_real_LBS = pd.read_excel (r'C:\Users\ceglo\Documents\1_Spring 2022\Tests\LBS_Python\
T_real_wall = pd.read_excel (r'C:\Users\ceglo\Documents\1_Spring 2022\Tests\Wall_Pytho

#Get to 1dim array for LBS
T_real_data_LBS = pd.read_excel (r'C:\Users\ceglo\Documents\1_Spring 2022\Tests\LBS_Py
T_real_prep_LBS = T_real_data_LBS.values
T_real_1dim_LBS =T_real_prep_LBS[:,0]

#Get to 1dim array for outside wall
T_real_data_wall = pd.read_excel (r'C:\Users\ceglo\Documents\1_Spring 2022\Tests\Wall_
T_real_prep_wall = T_real_data_wall.values
T_real_1dim_wall =T_real_prep_wall[:,0]

#Calc average error
def calc_average_error(temp_sim, temp_real_1dim):
    mean_sim = np.mean(np.abs(temp_sim))
    mean_real = np.mean(np.abs(temp_real_1dim))
    mean_error = np.abs(mean_real-mean_sim)
    return mean_error

av_error_LBS = calc_average_error(T_LBS,T_real_1dim_LBS)
print ("Average error for LBS [degree C]:","%.2f" % av_error_LBS)

av_error_wall = calc_average_error(T_wall,T_real_1dim_wall)
print ("Average error for outside wall [degree C]:","%.2f" % av_error_wall)

fig = plt.figure()
l1 = plt.plot(time, T_LBS, 'b', label = "simulated LBS")
l2 = plt.plot(time_real, T_real_LBS, 'b--', label = "real LBS")
l3 = plt.plot(time, T_wall, 'r', label = "simulated wall")
l4 = plt.plot(time_real, T_real_wall, 'r--', label = "real wall")
plt.legend(loc = 'upper left')
plt.title('Sim vs real. I = 630A and later overloaded to I = 850A.')
plt.xlabel('Min' )
plt.ylabel('Temp [Degree C]')
plt.axis([0,510,0,120])
plt.grid('on')
plt.show()
```

Appendix H

Average deviation for overload cases

The calculated average temperature deviation between the real and simulated model for the temperature rise tests with overloading (not adjusted time constant at overload) is presented in the following tables. The error is calculated based on Equation (8.1). I_2 is the overload current.

Initial current is 400A:

	I_2 = 700A	**I_2 = 800A**	**I_2 = 850A**
LBS ΔT [˚C]	80.4	88.7	91.1
LBS error [˚C]	4.3	3.5	4
LBS error [%]	5.3	3.9	4.4
Outside wall ΔT [˚C]	7.1	10.5	7.5
Outside wall error [˚C]	0.8	0.6	0.5
Outside wall error [%]	11	5.7	6.7

Initial current is 500A:

	I_2 = 700A	**I_2 = 800A**	**I_2 = 850A**
LBS ΔT [˚C]	82.5	90.2	90.3
LBS error [˚C]	3.6	0.9	0.3
LBS error [%]	4.4	1	0.3
Outside wall ΔT [˚C]	9.6	7.6	9.2
Outside wall error [˚C]	1.9	0.6	0.8
Outside wall error [%]	19.8	7.9	8.7

Initial current is 630A (nominal):

	I_2 = 700A	**I_2 = 800A**	**I_2 = 850A**
LBS ΔT [˚C]	78.9	88.9	88.8
LBS error [˚C]	0.6	1	6.9
LBS error [%]	0.8	1.1	7.8
Outside wall ΔT [˚C]	12.5	5	7.9
Outside wall error [˚C]	0.2	0.3	1.7
Outside wall error [%]	1.6	6	21.5

Average deviation for overload cases – adjusted τ

The average temperature deviation between the simulated thermal model and the real data is calculated for the temperature rise tests with overloading with adjusted time constant τ (in the overload period). The result is presented in the following tables. I_2 is the overload current and the error is calculated based on Equation (8.1).

Initial current is 400A:

	I_2 = 700A	**I_2 = 800A**	**I_2 = 850A**
LBS ΔT [˚C]	80.4	88.7	91.1
LBS error [˚C]	1.5	1.6	2.7
LBS error [%]	1.9	1.8	3
Outside wall ΔT [˚C]	7.1	10.5	7.5
Outside wall error [˚C]	0.1	0.3	0.2
Outside wall error [%]	1.4	2.9	2.7

Initial current is 500A:

	I_2 = 700A	**I_2 = 800A**	**I_2 = 850A**
LBS ΔT [˚C]	82.5	90.2	90.3
LBS error [˚C]	1.3	2.8	4.1
LBS error [%]	1.6	3.1	4.5
Outside wall ΔT	9.6	7.6	9.2
Outside wall error	0.2	0.06	0.4
Outside wall error [%]	2.1	0.8	4.3

Initial current is 630A (nominal):

	I_2 = 700A	**I_2 = 800A**	**I_2 = 850A**
LBS ΔT [˚C]	78.9	88.9	88.8
LBS error [˚C]	1	0.9	5.3
LBS error [%]	1.3	1	6
Outside wall ΔT [˚C]	12.5	5	7.9
Outside wall error [˚C]	0.25	0.2	0.7
Outside wall error [%]	2	4	8.9

Appendix I

Overload time for different currents

The possible overload times are presented as a chart which describes possible overload currents based on initial current and wanted overloading time. The data used to develop the chart is gathered from simulations in Appendix G with changed time constant for the LBS and wall. The time constant used for the LBS is shown in the table below. The time constant for the wall is set fixed to 140min as described in section 8.2.3.

	400A	**500A**	**630A**	**700A**	**800A**	**900A**
Time constant [min]	90	80	70	60	50	40

Changing the time constant changes the possible overload time. This means that previous simulated thermal model results will not correspond to this solution. Neither will the real data from the temperature rise test on the lab system. This is accepted to develop an approximately overview of possible overload times based on a simplified thermal model.

The main gathered data from the simulation is plotted in the figure below. Trendline function in excel is used to get the equations. The rated current is 630A.

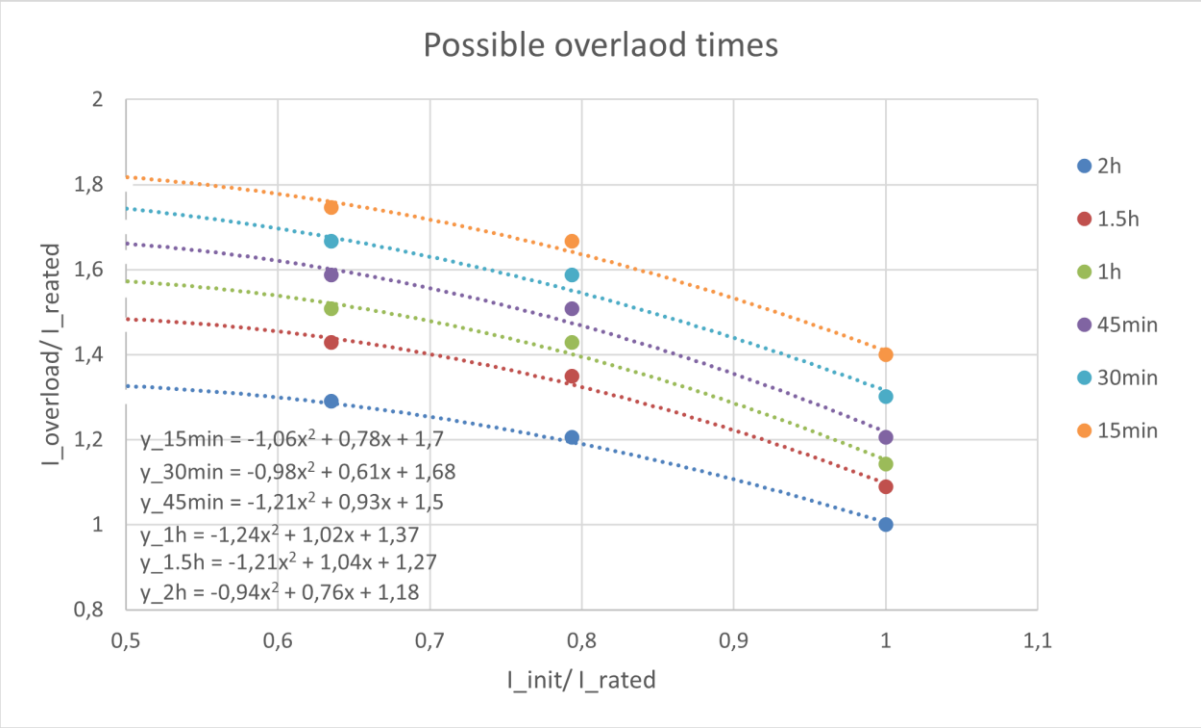

A Python script is developed to plots the possible overload times, based on the equations. The script is shown below.

```
import matplotlib.pyplot as plt
import numpy as np

x = np.linspace(0, 1.5, 50)

y_15min = (-1.06*x**2)+(0.77*x)+ 1.70
y_30min = (-0.98*x**2)+(0.6*x)+ 1.68
y_45min = (-1.21*x**2)+(0.92*x)+ 1.5
y_1h = (-1.24*x**2)+(1.02*x)+ 1.37
y_1point5h = (-1.21*x**2)+(1.04*x)+ 1.27
y_2h = (-0.94*x**2)+(0.76*x)+ 1.18

fig = plt.figure()

l1 = plt.plot(x, y_15min ,'y', label = "15min")
l2 = plt.plot(x, y_30min ,'m', label = "30min")
l3 = plt.plot(x, y_45min ,'r', label = "45min")
l4 = plt.plot(x, y_1h ,'b', label = "1h")
l5 = plt.plot(x, y_1point5h ,'g', label = "1.5h")
l6 = plt.plot(x, y_2h ,'k', label = "2h")

plt.title('Possible overlaod time')
plt.legend(loc = 'upper right')
plt.xlabel('I_init/ I_rated' )
plt.ylabel('I_overload/ I_rated')
plt.grid('on')
plt.axis([0.5,1.0,1.0,2])
plt.show()
```